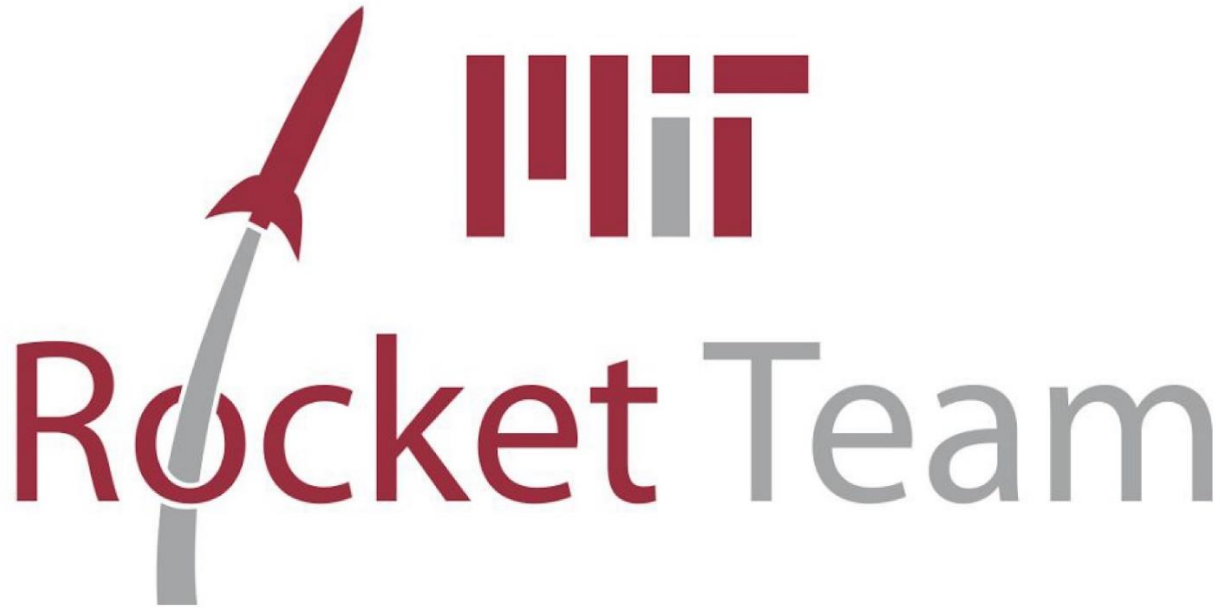

Viper2

Preliminary Design Review

February 10th, 2017

Table of Contents

Viper2 PDR | 2017-02-10

Contents

Overview

Charlie Garcia | 2017-02-09

This document outlines a methane-oxygen bipropellant rocket engine named Viper-2, currently under development by MIT Rocket Team. The engine is an initiative to build experience and infrastructure on the team to operate cryogenic liquid rocket engines. This engine is designed to validate combustion stability, cooling, fueling, manufacturing, and other critical aspects of a methane oxygen rocket engine. The engine is designed to produce 2 kN of thrust when running at a chamber pressure of 3.4 MPa. It is designed for an operating time of 30 seconds, scheduled for a successful hot fire test by May 2017. The scope of this development project runs through the first test of a non-flight weight engine. This document serves as both an external review and internal reference for the design to this point.

The engine is operating under both financial and chronological pressure. In some cases, either financial or chronological pressures played a significant role in design decisions. In these cases, we held safety as an immutable factor, and only accepted solutions that maintained high safety standards.

The remainder of this document outlines in detail the injector and chamber geometries and manufacturing processes, tank structures, test stand architecture, fluid handling procedures, ignition procedures, engine thermal performance, and safety considerations. Outlined are the assumptions and methods we used to devise the design so far, as well as analysis and validation that has been done to this point.

Injector Design

Ethan Perrin | 2017-02-01

This section presents the injector design for Viper2. The design is composed of three 316 stainless steel components, A286 bolts, Grafoil gaskets, and PTFE O-rings. The injector topology is unlike doublet with two concentric rings of 16 orifice pairs, forming 32 impingement and atomization planes.

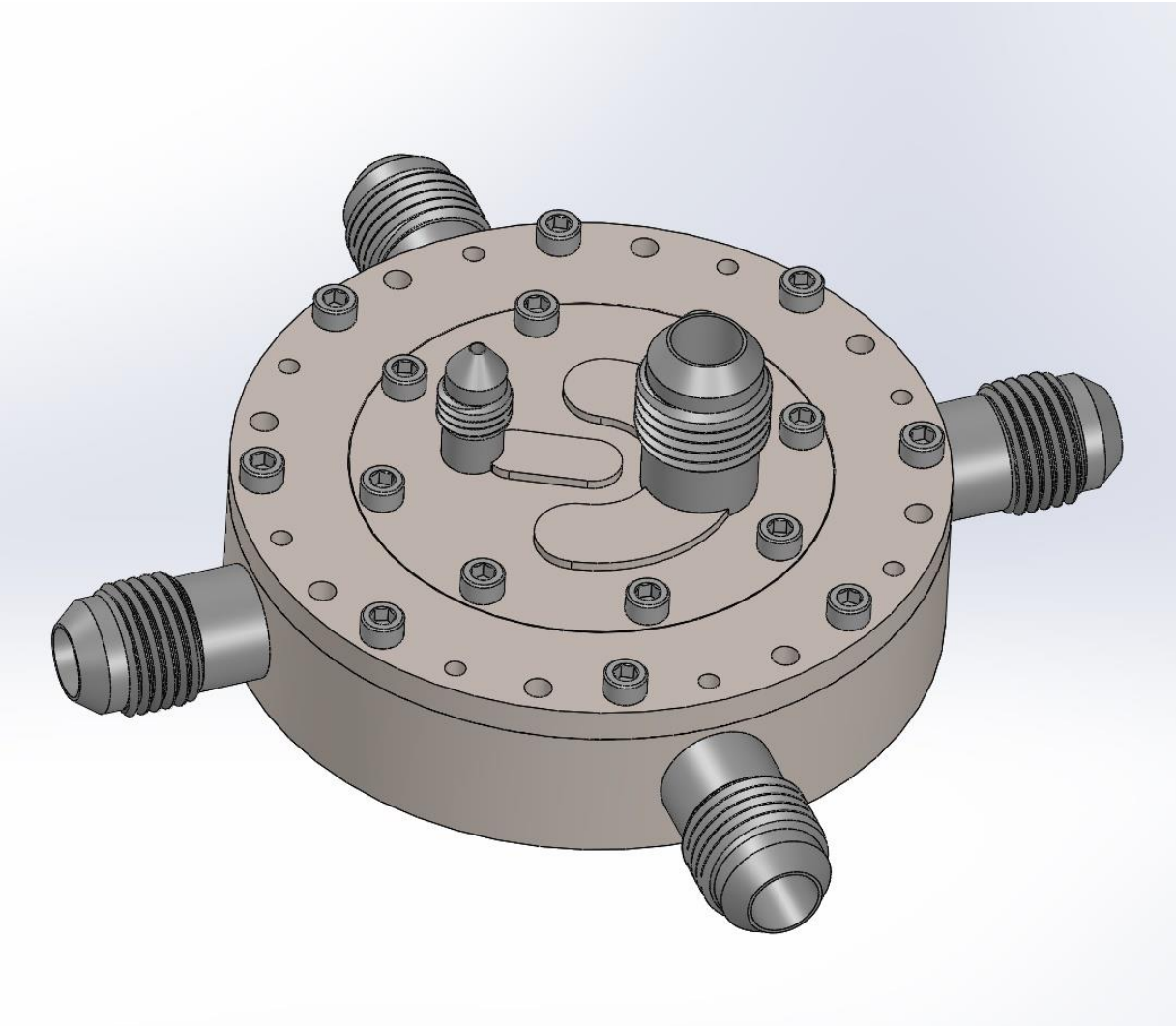

1 Injector Topology

The purpose of the injector is to atomize and mix the two propellants in preparation for combustion, ensuring rapid, uniform reactions. The unlike doublet design forces the propellants through small orifices, increasing their flow velocity and momentum until they collide at the impingement point, where the collision atomizes the stream into fine droplets. Two similar topologies include like doublets and unlike triplets. In the former, the oxidizer and fuel are impinged with streams of the same propellant and the atomized clouds mix in the chamber. In the triplet, there is a central stream of one propellant impinged by two streams of the other.

1.1 Injection Schemes

Detailed in Huzel & Huang [6], there are generally three types of injection elements – nonimpinging, unlike-impinging, and like-impinging. Non-impinging elements include the coaxial injector used in the SSME, "shower head" type axial streams, and fan formers are popular in larger engines or other types of engines, but are disadvantageous in Viper2 for their complex design (coaxial), or ineffective mixing (shower head/fan former) compared to impingement schemes.

Due to simple design and manufacturing requirements, good mixing and atomization, the unlike doublet was chosen for the Viper2 injector.

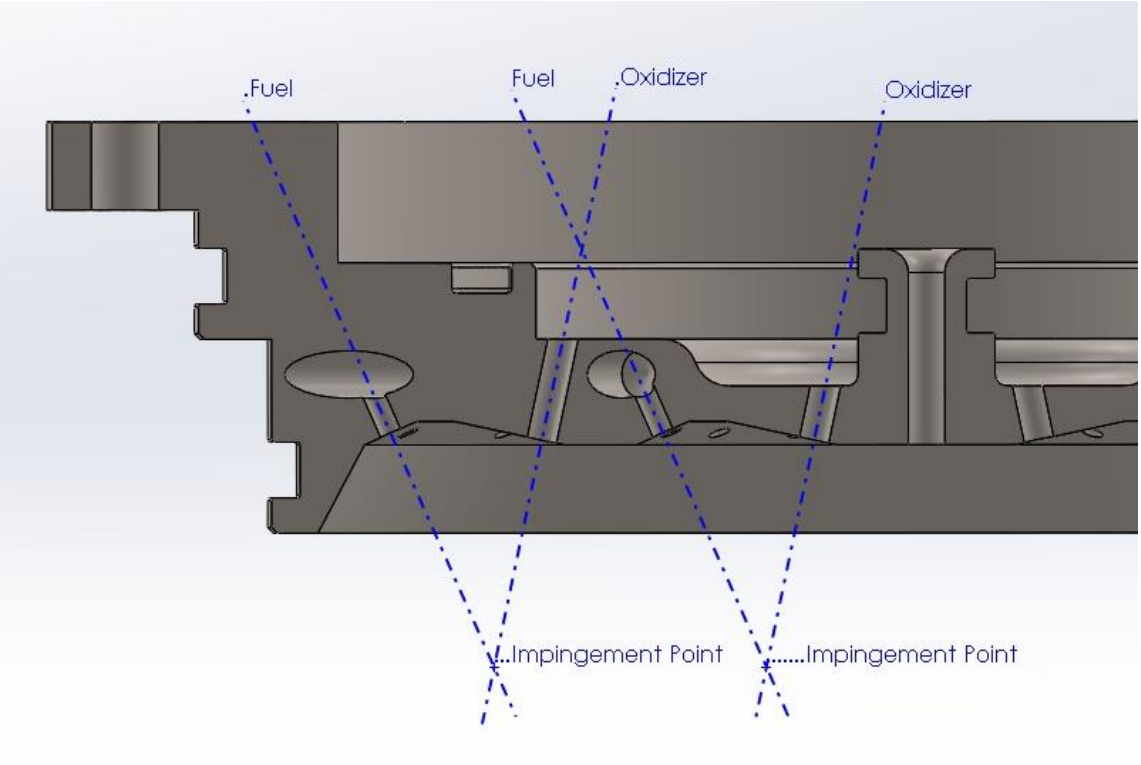

Figure 1.1: Cross-section of Viper2 injector, showing fuel and oxidizer impingement points and orifice angles. The oxidizer incident angles with respect to the vertical axis are 12 and 24 degrees for oxidizer and fuel, respectively.

1.1.1 Unlike Elements

The simplest unlike-type injection element is to impinge one stream of each propellant at a point in space in front of the injector surface. The collision of the propellants produces a finely atomized, mixed

spray fan perpendicular to the plane formed by the fluid streams. The velocity of the streams and their angle of impingement directly impacts the effectivity of the atomization and orientation of the droplet plane. Unlike elements do not produce a perfectly distributed mix of propellants, subject to stream diameter mismatch and turbulent radial winds propagating from combustion below the impingement point. Unlike triplets, quadruplets, pentads, etc. also exist, whereby multiple streams of one propellant impinge on a central stream of the other. This is slightly advantageous to better match the momentums and stream diameters of the propellants, and achieve better mixing at the cost of significant manufacturing and manifold complexity [6].

1.1.2 Like Elements

Like injection elements follow the same layout patterns as unlike elements, but without implicit mixing due to the impingement. Atomized planar clouds of each propellant must be made to impinge by arrangement of like-doublet pairs. Like injection elements are superior in matching the momentum and diameter of impinging streams, resulting in more stable atomization and no pre-combustion of hypergolic propellants or heat transfer. This comes at the cost of (often) more injection elements and inferior mixing due to the two-step nature of atomization and mixing.

1.1.3 Comparison of Injection Elements

Table 1.1 offers a comparison of unlike and like injection elements in terms of relative atomization, mixing, and complexity. Due to the small size of the engine, restricted manufacturing capabilities, and similar propellant liquid properties, the unlike doublet was chosen.

Topology	Atomization	Mixing	Orifices per Element
Unlike Doublet	Good	Good	2
Unlike Triplet	Good	Excellent	3
Like Doublet	Excellent	Fair	4
Like Triplet	Excellent	Fair	6

Table 1.1: Comparison of injection elements

1.2 Injection Element Design

The injector, by nature of restricting fluid flow through orifices, has an associated pressure drop for each propellant. This characteristic has utility in reducing pressure for an increase in fluid flow velocity (and consequently momentum) that directly contributes to better mixing and atomization at impingement. A secondary and equally important effect of the pressure drop is isolation from combustion disturbances and local propellant flowrates through each orifice. The proposed design utilizes a pressure drop of 100 psi, equal to 20 percent of the chamber pressure of 500 psi. Across 32 orifices for each propellant, this computes to diameters of 0.972 mm and 0.720 mm for LOX and methane respectively, with fluid streams impinging at 12 and 24 degrees respectively.

1.2.1 Injector Pressure Drop

During combustion, instabilities and pressure deviations can locally change the chamber pressure near injection elements, disturbing the instantaneous mass flow rate and local reaction rate. The pressure wave and further propagating oscillations can compound and lead to destructive instabilities if the frequency of oscillation couples with another part of the system [6]. NASA specifications allow up to a 5 percent oscillation in chamber pressure for stable combustion. This necessitates a pressure drop of at

least 5 percent to avoid stagnating local flow through injection elements. Huzel & Huang further recommend a 20 percent pressure drop as a starting point, which was used for this design [6].

1.2.2 Number of Injector Elements

The number of injector elements has an adverse impact on complexity in terms of orifice size and quantity, and a positive correlation with propellant mixing and distribution throughout the combustion chamber. Given the combustion chamber diameter and manufacturing capabilities available on campus and in the local area, optimization was chosen on the side of good propellant mixing in exchange for more complex manifold design. The proposed design has two concentric sets of injection elements, each with 16 elements composed of one orifice for each propellant (total of 32 injection elements, 64 orifices).

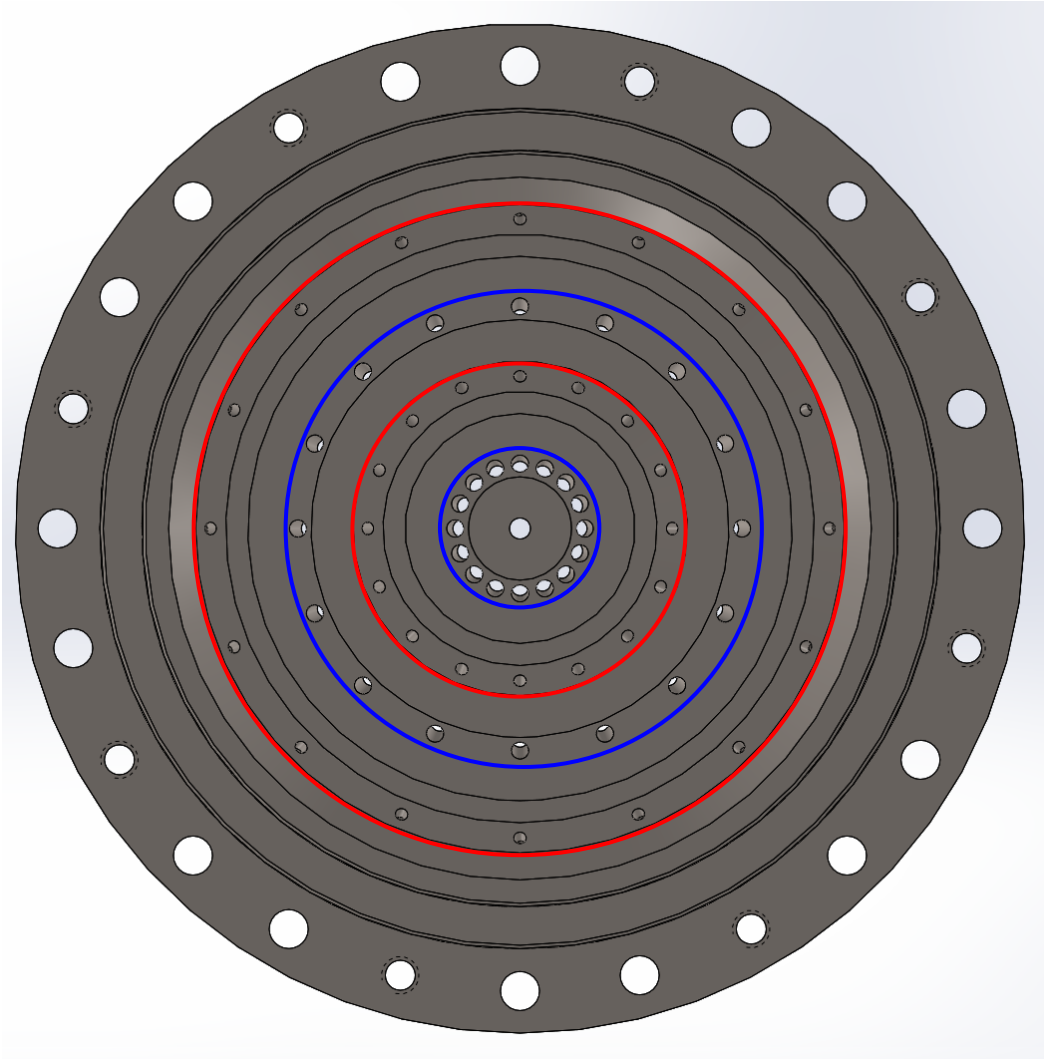

Figure 1.2: Bottom view of the Injector from inside the combustion chamber. Four concentric rings of orifices are visible, oxidizer encircled in blue and fuel encircled in red.

1.2.3 Diameter of Injector Orifices

Given the desired pressure drop, mass flow rate, and propellant density, the sum total area of all injector orifices can be calculated by equation 4-43 in Huzel & Huang, rewritten here with standard SI units [6].

$$A_{inj} = q\sqrt{\frac{K}{\rho \Delta P}}$$

Where q = mass flow rate (kg/s), K = head-loss coefficient, ρ = fluid density (kg/m^3), and ΔP = pressure drop (Pa). The engine was parameterized with a desired operating atmosphere of 0.10133 MPa (1 atm), a chamber pressure of 3.4474 MPa (500 psi), and mixture ratio of 2.90 (O/F).

Parameter	Fuel	Oxidizer	R_m (O/F)	P_c (MPa)	F (N)	P_c/P_e
Input	CH4(L)	O2(L)	2.90	3.4474	2355	34.023

Table 1.2: Inputs for NASA CEA Run rocket combustion simulation

Thermodynamic properties including combustion temperature, molar mass of exhaust products, and thermodynamic constant k were taken from NASA's online CEA Run program and tabulated below in Table 1.2 [9].

Parameter	k	T_c (°K)	M (mol)
Result	1.21	3356	19.96

Table 1.3: Results of NASA CEA Run simulation

These outputs can then be used in calculation of the exit velocity in equation 1.22 from Braeunig.us [8]. Rearranging equation 1.6 with a desired thrust value of 2355 N and iterative solving with Excel yields a total mass flow of 0.8671 kg/s, which can be broken down into specific mass flows for each propellant based on the mixture ratio.

Calculation with equation 4-43 yields a total orifice injector area of 30.23 mm^2 for LOX and 16.59 mm^2 for methane. Introducing the number of injection elements, we can calculate the diameter of each orifice using equation 4-44, again rewritten in SI units [6].

$$d_{orifice} = \left(\frac{Kq^2}{\rho \Delta P N^2}\right)^{0.25}$$

Where N = number of orifices. With 32 orifices per propellant, this calculates to diameters of 0.972 mm for LOX and 0.720 mm for methane.

1.2.4 Impingement Angle

Impingement angle of propellant streams was set to produce a droplet fan that is approximately planar with the central axis of the combustion chamber. Using the inelastic collision equation below from Huzel & Huang, the resultant beta angle of the droplet plane with respect to the axis of the chamber is calculated [6].

$$\tan\beta = \frac{q_1 v_1 \sin\alpha_1 - q_2 v_2 \sin\alpha_2}{q_1 v_1 \cos\alpha_1 + q_2 v_2 \cos\alpha_2}$$

Where q = stream mass flow (kg/s), v = stream velocity (m/s), α = stream angle from axial, and θ = resultant droplet plane angle in reference to figure 4-48 below from Huzel & Huang [6].

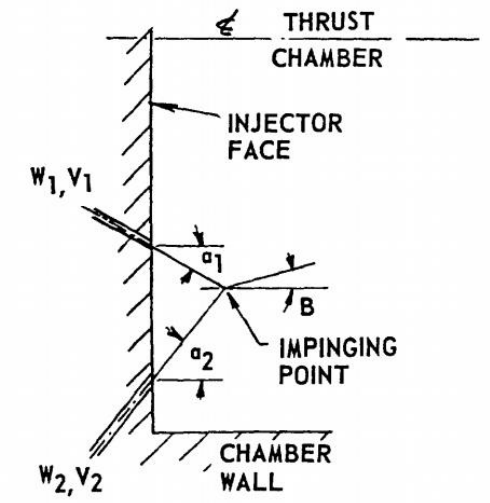

Figure 4-48.–Resultant angle of impinging streams.

Injection elements are arranged with the LOX orifices angled towards the chamber wall and methane orifices angled towards the central axis. This provides minor film cooling with the spray deflection on the outer ring angled back towards the chamber wall. The opposite arrangement would expose the chamber wall to oxidizer spray and contribute to corrosion and deterioration.

Calculation of stream momentums reveals the LOX stream has nearly double the momentum of the methane stream, necessitating a shallower stream angle α_1 compared to α_2 to provide a near axial (near-zero) θ angle. Analysis reveals a LOX stream angle of 12 degrees and a methane stream angle of 24 degrees results in a droplet plane angle θ of 0.59 degrees, angling slightly towards the interior of the chamber. This is desirable to keep combustion distributed throughout the chamber, but away from the chamber wall to prevent excessive heating. The resultant impingement point is 8.89 mm below the nominal plane of the injector surface. Impingement angles and the impingement point are displayed in Figure 1.1.

2 Manifold Design

The manifolds for each propellant serve to deliver propellant to each orifice before injection into the combustion chamber. The proposed design uses a LOX-dome type manifold for oxidizer and radial distribution paths joined by a circumferential manifold to distribute methane. This design allows for a monolithic injector face and minimal sealing requirements, with a total of three components making up the finished injector assembly.

2.1 Desired Properties

2.1.1 Low Pressure Drop

The injector assembly as a whole is designed to have a specific total pressure drop for reasons discussed in 1.2.1. In order to alleviate feed pressure requirements into the injector assembly and reduce the tank weight, pressurant volume, and stress on upstream components, it's optimal for the injector assembly

to have no more than the design pressure drop. This pressure drop is most easily controlled via orifice diameter, so providing consistent feed pressure across the numerous injection orifices is critical to consistent and distributed mass flow between elements. General design of fluid manifolds dictates the use of large passageways, rounded corners, smooth finishes, and even mass flow delivery to each feed path from the supply source. Increase of friction, cavitation sites, turbulent regions, and restrictions in the pathway are all detrimental to consistent mass flow and achieving a manifold low pressure drop.

2.1.2 Construction & Assembly Simplicity

The manifolds, whether integral to the injector face or product of an assembly, must deliver the requisite propellant to each injection element. A more complex array of many small injection elements is desirable for even droplet distribution and mixing in the chamber, but can quickly make manifold design challenging and complex. The more complex the manifold, the more difficult it is to design and manufacture which drives up design and manufacture time, tolerance requirements, and resource demands.

2.1.3 Even Mass Distribution

Each injection element is designed to receive a certain portion of the total mass flow, equal to the total mass flow divided by the number of elements. Without consistent mass flow to each element, mixture ratios, atomization, and combustion can vary widely across the chamber and contribute to low performance and instabilities. Designing a free-flowing manifold that provides even flow to each element favors a large manifold volume to dampen the effects of the inlet velocity head causing inconsistent mass flow, but this is constrained by size and packing requirements [6].

2.1.4 Manifold Volume

Manifold volume is the volume of fluid that remains inside the manifold between the inlet and the injection elements. A large manifold volume helps to alleviate uneven mass distribution due to inlet geometry, but has many adverse effects. The “dribble volume” remaining in the manifold after inlet valve cutoff has a propensity to produce a lag in response time between engine cutoff and the end of combustion, which is very unpredictable and inefficient due to the drop-off in mass flow as the manifold volume comes to rest. Large dribble volume decreases response time and repeatability of the engine.

Further, a large manifold volume acts as a fluid resonance chamber which can amplify pressure fluctuations in the combustion chamber and destructively propagate upstream to larger volumes in the feed lines and tanks. Between the opposite pulls of even mass distribution associated with high manifold volume and instability isolation associated with low manifold volume, an engineering compromise is to design the manifold to have four times the flow area of the total group of orifice areas fed by it [6].

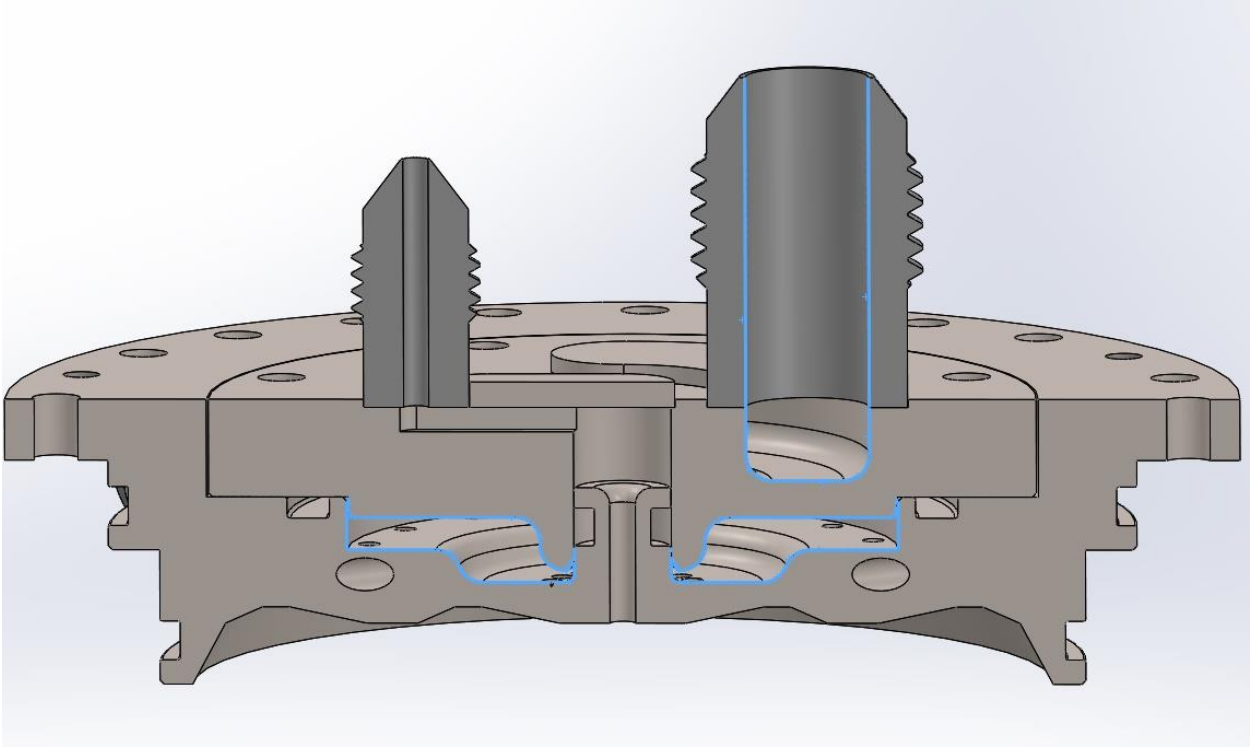

Figure 1.3: Cross section of the injector face and the LOX dome manifold. The highlighted areas are profiles that enclose the manifold or "dribble" volume. The connection duct between the AN flare inlet fitting on the right side and the lower torus manifold volume is obscured.

2.1.5 Minimal Velocity Impacts

Construction and geometry of the manifold and orifices has a propensity to impact orifice feed pressure due to velocity of the fluid interacting with the surfaces of the manifold. Knowledge of these interactions and impacts is crucial to achieving even mass flow between orifices.

2.1.5.1 Burrs & Orifice Edges

Sharp corners and burrs on the edges of holes produces a baffle or scoop effect, producing a negative or positive imbalance in mass flow and pressure variation [6]. While rounding or chamfering the edges of orifices is optimal, this is unfeasible with manufacturing available. Deburring accessible holes and careful cleaning helps reduce mass flow variation due to burrs and sharp edges.

2.1.5.2 Velocity Head

Similarly, proximity of the inlet to some orifices opposed to others subjects them to velocity head that can cause significant deviations in mass flow of up to 20 percent in simple ring-manifold designs with a single inlet collinear with the injector axis [6].

These effects can be mitigated with a larger manifold volume and preventing axial alignment of inlets and orifices.

2.2 Manifold Mechanical Interfaces

Viper2 is a ground test engine designed for research and development into methane-LOX engine design, performance, cooling, and operating parameters. Emphasis is therefore placed on usability and

reliability as opposed to a flight weight engine designed to be ultralight and deliver the peak performance.

The injector is designed as a bolt-together assembly with PTFE O-ring seals compatible with LOX and methane propellants [4, 10]. Inlet connections are comprised of durable, high pressure AN flare fittings that offer reusability and high pressure metal-metal seals. Compared to other fitting types like tapered NPT or double-ferrule compression, standard 37 degree AN fittings offer clocking adjustment, superior reusability, and a small form factor.

Each manifold is held in place by eight 4-40 bolts in a circular bolt pattern. Bolts are loaded in tension against the internal pressures of the manifold.

2.3 LOX Dome

The arrangement of the LOX orifices pointing outwards towards the chamber wall locates them on the central side of each injector element ring. This arrangement lends itself to a common cavity on the top side of the injector face, where a contoured cap reduces manifold volume. The face contour of the LOX dome was driven to reduce dribble volume inside them manifold, visible in Figure 2.1.

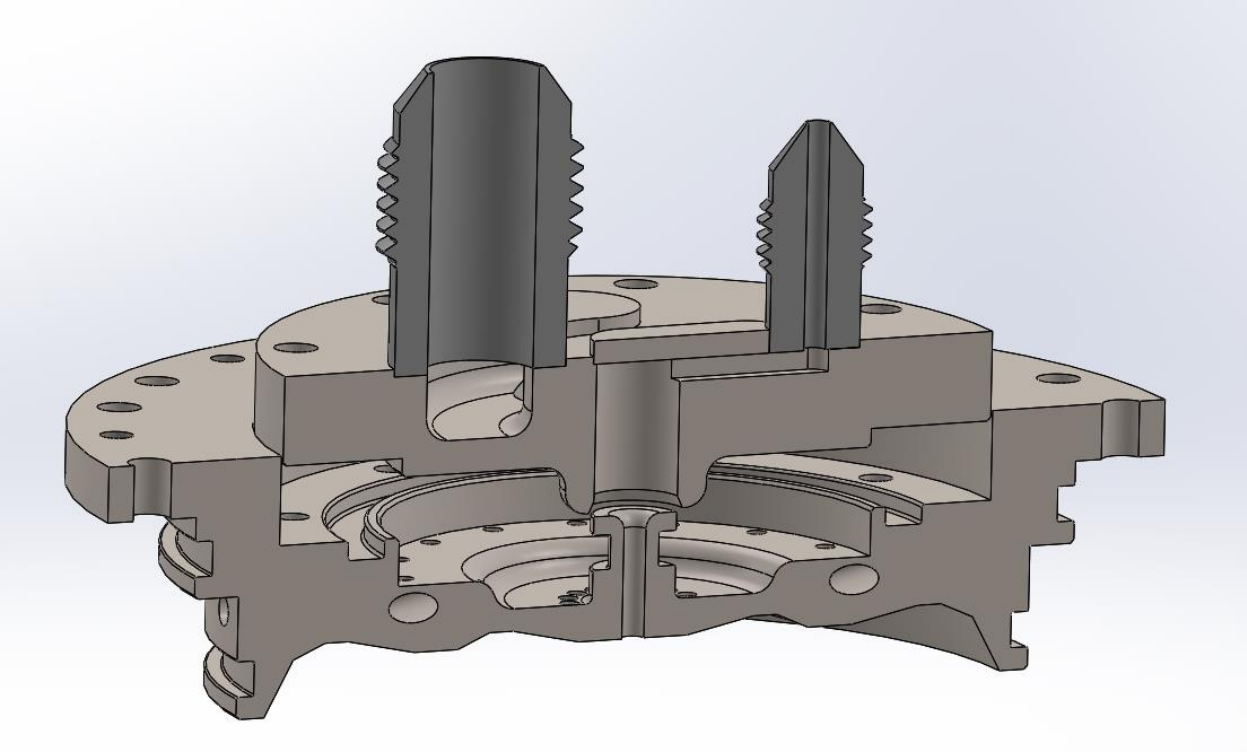

Figure 2.1: The LOX dome shown above the injector. Visible is the LOX inlet AN fitting, the pressure tap post in the center of the injector and mating port in the LOX dome, and the grooves for o-ring sealing.

2.3.1 Inlet Connections

The inlet fitting on the LOX manifold is a AN-6 flare fitting, the largest that would fit within the dimensions available. The inlet directly feeds a circular slot in the top of the LOX dome which splits the mass flow between two ducts 180 degrees apart, which then enter the dome cavity and feed the orifices directly. Direct inlet from the offset flare fitting to the injector oxidizer cavity would cause a large variation in orifice mass flow due to proximity to the inlet subjecting the orifices to significant velocity

head. Distributing the inlet to two ports helps provide more even mass flow distribution at a small cost to manufacturability. The distribution channel is visible in Figure 2.2.

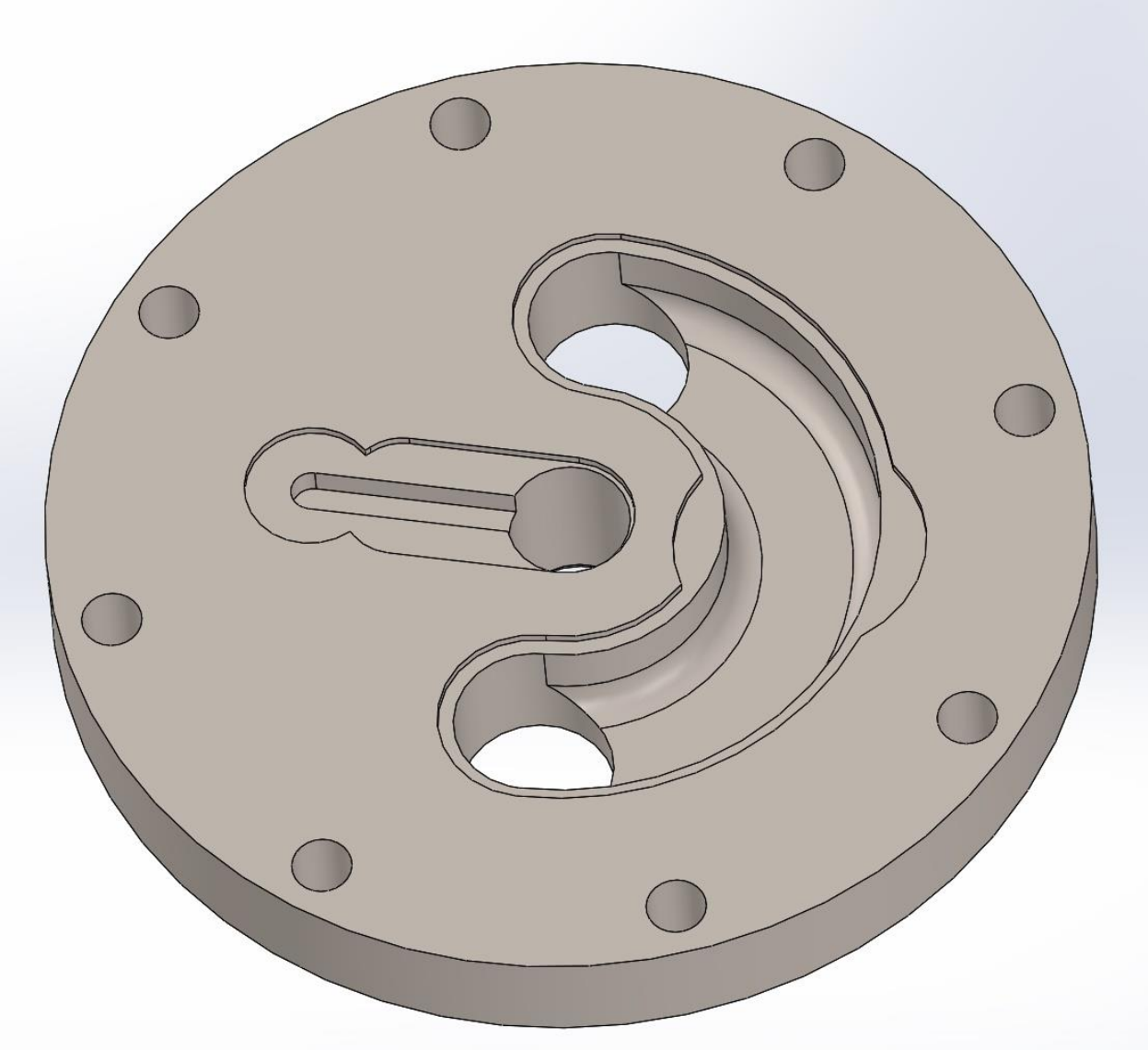

Figure 2.2: The top side of the LOX dome where the inlet connections attach. Visible are the milled channels used to offset the LOX inlet fitting and pressure tap connection. Flare fittings are welded in the circular pockets and the channels capped by welding stainless steel covers in place.

2.3.2 Pressure Tap Port

Chamber pressure is a valuable data point for measuring engine performance during operation, allowing calculation of effective exhaust velocity (C*) in combination with measured mass flow and nozzle geometry. Arrangement of the injector orifices in concentric rings leaves room in the center for a small port directly to the combustion chamber, where a feed-through is created through the pressure manifold to a remote pressure sensor. An O-ring groove seals against a hole in the manifold where a slot on the top leads to an offset AN-2 flare fitting welded in place. This interface is visible in Figures 2.1 and 2.2.

2.3.3 LOX Manifold Assembly Interface

A face groove is machined in the injector for a face-sealing O-ring with dimensions to fit a standard sized O-ring based on the Parker O-ring Handbook, with tapped blind holes behind the face groove for retention of the LOX dome [11].

Using a standard static circumferential O-ring seal on for the pressure tap and a face sealing O-ring on the outside of the manifold reduces feature concentricity tolerance requirements. Use of PTFE O-rings forms a cryogenic and oxygen-compatible seal. Eight 4-40 bolts retain the manifold against the injector flange. The two O-ring grooves and bolt holes are visible in Figure 2.1.

2.4 Methane Distribution Manifold

The radial methane ducts feeding the fuel orifices are angled such that they avoid intersection with LOX orifices (Figure 2.3). These ducts are enclosed by a circumferential manifold that seals against two O-ring grooves on the injector (Figure 2.3a) and is retained by eight 4-40 bolts.

2.4.1 Fuel Ducts

The sixteen fuel ports each feed two orifices. An ideal fluid manifold would reduce in diameter after feeding each orifice to maintain even mass flow between the orifices, but this complicates manufacturing due to the need to drill deep, small diameter holes [6]. Because there are only two orifices per duct it is deemed acceptable to use a single manifold diameter.

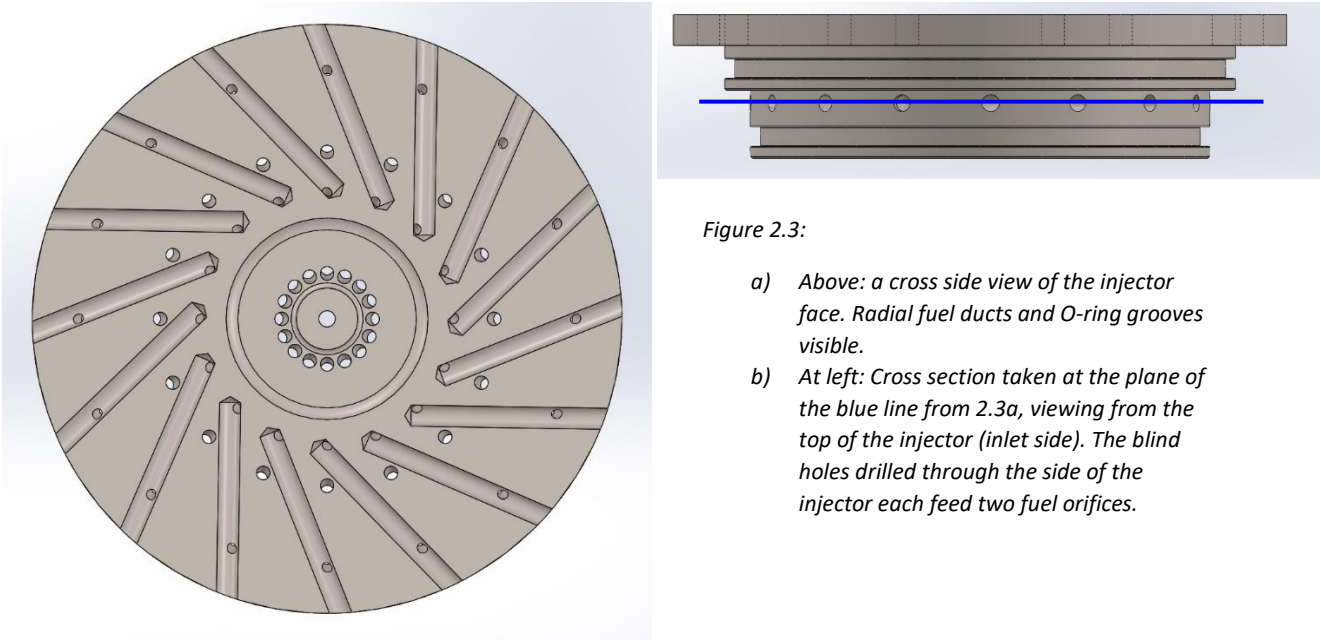

Figure 2.3:

a) Above: a cross side view of the injector face. Radial fuel ducts and O-ring grooves visible.

b) At left: Cross section taken at the plane of the blue line from 2.3a, viewing from the top of the injector (inlet side). The blind holes drilled through the side of the injector each feed two fuel orifices.

2.4.2 Inlet Connections

The inlet to the fuel ring manifold is divided between four AN-6 flare fittings to reduce pressure deviations between orifices. These fittings are welded directly to the outer diameter of the manifold (Figure 2.4a).

Each inlet is oriented radially and is placed between fuel ducts to reduce pressure variability due to velocity head. Each tube stub effectively feeds four ducts and eight orifices. Using the manifold diameter rule of thumb referenced in 2.1.4, this corresponds to an inlet manifold cross sectional area of

50.8 mm^2 and a circular diameter of 8.04 mm. The proposed manifold fittings each have a cross sectional area of 7.62 mm and a cross sectional area of 45.6 mm^2, which is 90 percent of the ideal value but limited by dimensional boundaries and standard available fitting sizes.

In order to maintain circular seal surfaces on the inner diameters of the manifold, welding takes place before boring each ID to final dimension.

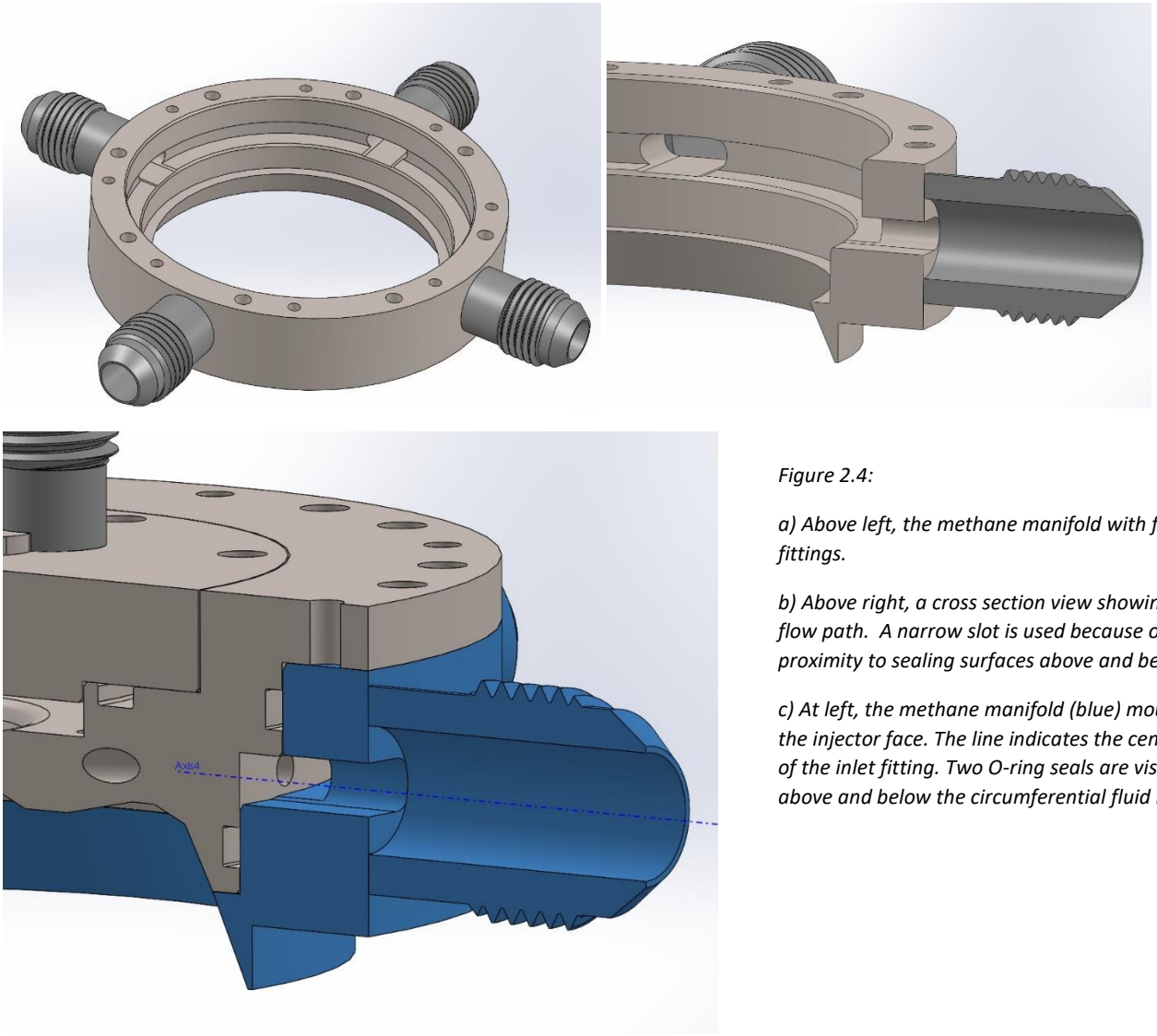

Figure 2.4:

a) Above left, the methane manifold with four inlet fittings.

b) Above right, a cross section view showing the flow path. A narrow slot is used because of proximity to sealing surfaces above and below.

c) At left, the methane manifold (blue) mounted on the injector face. The line indicates the central axis of the inlet fitting. Two O-ring seals are visible, above and below the circumferential fluid manifold.

3 Chamber Interface

3.1 Chamber Seal

The combustion chamber must mate to the injector face through a high temperature, leak-free, combustion compatible solution. Because of the dissimilar characteristics of aluminum and stainless steel, ceramic adhesive sealant Resbond 904 is used to bond Grafoil flange packing against the mating surfaces. This joint takes approximately 24 hours to cure fully into a dense, single-use gasket capable of withstanding the high temperature conditions of the chamber.

Grafoil gasket material is easily cut and formed into custom sized flange gaskets with steel dies. Resbond 904 adheres tightly with the metal surfaces and the Graphoil gasket placed in between, held in compression with bolts until the ceramic cures (Figure 3.1).

Grafoil and ceramic paste are susceptible to failure due to inconsistencies and defects in the materials, which can lead to cracks, hotspots, and eventual burn through of the gasket. Adherence to procedures and experience with the process is necessary to ensure proper application.

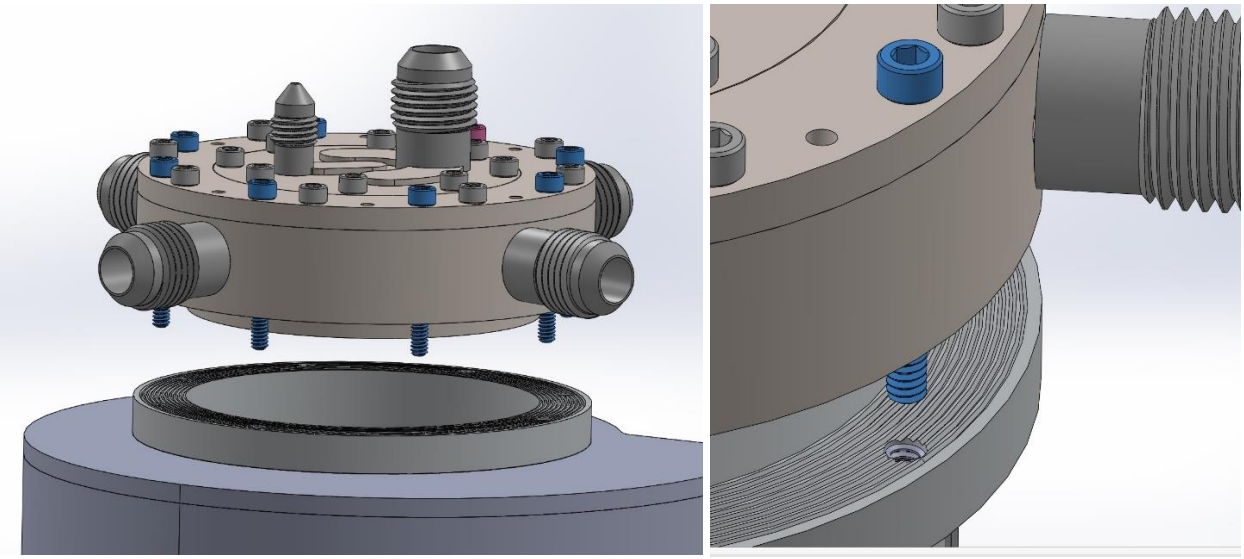

Figure 3.1: a) At left, the injector assembly above the chamber. Eight screws used for mechanical retention highlighted in blue. Grafoil gasket not shown for clarity. b) At right, a close up of the seal interface showing the Helicoil insert, the blue A286 fastener, and the surface grooves for the Grafoil mating surface. Grafoil gasket not shown for clarity.

3.2 Mechanical Connection

The mechanical connection between the chamber and the injector is accomplished with eight 4-40 screws extending from the top of the injector flange, through the methane manifold, into Helicoil threaded inserts in the aluminum thrust chamber. Helicoil inserts are used to aid in thread strength and durability; the aluminum is a soft material relative to the A286 bolts and is prone to thread wear and distortion with repeated use. Use of a stainless steel insert increases the thread depth (and therefore pull-out strength) and provides a steel-on-steel wear surface for thread engagement. Detail of this connection is shown in Figure 3.1b.

4 Thrust Take-up Structure

The large number of bolted connections taking place on the top surface of the injector leaves little room for mounting a thrust take-up structure to mount the engine and transfer load to the test stand. The take-up structure must allow tubing connections into the LOX dome and chamber pressure port after installation and provide a rigid connection with the test stand.

The proposed design uses a waterjet stainless steel plate to provide a mounting surface that clears all the bolts in the injector flange. A large steel plate with a central hole, providing clearance for the LOX inlet and pressure port, is then bolted through the spacer into the injector. This steel plate can then be

bolted onto the load cell adapter plate with additional hardware. The injector mounted to the thrust take-up plate is shown below in Figure 4.1.

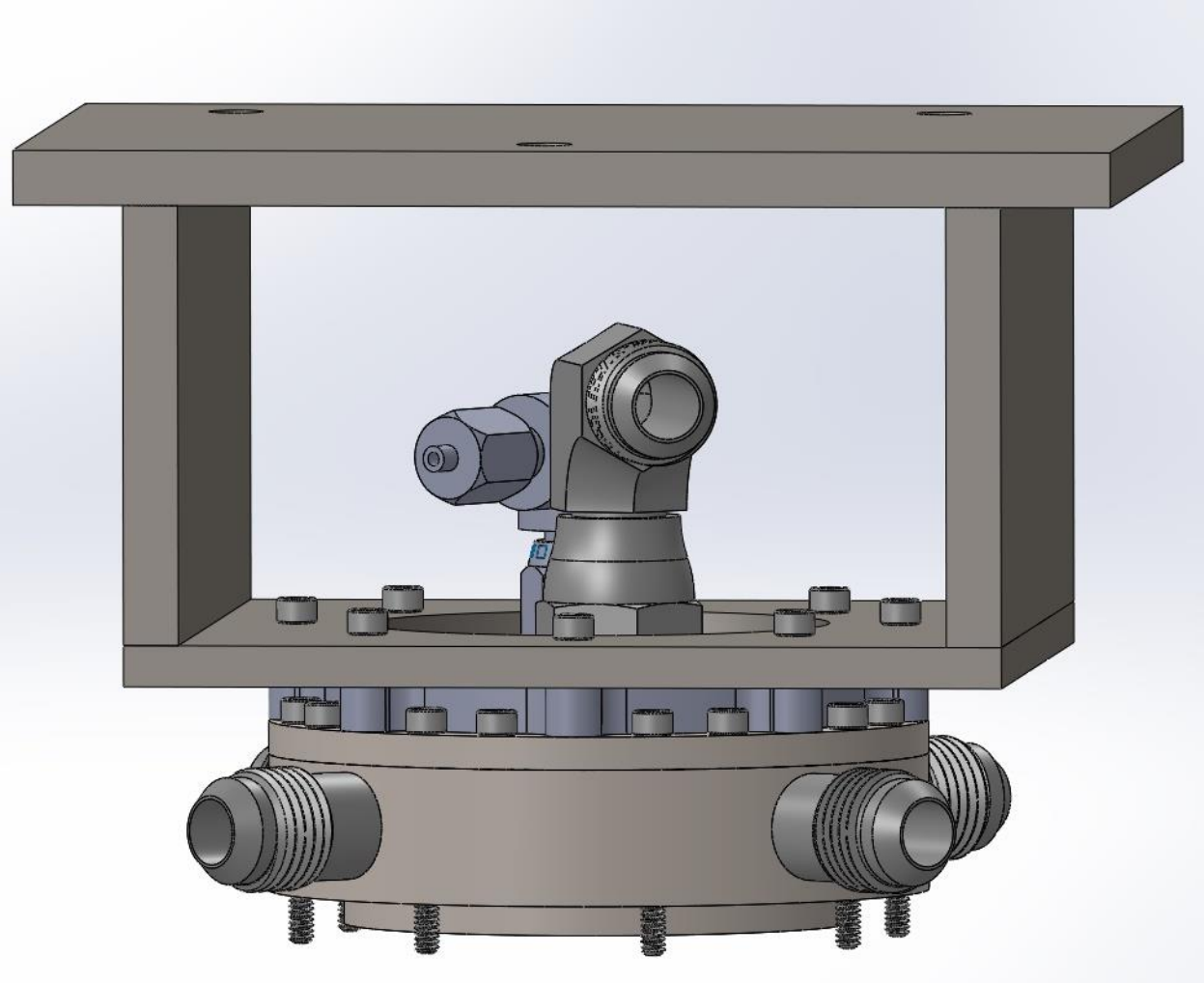

Figure 4.1: Complete injector assembly with thrust take-up structure. The light-grey spacer plate allows the structure to clear the bolt heads in the injector plate.

5 Material selection

Each component of the injector is manufactured from 316 stainless steel. 316 is a LOX compatible material that is inexpensive, machinable, and readily weldable. While not possessing high specific strength compared to other steel and nickel alloys, the small size of the injector and few features make the injector a fairly monolithic component which adds considerable strength to the design. Constructing all parts of the same alloy ensures identical thermal properties under operation.

5.1 Metals

5.1.1 Materials Compatibility

Materials of construction must be directly compatible with cryogenic methane and LOX.

5.1.2 Temperature tolerance

The material must retain suitable strength, ductility, and chemical resistance at cryogenic temperatures down to 90°K.

5.1.3 Manufacturability

Materials must be easily machined with available tools in a safe working environment. Weldability is also an important consideration for ease of manufacturing, especially for attachment of fittings.

5.1.4 Choice of Material

Low temperature compatibility rules out all steels except austenitic nickel-chromium alloys that maintain ductility. Copper, bronze, and brass, have low strength and durability for holding threads and less than ideal oxidizer compatibility. Aluminum becomes quickly impact sensitive if the oxide layer is scratched or abraded. Ignition sensitive alloys include titanium, zirconium, magnesium, and lead. Titanium is especially noted to be extremely impact sensitive.

The 300 series of austenitic stainless steel alloys maintains medium strength, excellent low temperature performance, material compatibility, ease of availability, weldability, and machinability and is the ideal material for construction.

5.2 Seal Materials

For use as a research engine, the ability to disassemble and analyze components of the injector assembly is important for development, cleaning, and inspection. O-rings were chosen for their balance of cost, ease of design implementation, versatility, and reusability. Where O-rings are unsuitable for high temperature sealing, such as the chamber interface, a crush gasket is used.

5.2.1 O-rings

Conventional O-rings offer very simple seal design through mechanical integration of an elastomer and operate up to extremely high pressures. O-rings come in standard sizes and a wide range of materials depending on fluid media and temperature of application. Kel-F, PFA, and PTFE are low-temperature compatible and insensitive to strong oxidizers such as LOX [4, 10].

5.2.2 Crush Seals

Crush seals offer high and low temperature durability, high pressure and vacuum use, wide range of materials and oxidizer compatibility, and minimal part features to accommodate. Low elasticity restricts applications to flange sealing applications. Surface finish requirements are moderate and replacement cost is low, with mechanical deformation allowing moderate tolerance requirements for proper sealing.

Crush gaskets and seal materials can be metallic or non-metallic materials depending on the application and desired properties. Copper, Iridium, and other soft metals are often used for example. Non-metallic seals include graphite (Grafoil) and ceramic based materials that are more flexible and have excellent high temperature performance.

5.3 Welding Consumables

ER316L filler is appropriate for welding 316 to 316. Midalloy and Sandvik produce low ferrite/cryogenic 316L filler rods, if vendors can be found. 100 percent argon shielding gas is best for stainless steel welding.

5.4 Fasteners

The injector assembly uses exclusively 4-40, A286 alloy stainless steel screws that maintain their strength and high corrosion resistance from cryogenic to high temperatures up to 700°C [13].

Stainless steel fasteners are prone to galling under high torques, temperature variations, and vibration that causes fretting. Using an antiseize compound designed for stainless steel in low temperature service greatly prevents galling. A suitable compound is available from McMaster, part number 1280K41, which corresponds to LP-250 antiseize manufactured by Armite Labs. LP-250 performs from -212°C up to 370°C and with all materials and chemicals except pure oxygen [12]. For this reason, it is critical to restrict contact of LP-250 to only the threaded areas protected by O-ring seals. LOX compatible antiseize compounds are available as expensive alternatives.

5.5 Fittings

All fittings used are 316 stainless to match composition of the components and permit welding. Use of 316 stainless steel is best for cryogenic oxidizer service and use with high pressure stainless steel tubing. Carbon steel and aluminum fittings and tubing are incompatible with liquid oxygen or not suitable for the MEOP of the test stand. Fittings are standard AN flare fittings that use metal-metal seals against the tubing flare surface.

6 Manufacturing

6.1 Machining Tools

The use of 316 stainless does not require special machines or considerations for manufacturing. Abiding by standard recommendations for tool selection and cutting parameters specific to the material is always advisable. Available resources include 2, 3, 4, and 5 axis CNC milling machines, CNC lathes, and other standard machine tools needed to complete the construction of the injector assembly.

6.1.1 Contour Turning

316 is machined with standard carbide insert tooling and flood coolant. The radially symmetric profile of the injector body and each manifold in the assembly allows the majority of machining to take place in turning operations. Recommendations for surface speed and feed rate can be found on the insert manufacturer's datasheets and in Machinery's Handbook [7].

6.1.2 Milling

Milling of 316 is also readily accomplished with standard tooling including carbide insert tools and carbide end mills. Flood coolant is necessary for chip evacuation and cooling of the cutting tool. Recommendations for surface speed and feed rate can be found in the tooling manufacturer's datasheets and in Machinery's Handbook [7].

6.1.3 Drilling

Drilling 316 stainless is accomplished with standard machinery with optimal RPM and feed rate settings for the drill diameter, found in Machinery's Handbook and in the drill manufacturer's recommendations [7].

6.1.4 Threading

Threading can be accomplished in two primary methods: single-point thread cutting and tapping. Due to the design of components and circular bolt patterns, single-point thread cutting in the lathe is not an option and will not be compared.

6.1.4.1 Thread Milling

Single-point cutting can be accomplished with a thread milling cutter in the CNC mill and a helical cutting path. Exact positional control of the tool allows for fine adjustment of thread depth, major and minor diameters and ultimate thread fit. Thread milling also allows the ability to thread holes nearly all the way to the bottom to increase full thread engagement. This adds considerable machining time at the benefit of flexibility and precision.

Single-point threading tools for 60-degree standard threads are widely available and thread milling is supported by CNC equipment available on campus.

6.1.4.2 Tapping

Tapping makes use of a form tool to impart the desired thread geometry into the part. Two options for tapping include thread forming taps and thread-cutting taps.

6.1.4.2.1 Form tapping

Forming taps use a zero-flute geometry that roll forms the parent metal into the thread geometry by cold working, with no creation of chips. The roll forming process by nature maintains the grain structure of the material, preventing fracture formation from discontinuities in grain structure. Further 316 stainless work hardens when cold worked, resulting in a thread form that is harder, stronger, and more durable than a cut thread.

Form tapping first requires drilling to a specified diameter before the form tap is used to roll form the threads. This initial diameter is chosen based on desired final thread engagement and is larger than the finished minor diameter of the hole, where the material is deformed into the valleys of the thread form tool and creates a smaller minor diameter. Because of the large forming forces involved in displacing the parent material, this process typically involves exerting higher forces on the cutting tool and work piece. To compensate, the roll-form tap has a very thick, rigid shank to avoid breakage. In comparison to mechanically cut or milled threads, it is very difficult to achieve high thread engagement with small threads due to the large forces required in the forming process.

6.1.4.2.2 Thread Cutting taps

Thread cutting uses a hardened form tool with many teeth that gradual cut the thread form into the parent material. Chips are formed as the tap rotates, each successive tooth cutting the thread deeper until the full thread depth is formed. Thread strength is governed by depth of the thread, limited by the strength of the tap and cutting forces required to shear off material as each tooth advances forward. The necessity of flutes to clear chips limits the strength of thread cutting taps and can contribute to breakage if excessive torque is applied. Thread cutting taps are additionally not able to cut to the bottom of a blind hole due to the tapered start and gradual cutting profile, requiring a deeper hole. Bottoming taps are available that can thread within 2-3 threads of the bottom of a blind hole, but must be started with a traditional starting tap.

Taps of all sizes are widely available and easily cut 316 stainless. The required drill diameter is found in Machinery's Handbook. Chips produced as a result of the cutting action must be cleared by retracting the tap periodically, or the flutes will clog and bind the tap in the workpiece [7].

6.1.4.3 Comparison & Selection of Threading Techniques

Table 6.1 compares the three threading techniques. The small volume of parts does not require low cycle times. Standard design practices call for the fastener to fail in tension before the threaded part does. By ISO standards the shear area of the female thread must be at least twice the tensile area of the fastener [14]. A286 fasteners have a rated tensile strength of 160 ksi and a tensile area of 0.00411 in^2 for a maximum tensile stress of 657 lbs. [13]. Provided the female thread was also A286, only 0.0547 in. of thread engagement would be required (~2 full threads). De-rating the calculation for use in 316 stainless steel threads with a tensile strength of 75 ksi requires a minimum engagement of 0.117 in. [5].

Because all threads in the design use more than this minimum number of threads, the resultant criteria of comparison are fracture resistance, durability, proximity to hole bottom, and machining considerations. Form tapping ultimately provides the most durable threads with high fracture resistance, fast machining times, and the ability to cut close to the bottom of the pre-drilled hole and is the chosen process.

Method	Relative Speed	Max Thread Depth	Proximity to hole bottom (thread pitches)	Advantages	Disadvantages	Special Considerations
Thread Milling	Slow	100%	1	Control of thread fit Low cutting forces	Slow Expensive tooling Fracture prone	Incremental testing for optimal thread fit
Form Tapping	Fast	75%	1.5	High strength Fracture resistance No chip formation	High cutting forces Limit to achievable thread depth	Chance for tool breakage is higher – testing required.
Thread Cutting	Medium	75%	3	Inexpensive tooling	Low control of thread fit Fracture prone	Tool must be retracted for chip clearing; risk of binding

Table 6.1: Comparison of threading methods

6.1.5 Waterjet Cutting

Two-dimensional features such as the welded duct caps in the LOX dome are best cut out of sheet material on the abrasive waterjet. Typical tolerances are within 0.005 in. so several iterations or post-processing of parts may be necessary to achieve a satisfactory fit with the LOX dome before welding. No special consideration is needed when waterjet cutting of stainless steel sheet.

6.1.6 Special Processes & Tools

6.1.6.1 O-ring Grooves

Specialized grooving and face grooving tools with the proper corner radius of 0.005 to 0.015 in. are required to form the grooves for proper O-ring sealing, as specified in design tables 4-2 and 4-3 in the Parker O-ring Handbook [11]. Appropriate tooling is available from Sandvik Coromant and Kennemetal.

For proper sealing the glands must have a surface finish of 32 RMS or better on the opposing seal surfaces and 63 RMS on the sidewalls (for both male glands and face seal glands). The surface finish produced by sharp and well-maintained carbide insert tools in turning operations produces concentric imperfections in surface finish which easily meet this requirement without further polishing [11].

6.1.6.2 Drills

Drilling small holes for the injector orifices and deep holes for the radial methane ducts presents significant challenges. Principally, small drills are sensitive to total runout in the holder and spindle, angular alignment of drill axis and feed axis, and feed pressure and cutting forces. Adequate lubrication and cooling is essential at the cutting tip for chip evacuation to prevent binding and to prevent overheating of the material, which dulls the cutting edge and hardens the workpiece. Flood coolant and through-spindle coolant are recommended, especially for deep drilling applications where chip clearing and cooling are paramount to avoid tool breakage and prolong tool life.

Drills for the small diameters of the injection orifices are available from Mitsubishi in the solid carbide Micro-MVS lineup, available with internal coolant holes up to 30xD depths and coatings optimized for hard materials like 316 stainless steel.

Current machines accessible on campus do not support through spindle coolant recommended for drilling of deep holes in the radial fuel ducts. While possible without through spindle coolant, Mitsubishi notes that very short pecking cycles and rapid retract is necessary which prolongs the drilling operations and increases risk of tool wear and breakage. This operation may require sending to an off-campus machine shop or significant testing.

6.1.6.3 Work holding

Alignment between various features in the injector components requires precise registration during machining setup. Several fixture plates and workholding techniques will be necessary to ensure proper alignment of component features.

A common feature on each of the manifold and the injector body itself is the circular bolt pattern of mounting screws which can be used as a locating reference on jig plates for holding in various orientations between different milling and turning operations. Careful drilling and reaming of the holes to form a close fit with the precise OD of the fixture screws ensures repeatable alignment with high rigidity.

Additionally, the part is sufficiently small that emergency collets purchased from vendors such as McMaster Carr can be machined to allow workholding while maintaining concentricity within 0.001 in. Turning centers and the 5-axis trunnion available on campus both take 5C collets for this type of setup.

6.1.6.4 Post-Weld Machining

Heat input during welding processes of the methane manifold will cause distortion in the machined surfaces of the O-ring fit. To achieve the necessary surface finishes and circularity, the O-ring sealing surfaces will be bored to final dimension after the part has fully cooled. Each machined surface will be 0.020” undersize before welding and brazing.

6.2 Welding

6.2.1 Welding Process

Welding of small stainless steel parts is best accomplished with Gas Tungsten Arc Welding (GTAW). GTAW allows fine control of heat input which is essential for heat-sensitive materials and thin workpieces subject to warping. GTAW is also usable on nearly all metals with appropriate shielding and filler material. Access to GTAW equipment is prevalent and consumable inexpensive.

6.2.1.1 Carbide precipitation

Carbide precipitation (also called sensitization) is the formation of chromium carbide in stainless steel at high temperatures (427°C to 871°C) [1]. It depletes the steel chromium content, which reduces its corrosion resistance.

Several strategies can mitigate carbide precipitation. Using chill bars and skip welding reduces the amount of time the steel's temperature is in the critical temperature range [1]. Using a low-carbon alloy (i.e. 316L instead of 316) for the base and filler material prevents carbide precipitation [2]. The part can also be heat treated after welding to re-dissolve the carbide [1]. Of these strategies, using low-carbon 316L is the most convenient for our application.

6.2.1.2 Ferrite formation

Ferrite and austenite are alternate iron-carbon microstructures which can occur in steel. The amount of ferrite in an austenitic steel is measured by the ferrite number (FN). Some amount of ferrite is required to prevent hot cracking of the weld [1], but excessive ferrite will reduce the toughness at low temperatures [3]. For cryogenic applications, a FN of 3-8 is best [3]. FN depends on the composition of the base and filler material used. It seems that 316 usually has FN < 15, but that the FN can vary from lot to lot. We should use filler sticks marked as "low ferrite" "LF" or "cryo" if available.

6.2.1.3 Preparation

Welding processing and weld strength is sensitive to inclusion of foreign materials that may burn or vaporize and cause porosity, lack of fusion, or adversely affect the base and filler metals. General guidelines for material cleaning and preparation for GTAW call for cleansing all weld areas with a strong oil and grease solvent such as acetone after abrading the surface with a stainless steel wire brush. It is also advisable to wipe down filler rods with acetone prior to use and avoid cross-contamination of abrasives used in preparation.

6.2.1.4 GTAW technique for stainless steel

Use gas backup to prevent oxidation on back side of weld. In our case this would be purging the areas on the backside of welds, most easily accomplished using an argon purge chamber since the workpieces are small.

Use the appropriate current to avoid overheating the material: 1 amp for every 0.001 inch of thickness [4].

Avoid distortion. Because of its higher thermal expansion, 316 is more susceptible to distortion than mild steel. Page 33 of [1] provides advice on avoiding distortion. The simplest approach is to place tack welds before welding. Because the work pieces are small, only a few tacks will be needed to hold fittings and caps in place.

Welds should be full-penetration to prevent entrapment of small particles and ground to a smooth finish to aid in cleaning for liquid service, if applicable [15].

6.2.2 Weld inspection

Visual inspection for fillet size, excessive warping, porosity, and oxidization should be sufficient for this application. Leak testing with water and bubble testing is advisable but may be difficult to accomplish.

6.3 Cleaning Post-manufacturing

After welding and machining processes are complete, a thorough flush with water, denatured alcohol, and finally acetone will purge the system of hydrocarbons, lubricants, solvents, and undesirable materials prior to testing. In all cases, components should be cleaned in isolation instead of relying on flushing the system with solvents which is not nearly as effective and does not necessarily wet and cleanse all surfaces. Exact cleaning procedures prior to LOX and cryogenic handling are a topic of current research to be reviewed before any manufacturing operations.

7 Strength Analysis

Strength analysis of the injector and manifolds beyond design hand calculations is a topic of ongoing research. Computer simulation with FEA is the ideal tool for this and built into SolidWorks available to members of the team. Although preliminary results look very promising, members of the team are still gaining experience with SolidWorks Simulation and review by other engineers is necessary before conclusions and design approval can take place. Ansys and OpenFOAM simulation software is also available for use.

8 Testing

The injector and manifold assembly will be subjected to leak testing under room temperature and cryogenic conditions with liquid nitrogen. Cold flow testing with water at low pressure will be done to measure the discharge coefficient of each set of orifices. Final high-pressure cold flow tests will take place with liquid nitrogen at operating pressure to assess sealing performance and atomization.

These tests can be conducted with available measurement tools. The test stand will be used as a LHS for both water and liquid nitrogen tests with appropriate cleaning before switch fluids.

9 Materials

Item	**Vendor**
316L Round Rod, Sheet, Plate	McMaster Carr, Online Metals
AN Flare Fittings	Swagelok, Hylok
PTFE O-Rings	The O-ring Store, LLC
Grafoil	Graftech, Lamons Gasket, Curtiss-Wright
A286 Bolts, Helicoils, Standoffs	McMaster Carr, Extreme Bolt
LP-250 Antiseize	McMaster Carr

Table 8.1: Materials and where to purchase.

10 References

[1] D. Kotecki and F. Armao, "Stainless Steels Welding Guide," Lincoln Electric.

[2] American Iron and Steel Institute, "Welding of Stainless Steels and Other Joining Methods," Nickle Development Institute, 1979.

[3] N. Friedrich, G. Posch, J. Tosch, J. Ziegerhofer and W. Berger, "Welding of austenitic stainless steels for cryogenic LNG applications".

[4] C. R. James and J. A. Letos, "Materials Compatability with Liquid Rocket Propellants," 1970. [Online]. Available: http://www.dtic.mil.libproxy.mit.edu/dtic/tr/fulltext/u2/866010.pdf.

[5] AK Steel, "Product Data Sheet: 316/316L Stainless Steel," [Online]. Available: http://www.aksteel.com/pdf/markets_products/stainless/austenitic/316_316l_data_sheet.pdf.

[6] D. Huzel and D. Huang, Modern Engineering for Design of Liquid-Propellant Rocket Engines, Washington, DC: AIAA, 1992.

[7] Oberg, E., & McCauley, C. J. (2012). *Machinery's handbook: A reference book for the mechanical engineer, designer, manufacturing engineer, draftsman, toolmaker, and machinist.* (29th ed.). New York: Industrial Press.

[8] R. Braeunig, Rocket Propulsion [Online]. Available: http://www.braeunig.us/space/index.htm

[9] C. Snyder, "CEARUN,". [Online]. Available: https://cearun.grc.nasa.gov/. Accessed: 2017.

[10] "Chemical Resistance Guide," in The O-Ring Store LLC. [Online]. Available: http://www.theoringstore.com/index.php?main_page=page_3. Accessed: 2017.

[11] Parker O-Ring Handbook. Cleveland, OH: Parker Hannifin Corporation, O-Ring Division, 2007.

[12] A. Laboratories, "LP-250 & LP-250F anti-seize thread & sealing compound," in Armite Lubricants, 2013. [Online]. Available: http://armitelabs.com/products/LP250_Anti-Seize_Thread.html. Accessed: 2017.

[13] "A-286 bolts," in Extreme Bolt & Fastener, 2016. [Online]. Available: http://extreme-bolt.com/a-286-incoloy-bolts.html. Accessed: 2017.

[14] "Minimum thread engagement equation and calculator ISO," in Engineers Edge, 2000. [Online]. Available: http://www.engineersedge.com/thread_strength/thread_minimum_length_engagement.htm. Accessed: 2017.

[15] National Aeronautics and Space Administration, "Safety Standards For Oxygen and Oxygen Standards," in NASA, 1996. [Online]. Available: https://www.hq.nasa.gov/office/codeq/doctree/canceled/1740151.pdf. Accessed: 2017.

Chamber & Cooling System Design

Nick Bain | 2017-02-05

This section presents the chamber geometry and cooling system design for Viper2. Due to thermodynamic inequalities between coolant heat capacity and heat flux, Viper2 isn't capable of regeneratively cooling the combustion chamber. Instead, the design involves pumping water through axial channels on the outside of an aluminum chamber coated with a thin ceramic. An optimal material choice for the combustion chamber wall was discovered to be the copper-nickel-beryllium alloy Ampcoloy 89, but manufacturing difficulty and high cost necessitate an alternative for initial testing. The water will recirculate through the coolant manifold at approximately 4 liters per second.

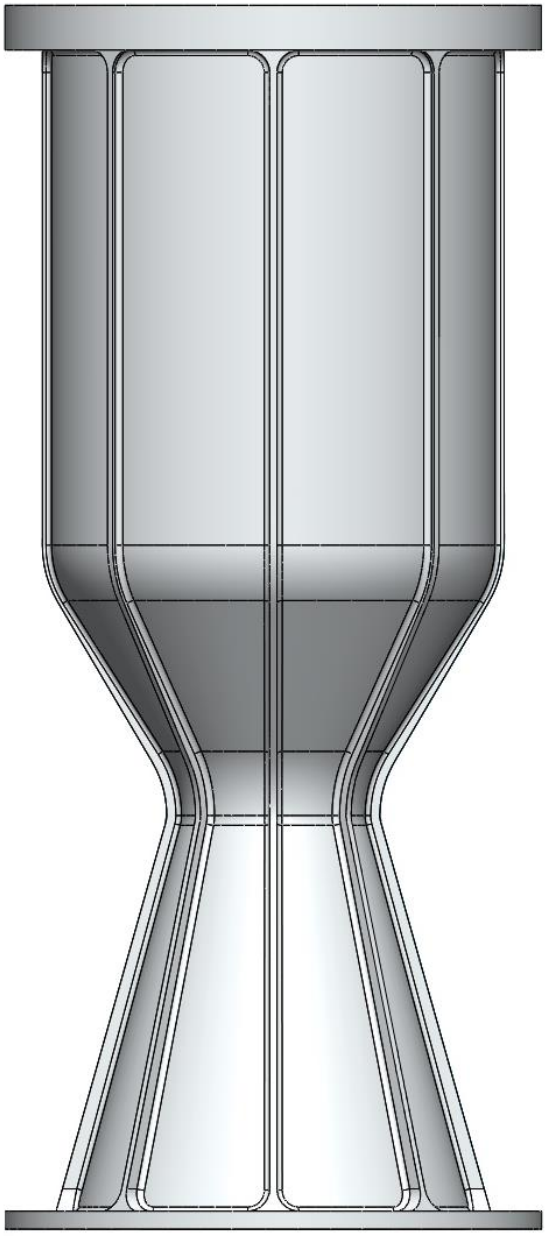

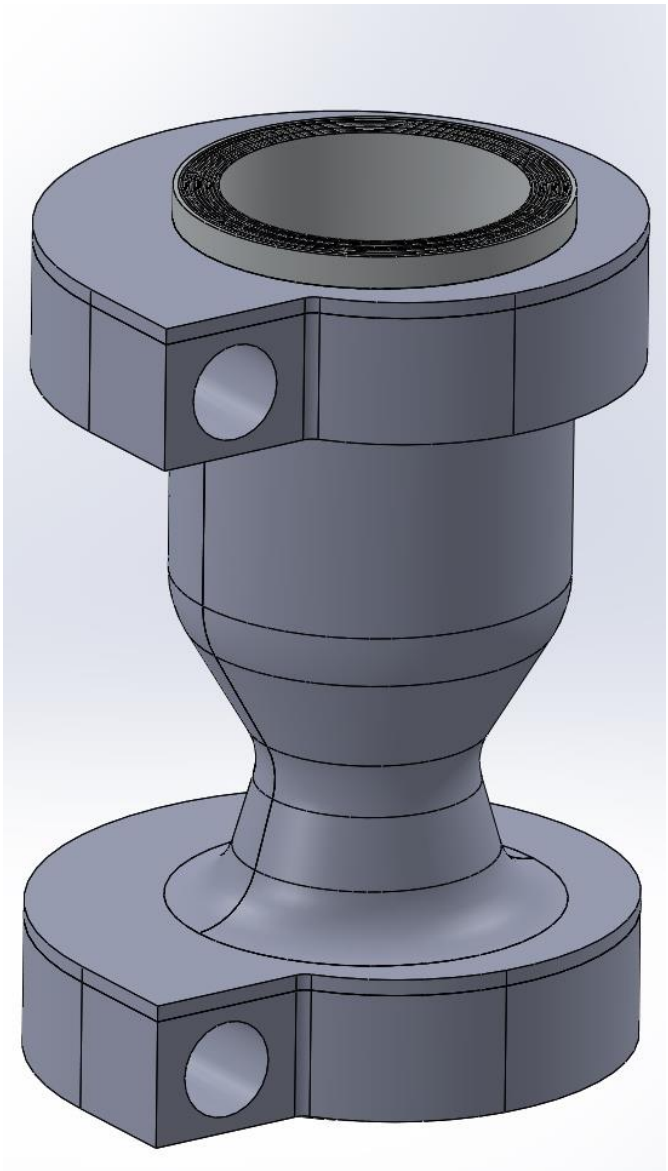

1 Combustion and Chamber Geometry

1.1 Throat and Chamber Area

The throat area is a function of chamber pressure, mass flow, and thermochemical features of combustion products. Substituting throat temperature and pressure into equation 1.26, we found throat area of the engine. (From braeunig.us)

$$A_t = \frac{q}{P_t}\sqrt{\frac{RT_t}{Mk}} \qquad P_t = P_c\left(1+\frac{k-1}{2}\right)^{\frac{-k}{k-1}} \qquad T_t = \frac{T_c}{\left(1+\frac{k-1}{2}\right)}$$

Eq. 1.26 *Eq. 1.27* *Eq. 1.28*

Thermochemical data (k, which is the specific heats ratio, and T_c, which is the chamber temperature) was calculated by NASA's Chemical Equilibrium with Applications (CEA) software. NASA CEA's inputs are chamber pressure, fuel and oxidizer selection, mixture ratio, and ambient pressure. The inputs used for these calculations are given in the Injector design section of this document.

The chamber diameter was found as a function of throat diameter using *Space Mission Analysis and Design*'s equation for chamber convergence ratio (Humble 222).

$$D_c = (8D_t)^{-0.6} + 1.25$$

1.2 Nozzle Geometry

A conical nozzle was selected over a parabolic nozzle for better manufacturability and because the geometrical differences between the two are negligible at this scale. A 15 degree half-angle was chosen based on Huzel & Huang's finding that a 15 degree half-angle is the best compromise between length and performance. The area of the exit was then computed from nozzle exit gas Mach number with the equations below. (From braeunig.us)

$${N_m}^2 = \left(\frac{2}{k-1}\right)\left[\left(\frac{P_c}{P_a}\right)^{\frac{k-1}{k}} - 1\right] \qquad A_e = \left(\frac{A_t}{N_m}\right)\left[\frac{1+\left(\frac{k-1}{2}\right){N_m}^2}{\frac{(k+1)}{2}}\right]^{\left(\frac{k+1}{2(k-1)}\right)}$$

Nozzle Exit Area Equations

1.3 Mass Flow Rate

The mass flow rate is found by solving for exhaust velocity (with outputs from NASA CEA) and rearranging equation 1.6. Because nozzle exit area is an input to this equation (which requires known mass flow), the values for mass flow and nozzle exit area were solved iteratively in Excel.

$$F = qV_e + (P_e - P_a)A_e \qquad V_e = \sqrt{\left(\frac{2}{k-1}\right)\left(\frac{RT_c}{M}\right)\left(1-\left(\frac{P_e}{P_c}\right)^{\frac{(k-1)}{k}}\right)}$$

Eq. 1.6 *Eq. 1.22*

1.4 Nozzle and Chamber Length

The nozzle length can then be found quite simply now that the nozzle half-angle, throat radius, and nozzle exit radius are known, using this diagram from Huzel & Huang.

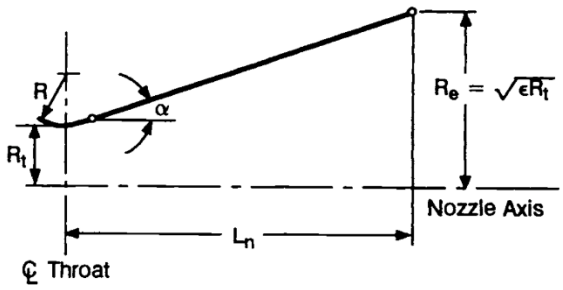

Fig. 4-12 Conical nozzle contour.

The chamber length was found as a function of throat diameter from Braeunig's experimentally derived relation equation below (Figure 1.1), and a chamber convergence angle of 30 degrees was chosen.

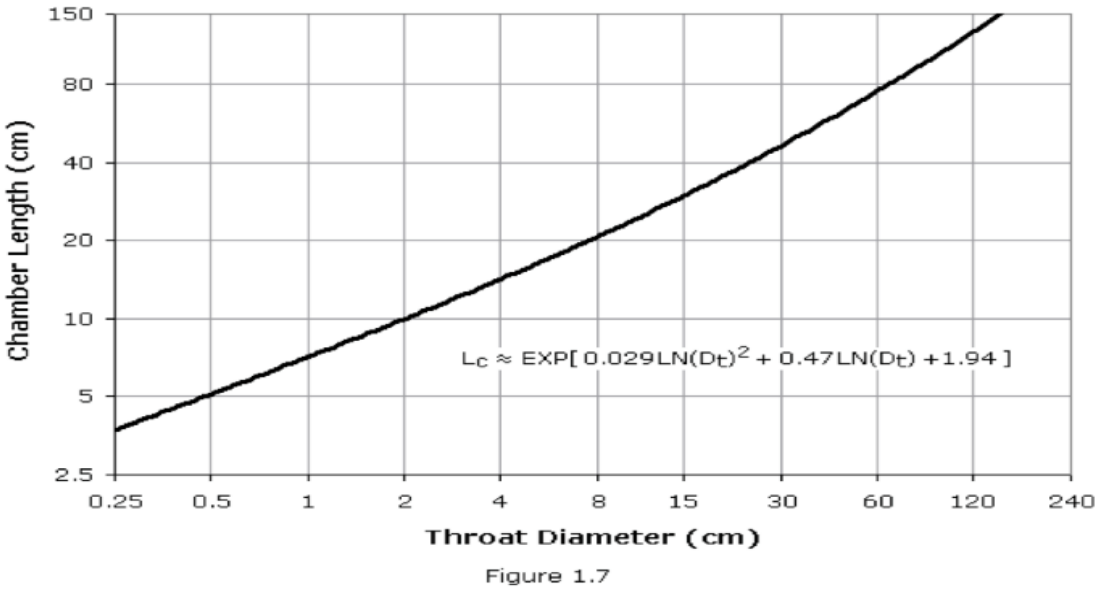

Figure 1.1: Experimentally determined relation between throat diameter and chamber length. From Braeunig.us.

The results of these equations are tabulated here:

Chamber Dia. (m)	Throat Dia. (m)	Exit Dia. (m)	Nozzle Length (m)	Chamber Length (m)	Mass Flow (kg/s)
0.05893	0.02413	0.05515	0.05788	0.10767	0.86715

Table 1.1: Results of thermodynic calculations to derive chamber & nozzle design parameters.

1.1.1. Mixture Ratio

We found the optimum mixture ratio using RPA's specific impulse vs. mixture ratio plotting tool, which yielded an optimum O/F of 2.9. This was validated using NASA CEA, which gave an optimum O/F of 3.0. Because of the negligible changes in specific impulse at optimum O/F and significant reduction in chamber temperature at slightly lower O/F's, 2.9 was chosen. Slight differences in calculation are due to variations in the semi-empirical relations used between programs.

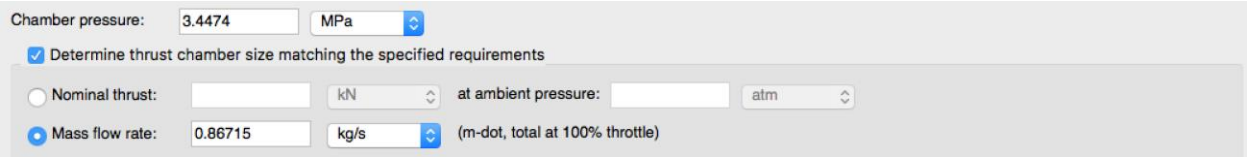

Figure 1.2: inputs to RPA's I_{sp} optimization tool.

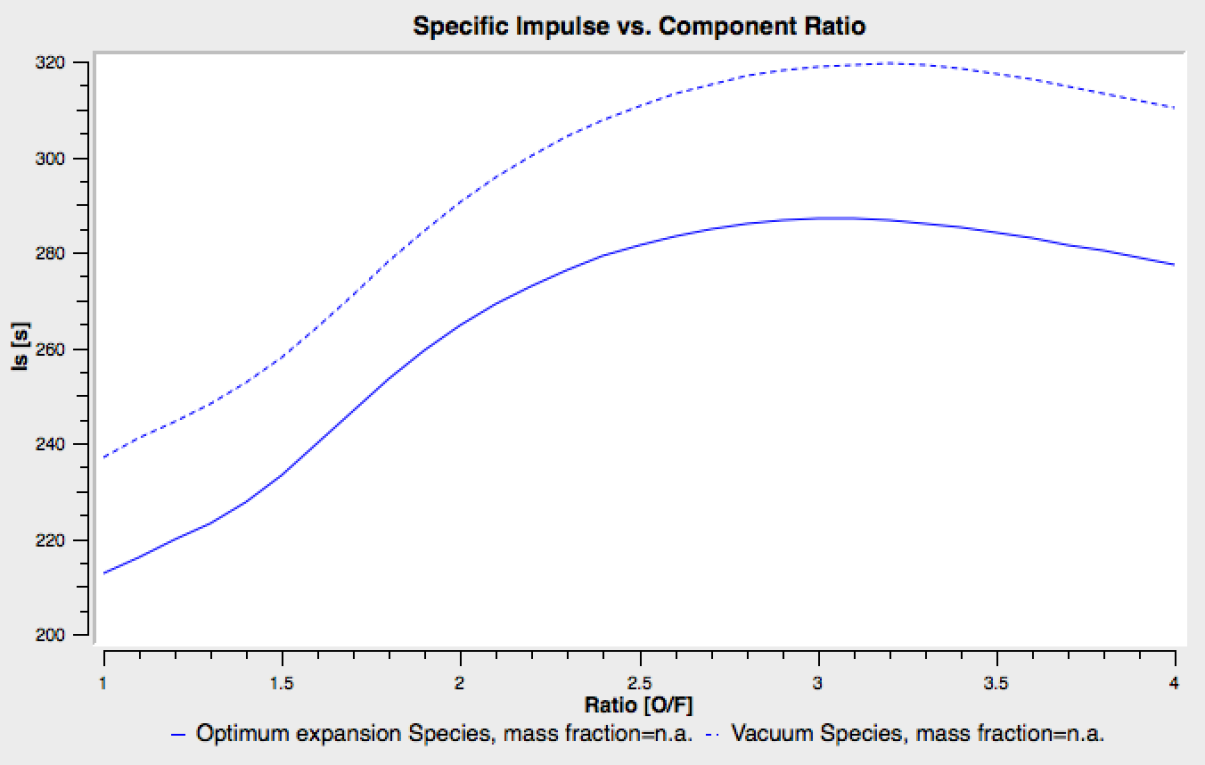

Figure 1.3: Results of I_{sp} vs O/F ratio plotted in RPA.

2 Thermal Analysis

2.1 Wall Thickness

Barlow's formula, shown below, was used to find required wall thickness at engine cross-sections, where *S* is allowable stress (the yield tensile strength of the wall material at operating temperature), *t* is wall thickness, *D* is chamber outer diameter, and P is the allowable pressure.

$$P = \frac{2St}{D}$$

In Luka Denies' *Regenerative Cooling Analysis of Oxygen/Methane Rocket Engines*, a chamber structural strength safety factor of 1.5 is used. Because this is a ground test, a minimum safety factor of 2 is met. The coolant channel ribs (discussed later) secured to the outer jacket will increase strength, but are ignored for simplicity, so a safety factor of 2 is conservative.

2.2 Coolant Selection

For this test, regenerative cooling with methane was ruled out because it is constrained by the relatively low mass flow rate going into the engine. As a result, wall temperatures are prohibitively high. The plot below shows wall and coolant temperature along the engine when methane is used. To illustrate the difficulty of using methane, this plot assumes a copper wall with the thinnest manufacturable wall thickness of 0.040" and cooling jacket pressure drop of about 400 psi. Despite these unrealistic conditions, the methane goes supercritical before reaching the throat and the wall temperature is well above the operating temperature of any copper alloy.

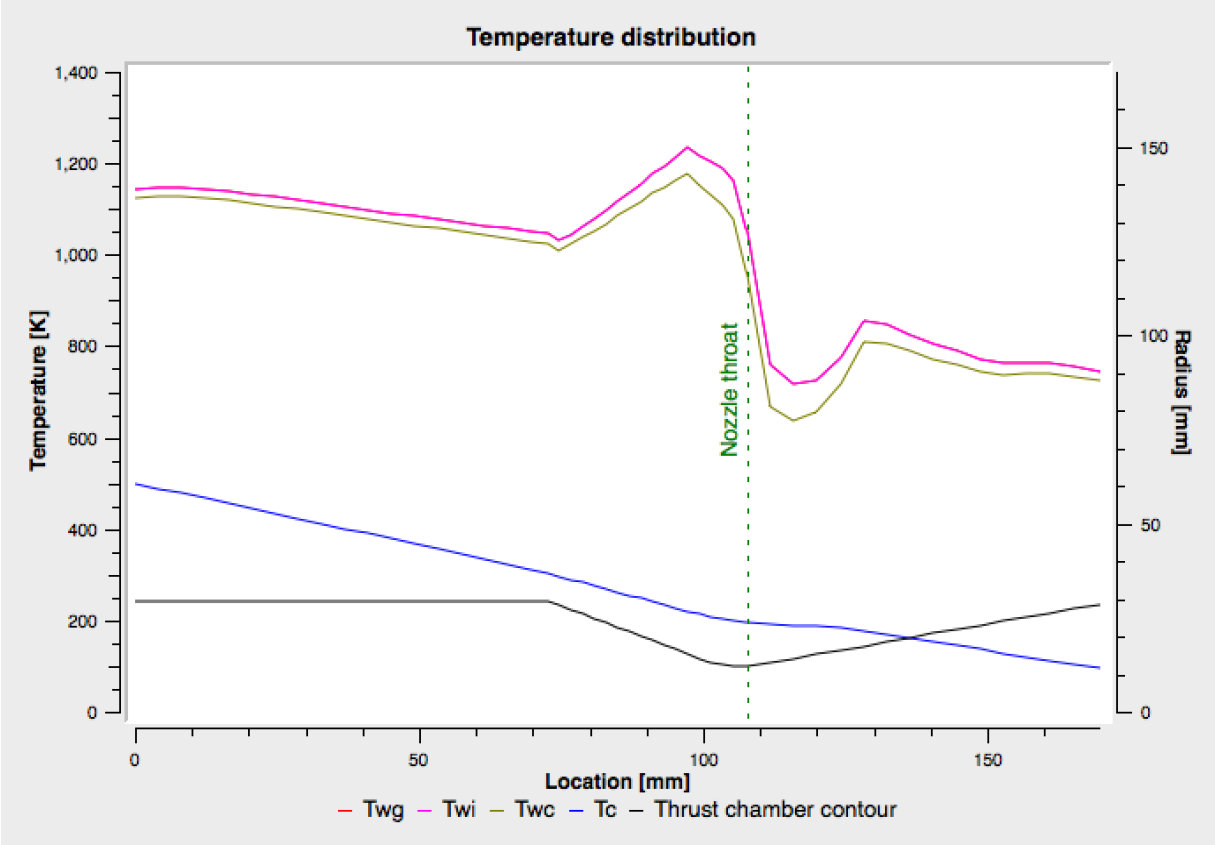

Figure 2.1: Plot of wall temperatures vs. location along the chamber wall with methane regen cooling in optimal conditions.

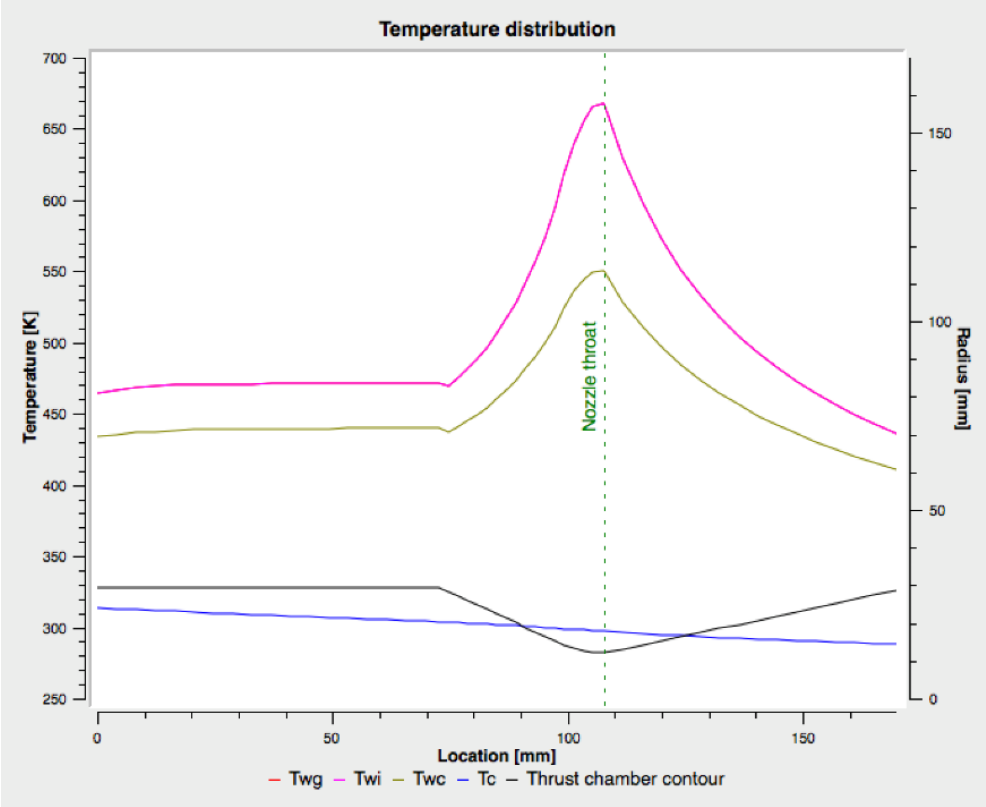

Figure 2.2: Plot of wall temperatures vs. location along the chamber wall with water cooling provided at one gallon per second.

For a ground test, a better option is water, which is not constrained by flow rate but only by the size of the pump used. The plot shown in Figure 1.5 shows the temperature profile using one gallon per second of water at a similar pressure drop through the cooling manifold.

2.3 Cooling Manifold Optimization

In the plots above, coaxial shells make up the cooling manifold. However, there are a number of ways cooling manifold geometry can be optimized to keep the chamber structure intact. Luka Denies' *Regenerative Cooling Analysis of Oxygen/Methane Rocket Engines* has a table of values showing the sensitivity of wall temperature and cooling manifold pressure drop to a range of factors:

Table 3.4: Summary of parametric analysis of generic engine

Change of	-10%		+10%	
Effect on	Δp_0	T_w	Δp_0	T_w
Wall conductivity	-0.79%	+0.14%	+0.66%	-0.12%
Number of channels	-21%	+2.3%	+31%	-2.3%
Channel depth	+37%	-6.9%	-24%	+6.7%
Wall roughness height	-3.3%	+1.2%	+3.2%	-1.1%
Coolant inlet pressure	+53%	+0.034%	-11%	-1.7%
Engine size	+2.7%	-1.2%	-5.2%	+1.2%

Figure 2.3: Tabulated sensitivity analysis of coolant pressure drop

In short, reducing temperature always incurs a pressure drop penalty, with the exception of increasing the pressure of the coolant entering the jacket. In order to reduce the pressure penalty, which can easily require prohibitively large pumps, the design should be optimized so that the structural safety factor is constant along the length of the engine. In other words, the wall temperature at every point along the engine should be the highest possible such that the material's yield strength at that temperature (after inputting into Barlow's formula with the chamber pressure and diameter at that cross-section) yields a safety factor of 2.

In uniformly spaced coaxial shells, the temperature profile is naturally highest at the throat and descends in the diverging and converging section until becoming relatively constant along the chamber, but optimization for constant safety factor causes the optimum temperature to be relatively constant from the throat to the nozzle exit and relatively constant at a lower temperature along the chamber section. The chamber must be lower temperature because of the combination of high pressure and large diameter. The nozzle throat and nozzle exit temperature are approximately the same because of the greater pressure but smaller diameter at the throat and inverse at the exit.

In order to determine this optimum temperature profile along the length of the engine quantitatively, the wall material's tensile strength vs. temperature curve must be known. To start, the wall thickness is assumed to be the smallest manufacturable thickness and then iteratively raised to optimize for lowest pressure drop. It would be theoretically possible to maintain minimum wall thickness along the chamber length, but the required pressure drop to maintain the optimum temperature profile would be unnecessarily and prohibitively high.

2.4 Wall Material Selection

The wall material should have a combination of high thermal conductivity to allow for effective cooling and high yield tensile strength at high temperature. Materials studied were specialized high-strength copper alloys (AMPCOLOY 89, Glid-Cop 15, NARloy-Z), found using matweb.com's database, searchable by yield tensile strength and thermal conductivity and also in Dinçer et al.'s "High Strength Copper Alloys for Extreme Temperature Conditions" and extensive internet research. A variety of types of Inconel, stainless steel alloys, and aluminum were also studied.

Most copper alloys become extremely ductile at relatively low temperature (around 300 Celsius), so they must be ruled out despite excellent thermal conductivity. Inconel has excellent strength at high temperature, but its extremely low thermal conductivity (about 3% of copper) forces the wall's necessary thickness (or thinness) to below what can be 3D printed or machined.

Strength vs. temperature curves for copper, aluminum, stainless steel, and nickel superalloys are shown in Figures 2.4a-d below. [3,10,11,12]

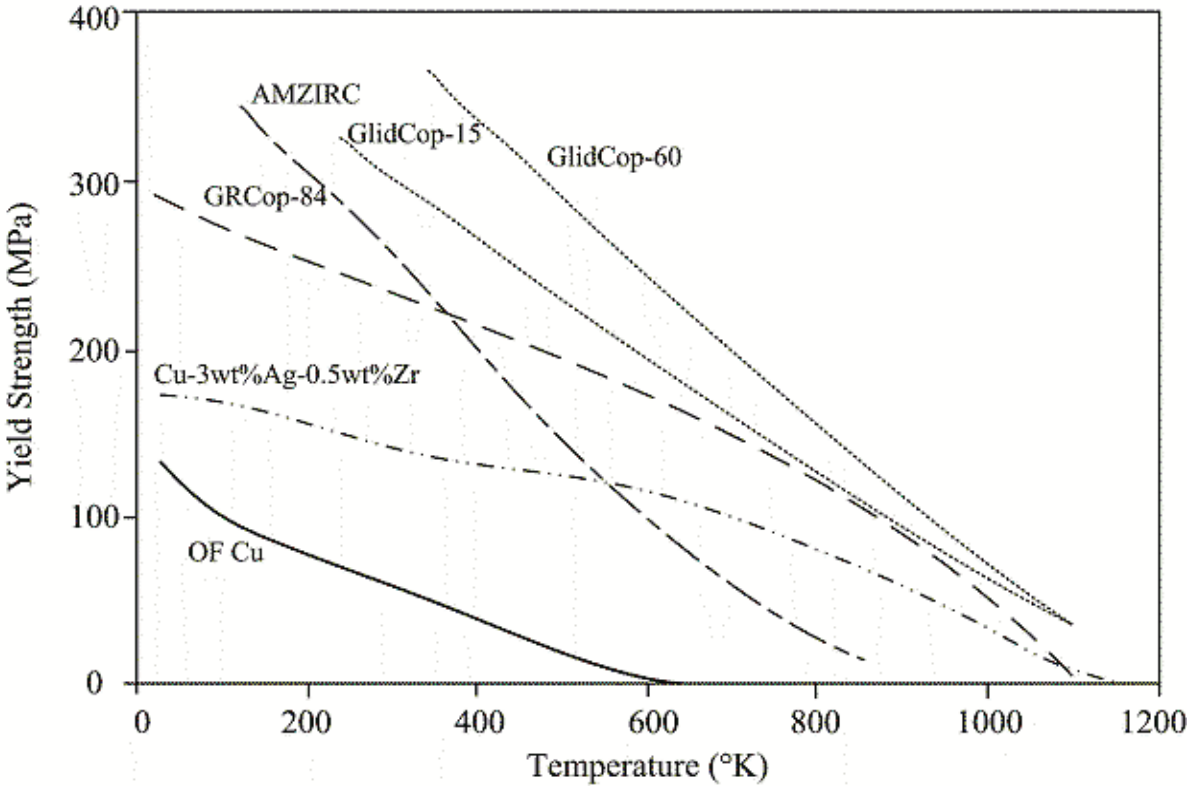

Figure 2.4a: Yield strength vs. temperature curve for high-strength copper alloys. GlidCop-15, GlidCop-60 significantly outperform oxygen free copper as a basis for comparison.

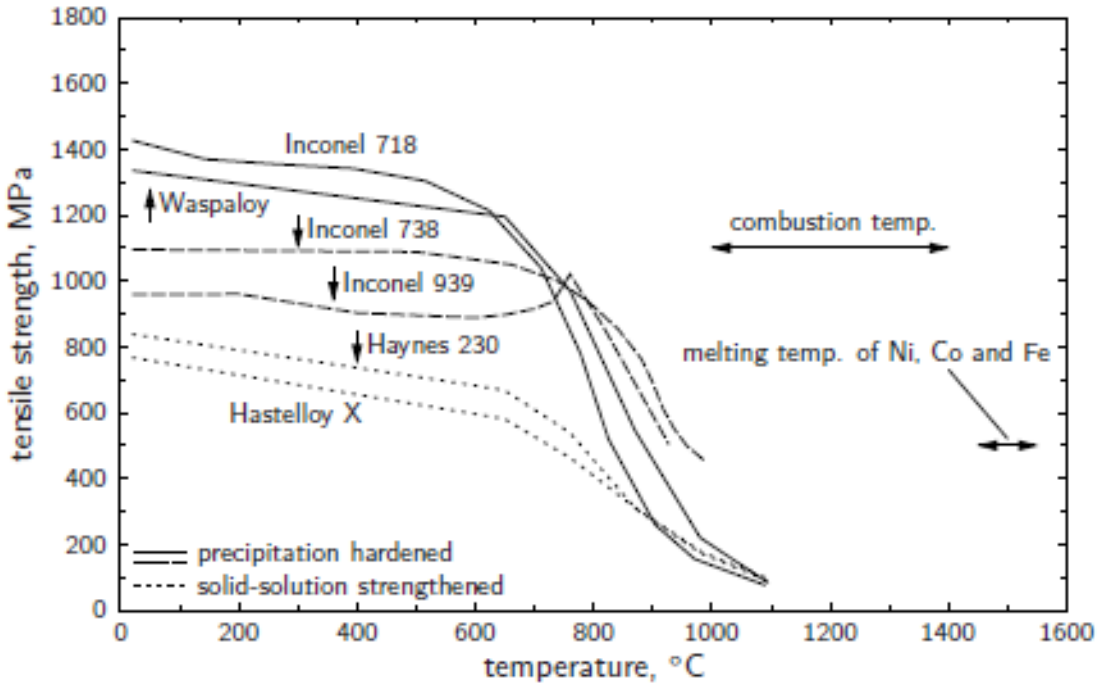

Figure 2.4b: tensile strength vs. temperature curve for high-strength nickel alloys. Inconel 718, Waspaloy, and Inconel 738 are front runners.

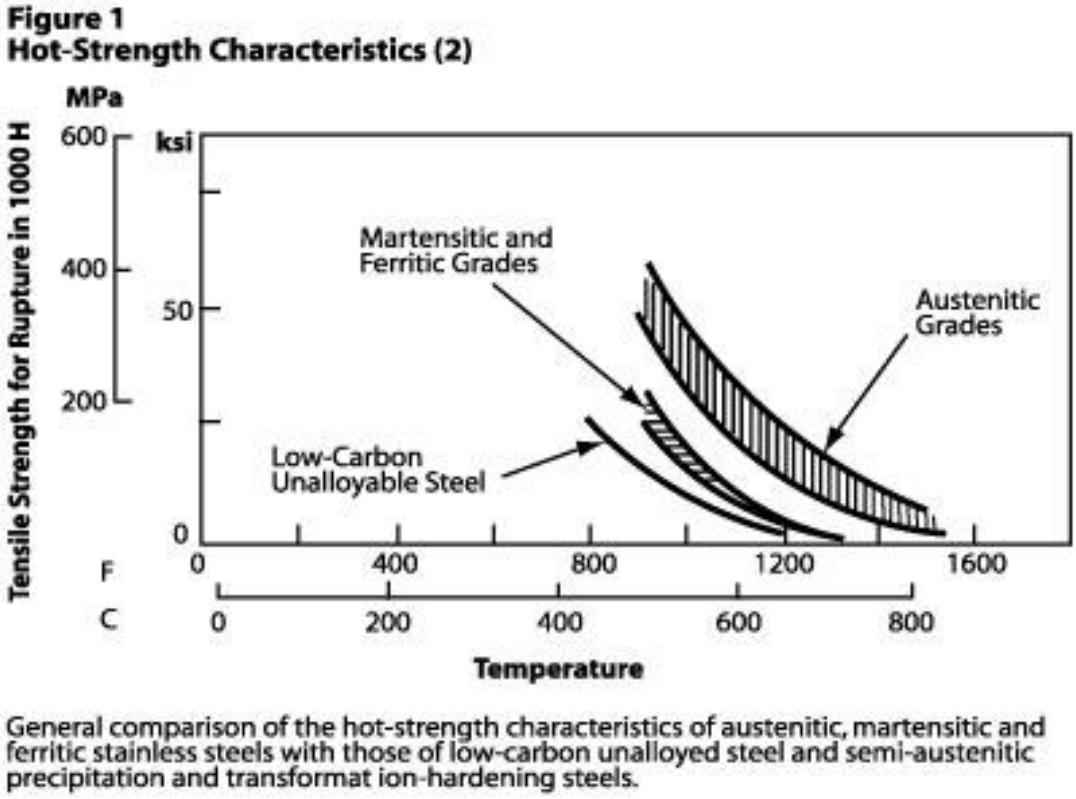

Figure 2.4c: Tensile strength vs. temperature comparison of various types of steels. Austenitic chrome-nickel alloys are notably better than Martensitic and Ferritic grades at high temperatures.

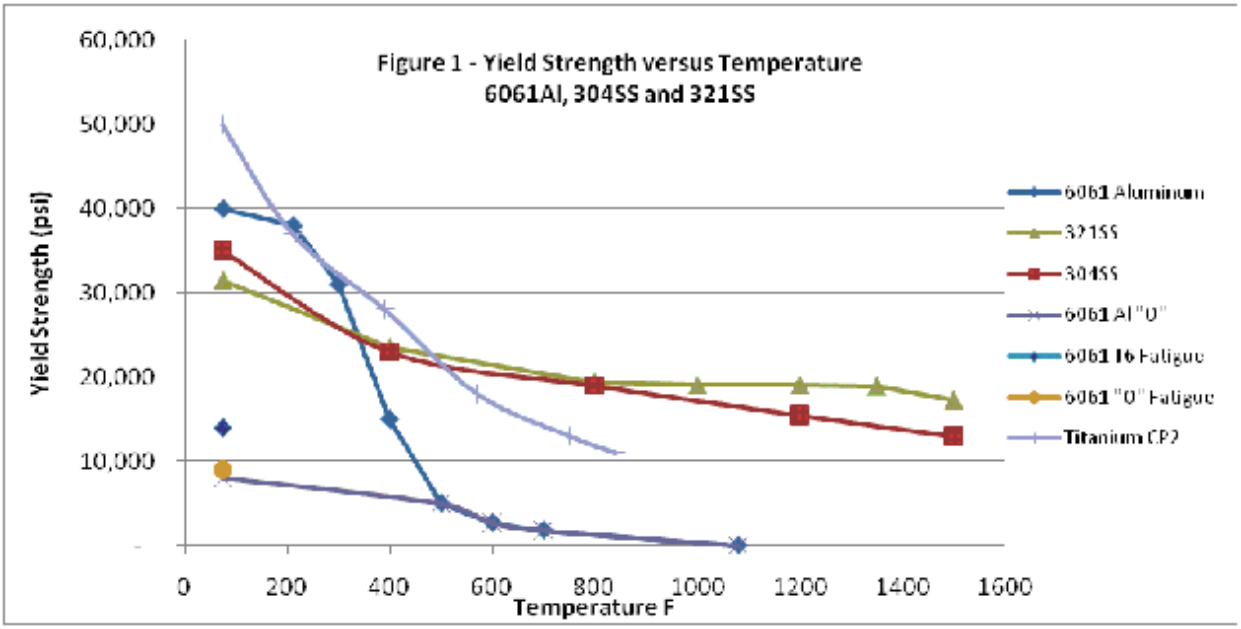

Figure 2.4d: Yield strength vs. temperature curve for aluminum alloys, stainless steels, and titanium CP2.

Stainless steel has approximately double Inconel's thermal conductivity, but is inferior for this application because its tensile strength is a small fraction of Inconel's throughout the operating regime of the engine. Despite being extremely expensive, exotic copper alloys are an excellent option. For the water-cooled test, however, finding a sufficiently large bar of exotic copper would be expensive (Ampcoloy 89 quoted at $2680) and its value would be diminished by the difficulty of machining the soft material reliably the first time along with limited or no reusability.

Aluminum is ultimately the best material for a preliminary test. Exotic copper alloys such as Ampcoloy 89 and Glidcop-15 are best utilized for the next generation engine and future flight engines. Both materials are evaluated in terms of design although aluminum 6061 will ultimately be used.

2.5 Optimum Temperature Profile

To find the optimum temperature at the combustion chamber, 480K was chosen from the tensile strength vs temperature curve of 6061 aluminum. After this temperature there is a rapid decrease in strength and is deemed the maximum working temperature. A necessary wall thickness from Barlow's formula was then found for that point. At the nozzle throat and nozzle exit, the combination of pressure and diameter are sufficiently low such that the wall thickness is limited only by manufacturability under Barlow's formula, so the allowable temperature changes as a function of allowable pressure. The parentheses in Table 2.5 indicate independent variables.

The nozzle exit is ideally under no pressure if the nozzle is correctly expanded, but a burst pressure of four times atmospheric pressure is used here in case of improper expansion or combustion instabilities. (Temperature vs. strength data from matweb.com, with linear interpolation).

At 480K	Injector Face	Nozzle Throat	Nozzle Exit
Required Wall Thickness (in.)	0.078	0.040	0.040
Allowable Pressure (psi)	(14900)	6500	2000
Allowable Temperature	(480K)	524K	644K

Table 2.5: Allowable temperatures at various locations along the chamber.

2.6 Variable Wall Thickness and Cooling Channel Depth Optimization

Of the parameters that cause change in wall temperature, channel depth is the only one that can be easily varied along the length of the engine to produce the optimum temperature profile. Using RPA, those optimum channel depths are found at different flow rates by iterating depth until the desired temperature is reached. Table 2.6 also shows the roughly inverse relationship between flow rate and pressure drop.

Flow Rate (gal/s)	Channel Depth at Injector Face (in.)	Channel Depth at Nozzle Throat (in.)	Channel Depth at Nozzle Exit (in.)	Resulting Pressure Drop (psi)
1	0.035	0.080	0.550	208
2	0.070	0.145	1.20	113
3	0.110	0.210	1.450	73

Table 2.6: Optimum cooling channel depths and coolant pressure drop to achieve optimal temperature profile at various coolant flow rates.

2.7 Ceramic Barrier

With aluminum, the pressure drop to maintain necessary wall temperatures is prohibitively high without a ceramic thermal barrier on the inside of the chamber. Rescor 760, a zirconium ceramic manufactured by Cotronics with an extremely high allowable temperature (2500K) was chosen to illustrate the feasibility of the system. The zirconium ceramic coating has a thermal conductivity of only 0.93 W/m-K, so the maximum layer thickness to prevent overheating of the ceramic is 1.5mm.

With that barrier and the channel depths found above, the following temperature profile is achieved.

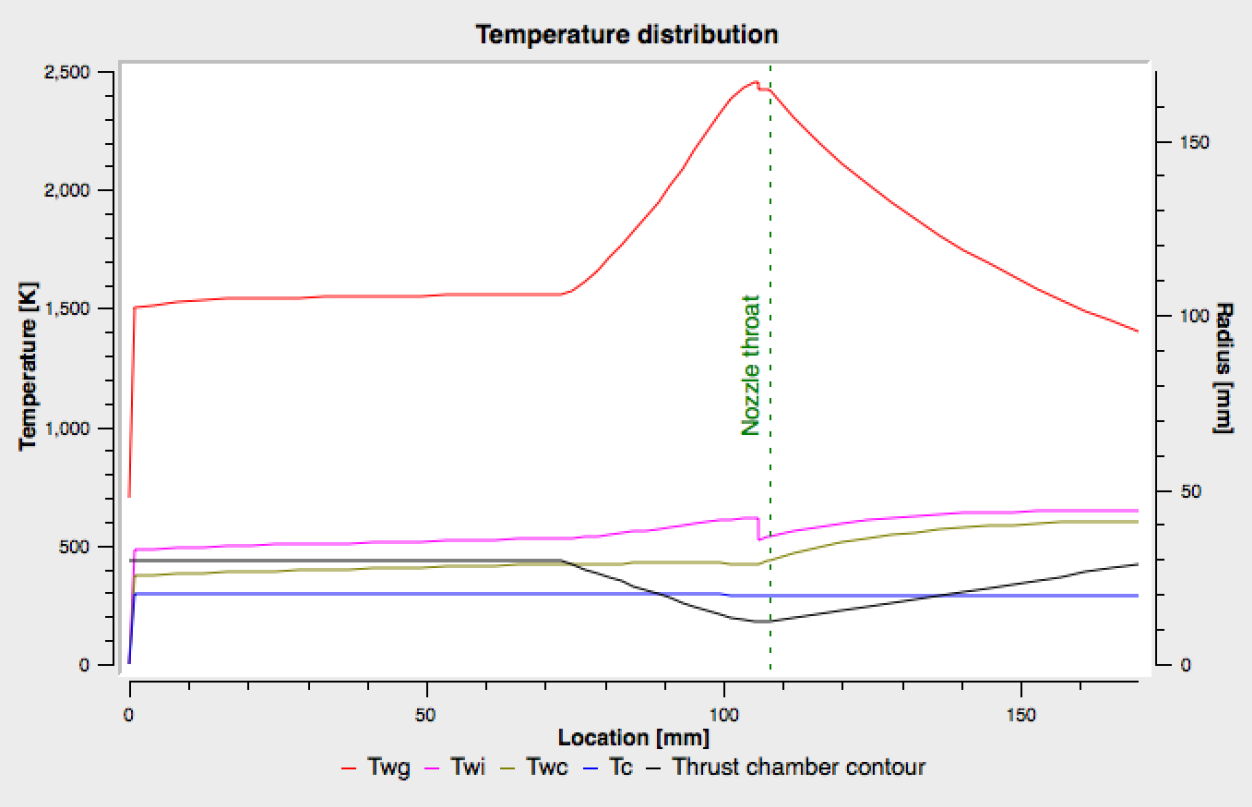

Figure 2.7: Temperature profile with aluminum chamber and ceramic thermal barrier.

(Note: the drop at the throat is due to RPA's inability to shift gradually from one wall thickness to another across the converging section)

2.8 Number of Channels

A greater number of channels increases pressure drop in the cooling manifold while decreasing wall temperature. The design is optimized when the fewest number of channels can cool the chamber. In this case, six channels are used. The changing channel width is a result of changing circumference and a constant rib thickness, which is 0.04" and limited by machinability. The constant channel number along the engine means that the channel width is smallest at the throat, and therefore has the best cooling performance at that point where fluid velocity is highest.

2.9 Chamber Jacket

The chamber material must have an outer shell to form the enclosed fluid ducts and force coolant upt he channels. The proposed design uses two half-shells of aluminum CNC milled to fit the contour of the ribs very closely and extend the length of the chamber. These shells each have a coolant port at the top and bottom of each channel to allow coolant to pass through the system. Once machined, the two haves are carefully aligned around the chamber and welded in place to form an enclose manifold.

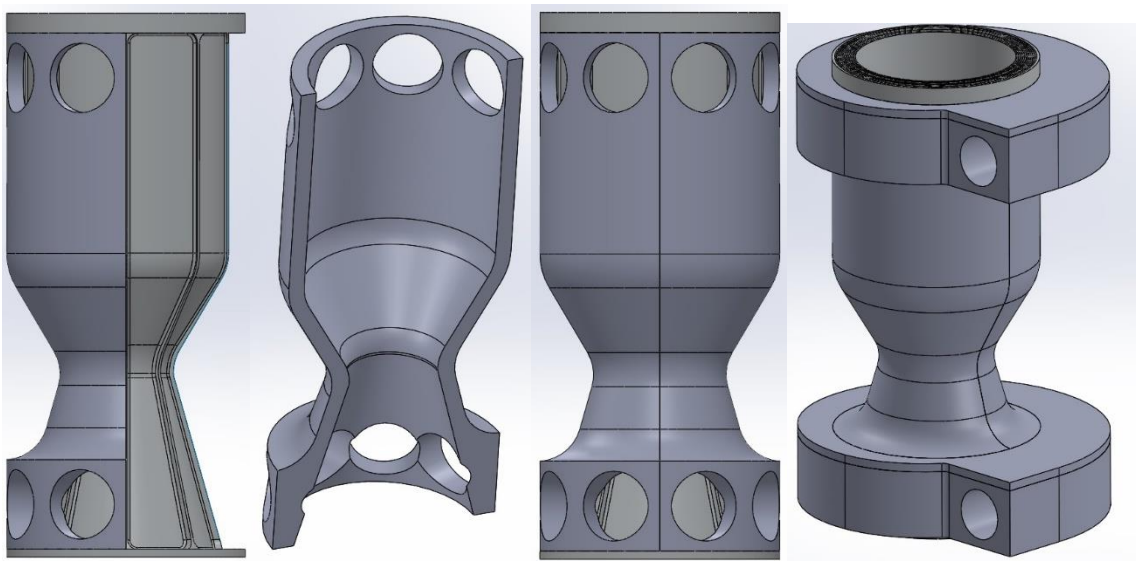

Figure 2.8: From left to right – chamber with half jacket, isolated jacket half-shell, assembled jacket on chamber, chamber assembled with manifolds.

Two circumferential spiral manifolds machined out of aluminum plate connect all the channels together at the top and bottom to provide a single inlet and single outlet for the water recirculation system. The shape of these manifolds spirals to evenly distribute mass flow among all the fluid ducts as it circles around the chamber. These manifolds are shown in the right-most image of Figure 2.8.

2.10 Water Pumps

To simplify and remain conservative, the approximate pressure vs. flow rate curve of a pump is linear with a y-intercept at maximum head pressure and x-intercept at maximum flow rate. To stay in an efficient operating regime, the water pump for the engine should have approximately 230 psi of maximum head pressure and a maximum flow of four gallons per second, or some similar combination with any drop in maximum flow rate made up for by a head pressure increase. Figure 2.9 shows a possible pump, though many variations exist and this one, the HH-80, is more powerful than necessary.

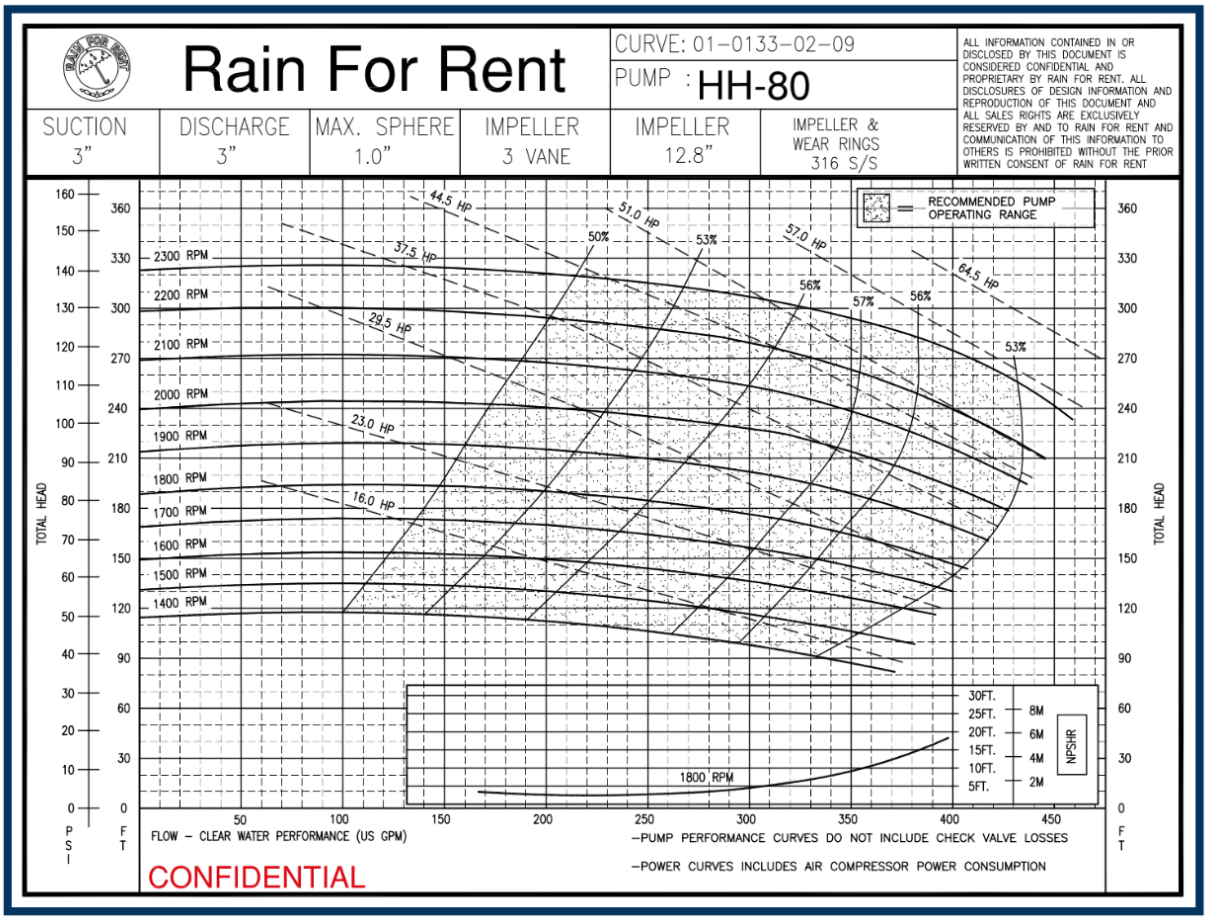

Figure 2.9: Prospective water pump for cooling Viper2 in aluminum chamber configuration.

It is possible to rent pumps by the day or week, usually with a charge for delivery and pickup (one quote from “Rain for Rent” estimated $350 each way and $1,200/week. Other companies, like Sunbelt, charge $50-$90/day).

These companies also provide the appropriate hosing, fittings, and reservoirs. The water, after leaving the cooling manifold, will return to the reservoir for recirculation. To avoid any debris that may enter the reservoir, a filter will be fitted onto the hose before the water enters the cooling jacket.

One concern is that the water will freeze in the cooling jacket before the engine starts because of its proximity (0.3 inches) to the reservoir of liquid methane in the injector. Given that the coolant channels are oriented axially, however, this seems unlikely at first approximation because the cool water near the stainless steel will be replaced by warmer water traveling up the engine. However, this can be ascertained without actually firing the engine and, if problematic, it would be possible to mix methanol with water in a 50/50 ratio to achieve a freeing point of -37 Fahrenheit or in a 70/30 mixture to achieve a -64 degree Fahrenheit freezing point (Martinez). Though the heat capacity of methanol is about half that of water, the coolant temperature delta through the jacket is very small (about 4°K at 3 gallons/second), so its much lower viscosity would increase the solution’s effectiveness as a coolant.

3 References

[1] Luka Denies, “Regenerative Cooling Analysis of Oxygen/Methane Rocket Engines” 2015. [Online]. Available: http://repository.tudelft.nl/islandora/object/uuid:90c8d527-7214-47ac-8a0b-0f03c40625cc?collection=education

[2] Ampco Metal, “Ampco Alloys Data Sheet," [Online]. Available: https://www.ampcometal.com/documents/datasheets/ampco_alloy_brochure.pdf

[3] O. Dinçer, M. Kaan Pehlivanoglu, and A. Dericioglu, “High Strength Copper Alloys for Extreme Temperature Conditions," [Online]. Available: http://www1.metalurji.org.tr/immc2016/693.pdf

[4] G.P Sutton and O. Biblarz, *Rocket Propulsion Elements.*

[5] D. Huzel and D. Huang, Modern Engineering for Design of Liquid-Propellant Rocket Engines, Washington, DC: AIAA, 1992.

[6] R. Braeunig, Rocket Propulsion [Online]. Available: http://www.braeunig.us/space/index.htm

[7] R. Humble, *Space Propulsion Analysis and Design.*

Ignition System

Matthew Campbell | 2017-02-04

1 System Overview

The proposed ignition system for the Viper2 engine is composed of a COTS GOX/MAPP blow torch attached to a rubber tube to a consumable igniter assembly inserted into the engine. The igniter assembly contains a narrow copper tube that acts as a nozzle for mixed GOX/MAPP gas delivered from the torch handle. Ignition of the gases at the end of the copper tube is piloted by a 20 gauge nichrome wire coil, using the copper tube as one conductor and 14 gauge solid core wire as the other. The igniter assembly is mounted on a FR4 plate with connectors for the gas line and power for the nichrome. This FR4 plate is compliantly affixed to the test stand with spring clamps for easy ejection from the engine and replacement after each test.

2 Theory of Operation

Both the GOX and MAPP gas tanks will each have a COTS pressure regulator (PR-A, PR-B) and solenoid valve (SV-A, SV-B) spliced between the regulator and the torch handle, allowing remote control of the fuel flow to the igniter assembly. The torch handle properly combines and mixes the two gasses into a single fluid stream which flows through a rubber tube to the igniter assembly inserted into the engine. The mixed gas flows up the copper tube and is ignited by nichrome at the tip. Upon ignition of the engine, the combustion will expel the igniter assembly from the engine.

-

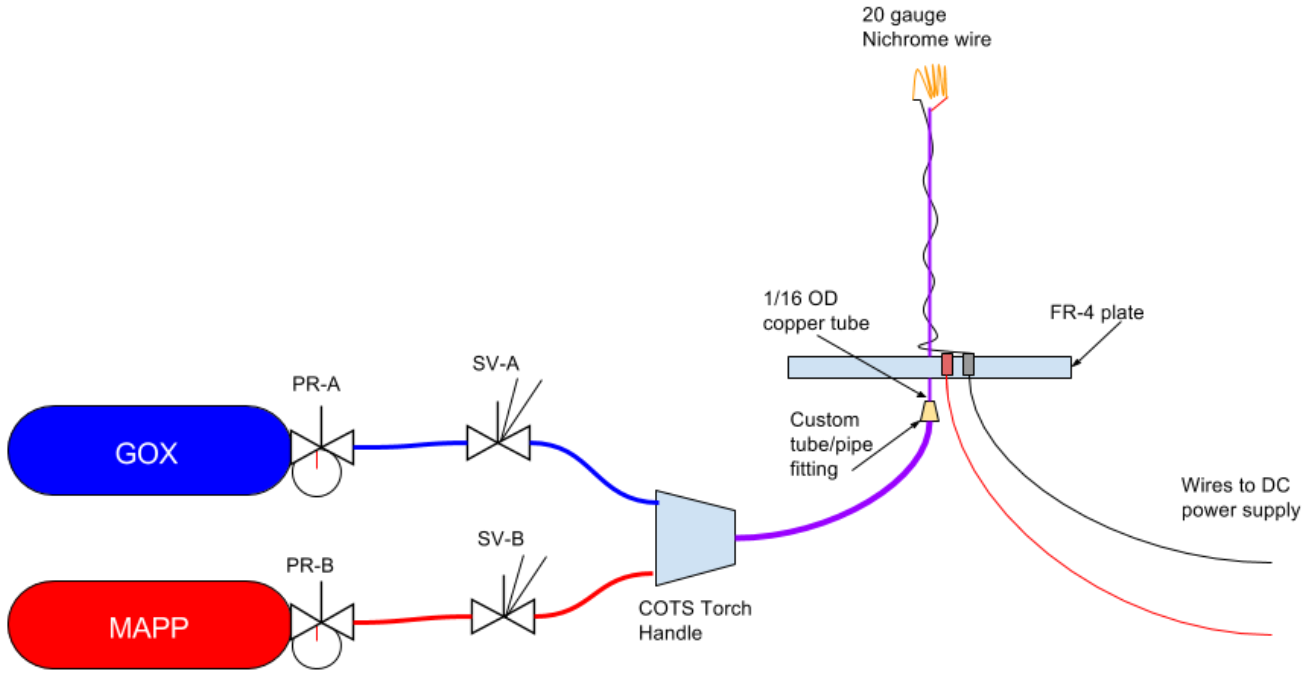

Figure 1: Ignition system schematic

3 Requirements

Table 3.1 details the requirements for the ignition system.

Igniter Requirements	Solution & Justifications
The ignition system shall provide sufficient energy to ignite cold propellants injected into the engine.	A similar igniter setup has worked reliably for a similar, but smaller engine (Lawn Dart by Tesla STEM High School in Redmond, WA). An increase in igniter propellant flow may be required for this larger engine.
The ignition system shall be robust enough for multiple ignition attempts or consist of easily replaceable consumables.	The only consumable part of the proposed system is the inexpensive igniter assembly. The torch handle, bottles, and regulator can all be used multiple times.
The ignition system shall be operated remotely from a safe distance of 500'.	The two solenoid valves and the nichrome wire are connected to relays operated by the control box.

Table 3.1: Requirements and Justifications

4 Propellant Selection

4.1 Fuel

The fuel proposed for this ignition system is MAPP gas commonly used for high temperature blow torches and is easy to obtain in small bottles at hardware stores. MAPP gas was chosen over propane or propylene because its flame is hotter and presents more energy in the combustion chamber. Energetic fuels like acetylene require more expensive and complicated equipment, and come in bottles larger than necessary for this system. If more ignition energy is needed, a system based on industrial gas bottles and regulators will be evaluated.

Gas	MAPP	Propane	Propylene
Flame Temperature (°K)	3200	3070	3140

Figure 4.1: Fuel comparison chart

4.2 Oxidizer

All values in the above chart compare fuels while oxygen-fed. Oxygen-fed combustion was chosen because it is almost 50 percent hotter than burning in atmosphere and can burn continuously inside the restricted volume of the engine [2]. The extra thermal energy available from these choices contributes to a higher chance of successful ignition.

5 Consumable Igniter Assembly

5.1 Tube Material

The material of the igniter tube was chosen because copper has a high melting point of approximately 1100°C. Prior experience with brass and copper tubes revealed the flame temp was sufficiently hot enough to melt brass after a few seconds, while copper was unaffected. Small diameter copper tube is manufactured by K&S Metals and sold by a number of online retailers, including McMaster Carr.

The narrow tube diameter increases the flow velocity of the mixed gases above the flame speed to prevent combustion inside the tube. Also, a thin design is necessary because it should fit easily inside the engine chamber with the lowest propensity to get caught during ejection after ignition. The tube is retained to the base plate with small shaft collars available from McMaster Carr.

5.2 Nichrome

20 gauge nichrome wire was chosen to light the fuel because it can sustain high temperatures for a reasonable amount of time. Using an online calculator for nichrome voltage, current, and temperature, 4.125 in. of 20 gauge nichrome wire supplied with 3.2V and 14.1A will reach about 925°C [1]. This temperature was deemed adequate because GOX/MAPP torches can be lit with a match which has a flame temperature of 600-800°C [4].

5.3 Baseplate material

The baseplate must be electrically insulating and withstand elevated temperatures to handle sustained ignition of the torch as heat conducts through the copper tube. FR4 is an inexpensive material easily cut and formed by available tools.

5.4 Plumbing & Wiring

The MAPP and GOX bottles attach directly to regulators provided with the COTS torch assembly. The short rubber tubing that leads to the torch handle will be cut and the normally-closed solenoid valves spliced in line to control flow of the propellants to the torch assembly.

The gas connection between the copper tube in the consumable igniter assembly and the torch handle is accomplished through a small rubber tube. The existing torch nozzle will be removed and fitted with a custom tube adapter. This intermediate tube between the COTS torch and the copper tube effectively extends the nozzle away from the torch handle, solenoid valves, and propellant tanks that should remain well protected from the engine under test.

The copper tubing acts as one conductor, connected to banana jacks panel-mounted to the FR4 with solid core wire. A secondary 14 gauge solid core will be heat shrunk to the copper tube and run alongside to provide the second electrical connection to the nichrome coil. 14 gauge wire is sufficiently large to carry the current of the nichrome and stiff enough to support the coil above the copper tube. Banana jacks permit easy replacement of the consumable igniter and are inexpensive enough to build many igniters at a reasonable cost.

6 Electrical & Control Requirements

The nichrome wire will need 3.2V and 14.1A DC from the power supply to run at the desired temperature. The solenoid valves will need 12V DC and 15W each, for a total of 2.5A. Each control relay should be normally open to prevent any excitation when not in use.

7 Risks/Mitigations

Risks	Mitigation
Lack of energy to light the fuel.	The amount of energy released by the GOX/MAPP combustion is estimated to be enough to light the fuel, supported by previous experience with a similar igniter and engine. If more energy is required, the proposed system can be adapted to work with higher gas flow and more energetic gases.
Open-loop control without visual feedback of igniter function	Repeated testing of each consumable assembly to find a repeatable design will be necessary. Each assembly is robust enough to withstand short duration tests without damage. Audio feedback from cameras at the test stand should be able to hear the torch burning inside the chamber.
Propellants are susceptible to environmental hazards (heat)	MAPP gas exists as a liquid at room temperature when in the pressurized canister, but elevated environmental temperatures change the mixture ratio of the torch and affect reliability. This can be mitigated with insulation of the MAPP cylinder to prevent large temperature swings, if necessary.
Igniter could cause damage to other components on or near the test stand.	Solenoid valves will be turned off after engine has started to avoid unwanted fire damage. All important components will be kept up away from the test stand and out of the firing zone.

Table 7.1: Risks and mitigation

8 References

[1] Jacobs-Online, “NichromeCalc” [Online]. Available: http://www.jacobs-online.biz/nichrome/NichromeCalc.html

[2] The Engineering Toolbox, “Flame Temperatures Gases” [Online]. Available: http://www.engineeringtoolbox.com/flame-temperatures-gases-d_422.html

[3] About.com, “Flame Temperatures Table” [Online]. Available: http://chemistry.about.com/od/firecombustionchemistry/a/Flame-Temperatures.htm

[4] Derose, “Flame Temperatures” [Online]. Available: http://www.derose.net/steve/resources/engtables/flametemp.html

Thrust Valve Actuator

Philip Phan | 2017-02-04

1 Overview

This section outlines the thrust valve actuator for the Viper2 engine test stand.

1.1 Design Requirements

The purpose of this system is to control the flow of fuel and oxidizer into the combustion chamber. The requirements for the system are as follows:

- The design must allow for the control of parameters such as opening speed and relative timing in order to aid in the development of a reliable start up sequence.
- All components must be able to work properly in cryogenic temperatures and be material compatible with propellants
- Incorporate reliable instrumentation to capture opening sequence of the valves at 100 Hz.
- The system must be as reliable as possible to reduce chances of inadvertent valve actuation and/or loss of control that can present a significant safety hazard.

1.2 Design Overview

A general diagram of the system is provided below in Figure 1.1.

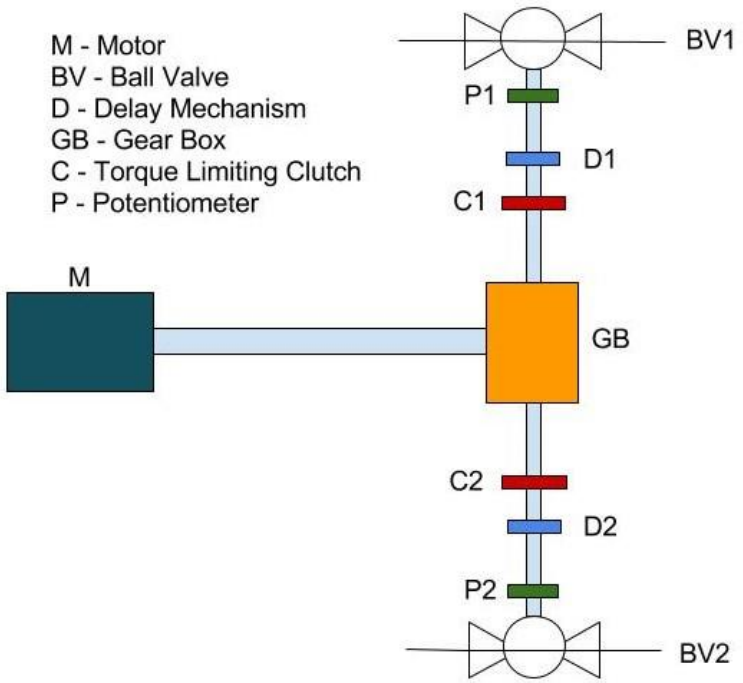

Figure 1.1: Diagram of the thrust valve actuator system.

A 12-24V motor controlled by a variable power supply will drive a shaft connected to a right angle gearbox. The gearbox will then actuate two ball valves that control the flow of fuel and oxidizer.

Between the gearbox and ball valves will be a delay mechanism to control the relative timing of the oxidizer and fuel. Torque limiting clutches will also be implemented to prevent any damage to the ball valves due to over actuation. Lastly, potentiometers placed right before the ball valves will measure how much the valves have been actuated.

1.2.1 Lead/Lag Mechanism

Figure 1.2 details a model of the lead/lag mechanism that will be used in the valve actuator.

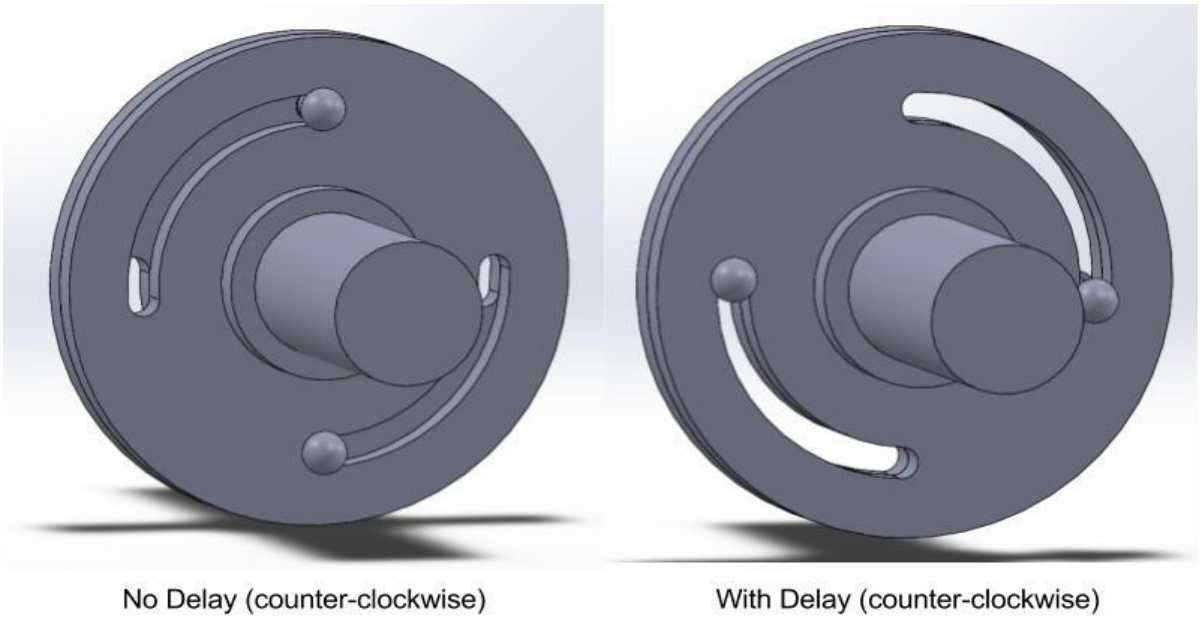

Figure 1.2: the angular delay mechanism controls the clocking of the valves with respect to each other.

A mechanical delay mechanism was chosen over an electrical one in order to minimize the number of issues that could potentially rise due to using electronics and software controls. A delay will be added to both outputs leading to the ball valves, giving us more control over which fluid will lead or lag entering the chamber.

1.2.2 Cold Temperatures

With cryogenics flowing through part of the system, nearly all of the components will be exposed to extremely cold temperatures. As a safety precaution for the motor and gearbox, the delay mechanism will be fabricated with a suitably insulating material to reduce thermal conductivity and optimized to reduce thermal transfer to rotating mechanical components. Stainless steel and titanium are two excellent materials for thermal insulation properties, with conductivities between 12 and 30 W/m-K depending on the alloy.

Another material choice to consider is Torlon, which exhibits exceptional mechanical and thermal insulating properties. By using a plastic rather than a metal components, the Torlon will add a substantial layer of thermal insulation to the motor with a thermal conductivity of only 0.26 W/m-K. Torlon could be implemented as an insulating washer between the delay mechanism flanges or as a shaft coupler on each side.

1.2.3 Slip clutches

To prevent any damage to the ball valves due to over actuation, two torque limiting clutches will be implemented. Both limiters will be placed between the gearbox and each ball valves. Whenever each ball valve reaches the limits of actuation, whether it is leading or lagging, the torque limiter slips to prevents the ball valves from excessive force. This means the motor can run continuously without any worry of damage to the system. Although this may seem very inefficient, it removes the need for a limit switch, which would have added another point of failure due to electronics. There is also a wide range of adjustability available by using a variable torque clutch and restricting the range of motion of each valve by a few degrees.

1.3 Component Selection

1.3.1 Ball Valves

One of the most important figures when it comes to choosing a ball valve is its flow coefficient, denoted as C_v. For our purposes, we needed a ball valve that could handle approximately 0.565 L/s of liquid oxygen flowing through its orifice with a maximum pressure drop of 5 psi. Using the following equation we calculated that we would need a valve with a C_v of at least 4.278.

$$C_v = Q\sqrt{\frac{SG}{\Delta P}}$$

$$Q = Rate\ of\ flow = 0.565\ Liters/Sec = 8.9554\ Gal/Min$$

$$SG = Specific\ Gravity = 1.141$$

$$\Delta P = 5\ PSI$$

Additionally, the ball valves have to be compatible with liquid oxygen. Although most ball valves are not rated for temperatures as low as that of liquid oxygen, they will be able to work as long as the materials that make them up are LOX compatible and cryogenic testing takes place before use. Using "Material Compatibility with Liquid Rocket Propellant," a document written by the Boeing Company, we picked ball valves that met these design requirements.

Below is a table of the valves that were chosen. Valves with close to a 1/2 in. nominal fitting size were selected to fit the rest of the components in our system.

Valve	Size	C_v	Seating Material	Packing Material	Fitting	Cost (USD)
SS-45TS8-T	1/2 in	12	PTFE	PTFE	Swagelok	264.20
SS-63TS8-T	½ in	7.5	PTFE	PTFE	Swagelok	222.22
B8VH-8T-UV-S316	½ in	12	PTFE	PTFE	Hylok	Unknown
8A-MB8LPFA-SSP	½ in	10.7	PTFE	PTFE	A-Lok	261.36

Table 1.1: Comparison of suitable ball valves.

Out of the four valves listed above, the Swagelok SS-45TS8 was ultimately chosen due to the documentation provided online. One of the biggest unknowns in designing this system is trying to figure out how much torque is required to open each ball valve. The SS-45TS8 is the only ball valve that has enough documentation to provide us with a reasonable estimate of how much torque would be required.

1.3.2 Motor, Gearbox, and Torque Limiter

In order to determine which motor, gearbox, and torque limiter we require, the torque needed to actuate the selected ball valve must be known.

Swagelok provides data points in order to determine how much torque is required to begin turning 40 series ball valves. Using these data points, linear extrapolation is used to conservatively determine torque requirements.

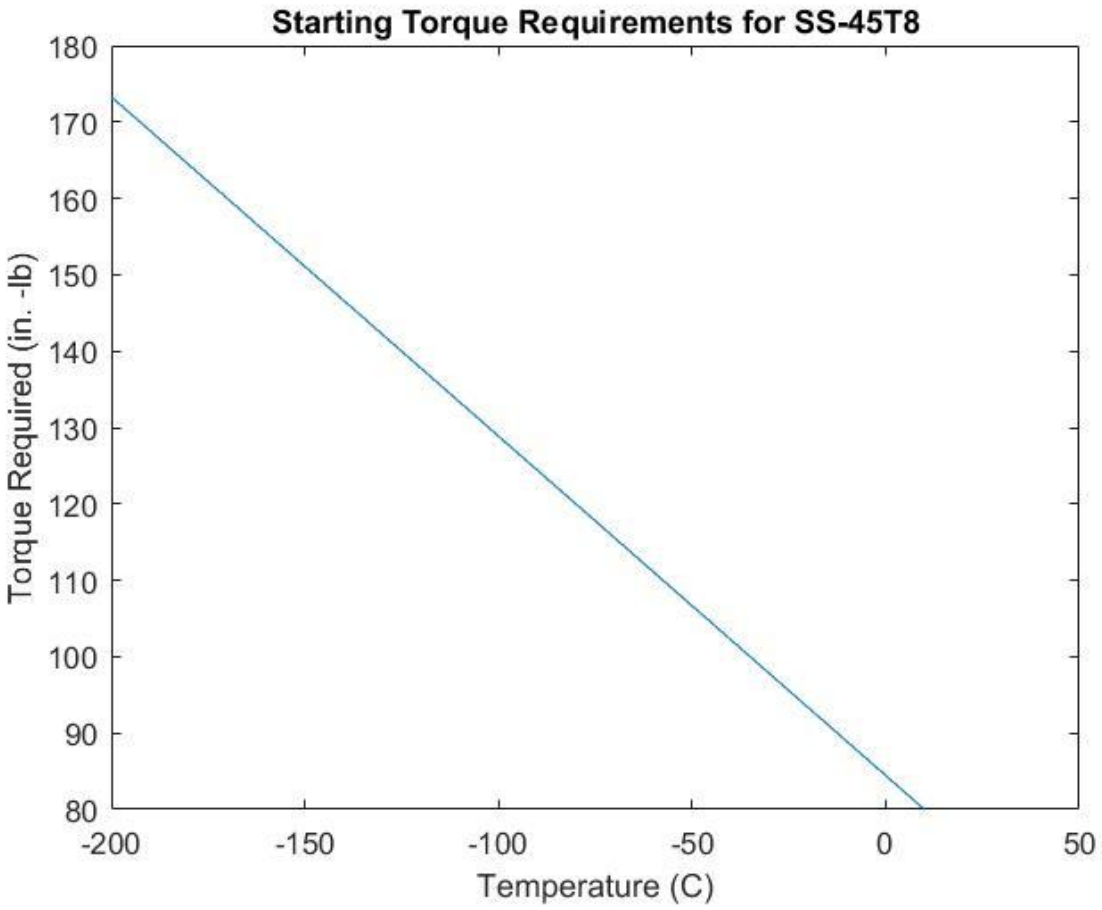

Figure 1.3: Linear extrapolation of provided starting torque data for SS-45T8

Liquid oxygen has a temperature of -182.6°C. This means approximately 165.6 in-lbs. of torque is required to open one valve.

However, this estimate is most likely conservative because it is outside the recommended data points provided by Swagelok. In order to get a better number, experimental analysis is necessary. Exposing the valve to liquid nitrogen, which has a boiling point 14°C lower than liquid oxygen, provides an accurate scenario for measuring operating torque under cryogenic conditions.

Using this experimentally determined value, the appropriate motor, gearbox, and clutches can then be selected. The maximum expected operating torque for the motor and gearbox are then set at twice the

experimentally determined value because they are driving two ball valves, while each torque limiter should be rated for the experimental torque at minimum. In order to have a safety factor of at least 2, we will choose components that have twice these requirements to account for mechanical inefficiencies and provide sufficient overhead to guarantee valve actuation.

1.3.3 Potentiometers

A sealed, through shaft potentiometers will be chosen to prevent condensation from forming inside and affecting the electrical components. The potentiometers should have at least 90 degrees of rotational range and consistently repeat performance at greater than 0.5 degree resolution. A wide range of suitable potentiometers is available from online distributors such as Mouser and Digikey.

Tank Design

Matt Vernacchia & Sam Austin | 2017-02-08

This section presents the design of a propellant tank for use in the LHS on the Viper2 engine test stand. The proposed design is welded from 316 stainless steel, is designed for use with liquid oxygen and liquid methane. The tank has an overall length of 1.300 m (51.20 in.), a diameter of 219 mm (8.625 in.), and a mass of 19 kg (42 lbs).

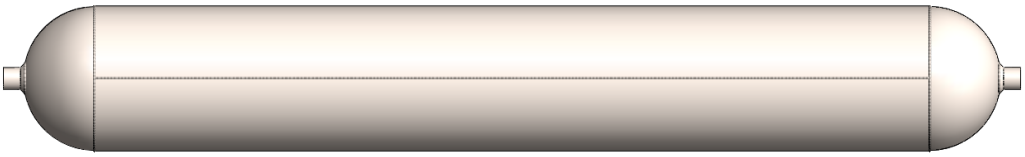

Figure 1.1: CAD rendering of the tank design.

1 Tank configuration

Separate fuel and oxidizer tanks should be used for the initial static fire tests, as opposed to a tandem tank configuration. Separate tanks will be easier to manufacture and reduce the risk of an inter-propellant leak, which could cause an explosion. However, tandem tanks (i.e. a common-bulkhead design) are lighter. In future revisions a tandem tank configuration may be preferrable to save mass on the flight vehicle.

2 Material selection

The tanks should be made from 316 stainless steel. 316 is the easiest to weld of the oxygen-compatible materials, so manufacturing the tanks from 316 will be cheaper and easier than with other metals. Also, the material properties of 316 reduce the likelihood of shrapnel generation from a tank failure. Unfortunately, 316 has a poor strength to density ratio, so using 316 will result in heavier tank than alternative materials. However, the manufacturing and safety advantages of 316 outweigh its mass-performance drawbacks.

2.1 Desired properties

2.1.1 Specific strength

Specific strength is the yield tensile strength divided by density, σ_y/ρ, and has units of N m kg^{-1} (m^2 s^{-2}). The mass of the tank is inversely proportional to the specific tensile strength. We desire a high specific tensile strength.

2.1.2 Ductility

Ductile materials yield (stretch) before breaking. Elongation at break is a reasonable quantitative metric for ductility. 5 percent can be a division between “ductile” and “brittle”.

A ductile tank is desirable so that a tank failure is safer. Ductile pressure vessels tend to peel open like a banana while brittle pressure vessels eject shrapnel.

2.1.3 Fracture toughness

The modeI fracture toughness K_{Ic} is the stress intensity factor at which a thin crack in the material will begin to grow. It has units of Pa $m^{1/2}$.

High fracture toughness means defects in the tank will grow more slowly. This will increase the lifetime of the tank, and make it more resilient to manufacturing or handling errors. Defects may exist in the tank due to:

- Defects in the stock material
- Weld defects
- Scratches or dents due to improper handling

2.1.4 Material compatibility

The tank material must be chemically compatible with liquid oxygen and liquid methane.

2.1.5 Temperature tolerance

The tank material must withstand cryogenic temperatures without becoming excessively brittle.

2.1.6 Weldability

Welding is the chosen manufacturing method, so an easily weldable material is greatly desired.

Fabrication will be easier if the material does not require post-weld heat treatment. Heat treatment uses specialized ovens and may require us to work with an off-campus site. Further, parts may deform during heat treatment and require mechanical straightening.

2.2 Comparison of materials

Titanium alloys are not compatible with liquid oxygen. Titanium will burn with oxygen, and this reaction is easily triggered by impact or ignition [1].

The aluminum alloys 7075, 2024 and 6061 are suitable for use with liquid oxygen [1]. Of these, only 6061 is weldable [2]. However, its tensile strength is poor in the as-welded (O temper) condition; it must be heat treated after welding to achieve a high specific strength.

The austenitic (304, 316) and semi-austenitic (17-7PH) stainless steels are also recommended for liquid oxygen service [1]. The austenitic stainless steels have poor specific strength. However, they are the easiest to weld of the materials considered, and usually do not require post-weld heat treatment [3]. The austenitic stainless steels are also very ductile, and have high fracture toughness. Semi-austenitic stainless steels have a higher specific strength, but require post-weld heat treatment and are less ductile.

Type	Alloy	Yield tensile strength (MPa)	Specific tensile strength (kN-m kg^{-1})	Elongation at break	Fracture toughness [MPa m$^{1/2}$]	Weldability
Aluminum	2024	290 (T3)	105 (T3)	14%	25	Not weldable [2]
	6061	276 (T6) 77 (O)	102 (T6) 28 (O)	12-17%	29	Weldable, heat treat and straightening required
	7075	480 (T6)	173 (T6)	7%	20-29	Not weldable [2]
Stainless Steel	304	290	36	55%	119-228	Weldable
	316	290	36	50%	112-278	Weldable
	17-7PH TH1050 [4]	1030 (TH1050)	135 (TH1050)	6%	76	Weldable heat treat required [5]

Table 2.1: Comparison of materials.

3 Welding

The tanks will be fabricated by welding. The following subsections describes factors to be considered in the welding process.

3.1 Welding process selection

Gas Tungsten Arc Welding (GTAW, also known as TIG welding) is the preferred method for welding austenitic stainless steel in thin pieces and tubes [6,7,8]. With manual GTAW, the operator has better control of heat and filler addition than in other processes. Manual GTAW is slow, but our production volume is small so this is not a concern. GTAW equipment is available on MIT campus in the D-Lab shop.

3.2 Metallurgical considerations with welding

3.2.1 Carbide precipitation

Carbide precipitation (also called sensitization) is the formation of chromium carbide in stainless steel at high temperatures (427 to 871°C) [7]. It depletes the steel chromium content, which reduces its corrosion resistance.

Several strategies can mitigate carbide precipitation. Using chill bars and skip welding reduces the amount of time the steel's temperature is in the critical temperature range [7]. Using a low-carbon alloy (i.e. 316L instead of 316) for the base and filler material prevents carbide precipitation [6]. The part can also be heat treated after welding to re-dissolve the carbide [7]. Of these strategies, using low-carbon 316L is the most convenient for our application.

3.2.2 Ferrite formation

Ferrite and austenite are alternate iron-carbon microstructures which can occur in steel. The amount of ferrite in an austenitic steel is measured by the ferrite number (FN). Some amount of ferrite is required to prevent hot cracking of the weld [7], but excessive ferrite will reduce the toughness at low temperatures [9]. For cryogenic applications, a FN of 3-8 is best [9]. FN depends on the composition of the base and filler material used. It seems that 316 usually has FN < 15, but that the FN can vary from lot to lot. "LF" and "cryo" marked filler rods are desirable if available.

3.3 GTAW technique for stainless steel

Use gas backup to prevent oxidation on back side of weld. In our case this would be purging the inside of the tank with argon.

Use the appropriate current to avoid overheating the material: 1 amp for every 0.001 inch of thickness [8].

Avoid distortion. Because of its higher thermal expansion, 316 is more susceptible to distortion than mild steel. Page 33 of [7] provides advice on avoiding distortion. The simplest approach is to place tack welds every inch before welding. If this is insufficient, a rigid jig may be required to hold the piece during welding. Acquisition of a rotary welding positioner would ensure extremely consistent welds, at a high equipment cost.

3.4 Filler material

ER316L filler is appropriate for welding 316 to 316. ER316L rods are available from McMaster and Lincoln Electric. Midalloy and Sandvik Coromant produce low ferrite/cryogenic 316L filler rods.

3.5 Weld inspection

An experienced welder (perhaps Jack Whipple from the D-Lab shop) should visually inspect our welds. A borescope camera will be required to inspect welds on the interior of the tank. A dye penetrant spray should be used to reveal cracks in weld beads.

More advanced inspection techniques (e.g. radiography) are necessary but difficult to acquire.

4 Mechanical design and fabrication plan

The tank is fabricated from 5 parts: a cylinder, two hemispherical ends, and two fittings (Figure 1). The cylinder is a 30.80 inch section of 8.625 inch OD, schedule 10, 316 stainless steel pipe. The ends are formed from sheet metal from a sheet metal forming manufacturer. Each end is attached to the cylinder with a circumferential butt weld. The fittings are turned from rod stock and tapped for ½ NPT pipe threads. Each fitting is joined to its end by a circumferential fillet weld.

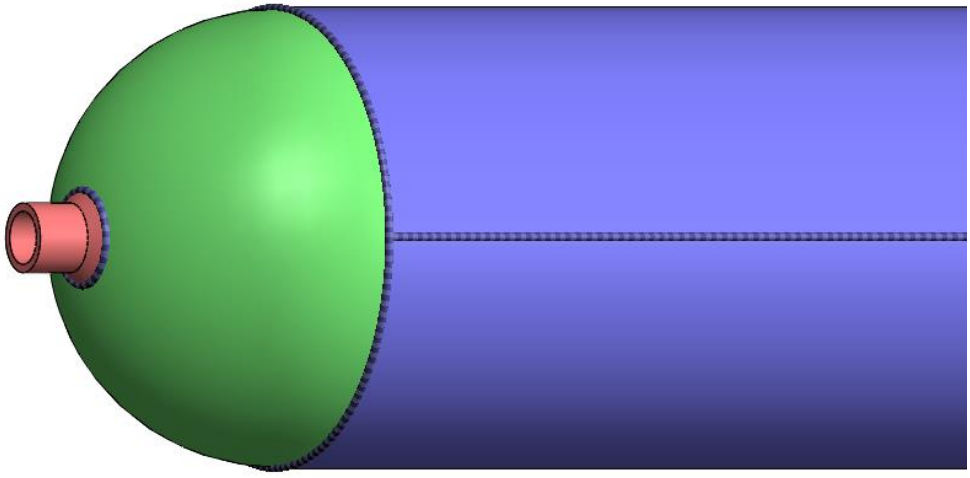

Figure 4.1: The tank is fabricated from 5 components: a cylinder (blue), 2 spherical ends (green, one shown), and 2 fittings (red, one shown). The components are joined by gas-tungsten arc welding. Four circumferential welds are used - the longitudinal weld shown here is from an earlier revision of the design.

5 Strength analysis and wall thickness

5.1 Maximum expected operating pressure

The tank is designed for MEOP of 800 psi (5.5 MPa). The engine design requires 600 psi inlet pressure at the injector, but there will be pressure losses in the feed system and manifold to account for so the tanks are designed for 800 psi to provide margin.

5.2 Maximum allowable stress

The maximum allowable stress in the tank wall is 232 MPa. AK Steel specifies the ultimate tensile strength of 316L stainless steel to be 558 MPa and the 0.2% yield tensile strength to be 290 MPa [10]. Applying the MIL-STD-1522A factors of safety (1.5 on ultimate and 1.25 on yield) gives a maximum allowable stress of 232 MPa.

The design stress is further discounted by a weld efficiency factor of 0.60, to 139 MPa. This value is recommended by the ASME pressure vessel code for welds with no backing and no radiographic inspection.

5.3 Wall thickness calculation

The required wall thickness is calculated using equations 8-15, 8-16 and 8-28 from Huzel and Huang [11]. A cylindrical tank was assumed with spherical ends, an OD of 8.625 in., and a wall thickness of 0.148 in. yielding an inside diameter of 8.329 in.

$$t_{cr} = \frac{p_t R}{2 S_w e_w} \qquad t_k = \frac{K p_t a}{S_w e_w} \qquad t_c = \frac{p_t a}{S_w e_w}$$

p_t = tank MEOP
R = tank-end crown radius
K = stress factor
t_k = wall thickness at knuckle, in
t_{cr} = wall thickness at crown, in
t_c = cylinder thickness, in
a = dome cap radius
S_w = maximum allowable operating stress of the tank
e_w = weld efficiency

The calculations yield a crown thickness of 0.0792 in., a knuckle thickness of 0.106 in., and a cylinder thickness of 0.159 in.

These thicknesses must be converted to gauge thicknesses in which sheet metal is sold. The ends must be at least as thick as the crown and knuckle thicknesses, so the ends will use 12 gauge (0.105 in) sheet. The cylinder wall will be made from Schedule 10 (0.148 in) pipe. This is 6% thinner than the calculated thickness and yields a safety factor of 3.478 on the burst pressure, which is acceptable.

5.4 Burst factor

The burst factor is the ratio of the burst pressure to the MEOP. The burst pressure for a cylindrical pressure vessel is given by the following:

$$p_{burst} = \frac{\sigma_u t}{r}$$

Where σ_u is the ultimate strength, t is the wall thickness and r is the radius. This design has a burst pressure of 19.0 MPa and a burst factor of 3.478.

6 Insulation

The tanks must be insulated to prevent excessive boil-off and propellant losses during testing and to ensure the safety of personnel while working near the tanks. An insulation system was designed consisting of expanding insulation foam inside a cardboard casting tube. The casting tube is a cement pouring tube, 14 in. in diameter. It will be held centered around the tank while the foam is poured in. The foam will be evenly distributed around the sides and on the end caps. After curing, the casting tube will be left in place for support and to provide additional insulation and protection. The casting tube will facilitate tank mounting as well. See Figure 8.1 for a cross section.

7 Mounting

The tanks must mount to the test stand in a stable and sturdy configuration. They will be mounted vertically and supported on the bottom by a shelf and supported horizontally by pipe clamps. In order to reduce the load borne by the tank and insulation, a hole will be cut in the shelf that the hemispherical portion of the tank will fit in. The casting tube will rest on the shelf, and a plastic ring at the bottom end of the casting tube will further support the assembly.

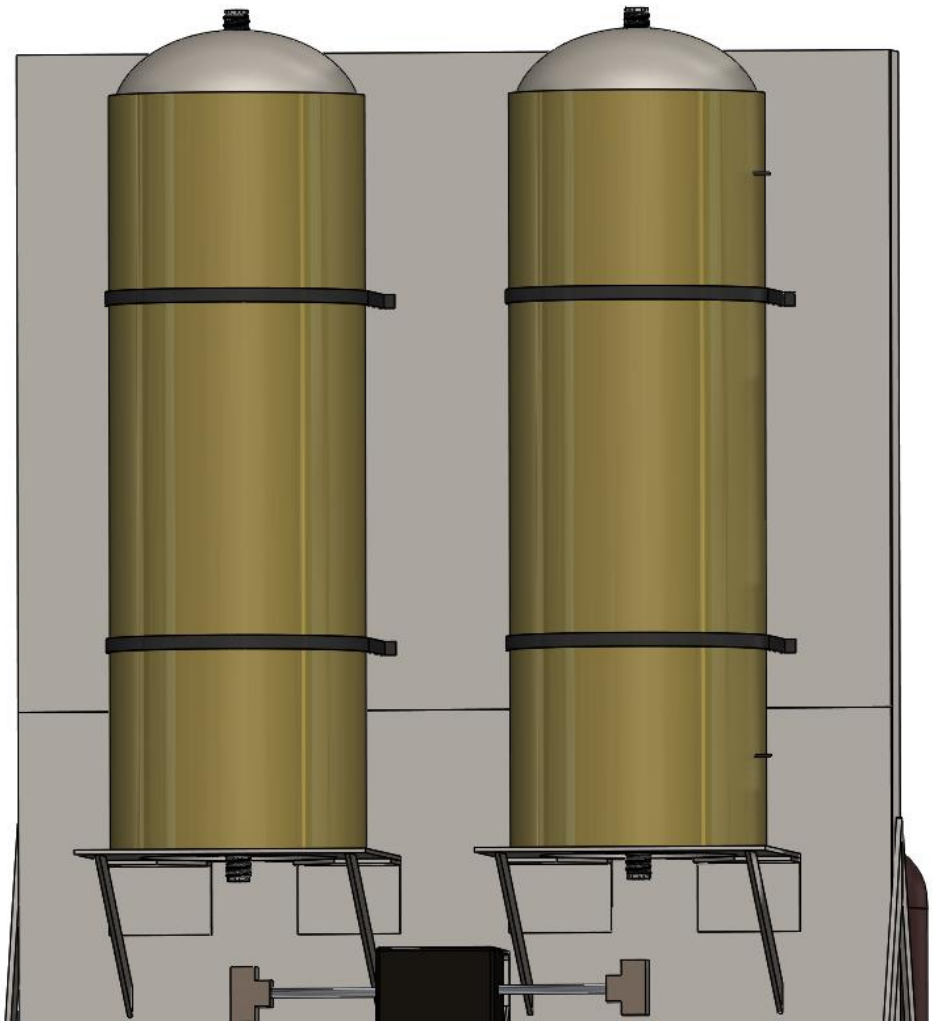

Figure 7.1: Tank Mounting Detail with Shelf and Support Straps

8 Instrumentation

Several instruments will be mounted on the tanks to collect temperature and pressure data. In particular, two thermocouples will be installed outside the tanks, with one at the top and one at the bottom to aid in the filling procedure. The thermocouples are type K and suited for cryogens and oxygen compatible. They will be installed on the tanks prior to insulation application and secured with aluminum tape.

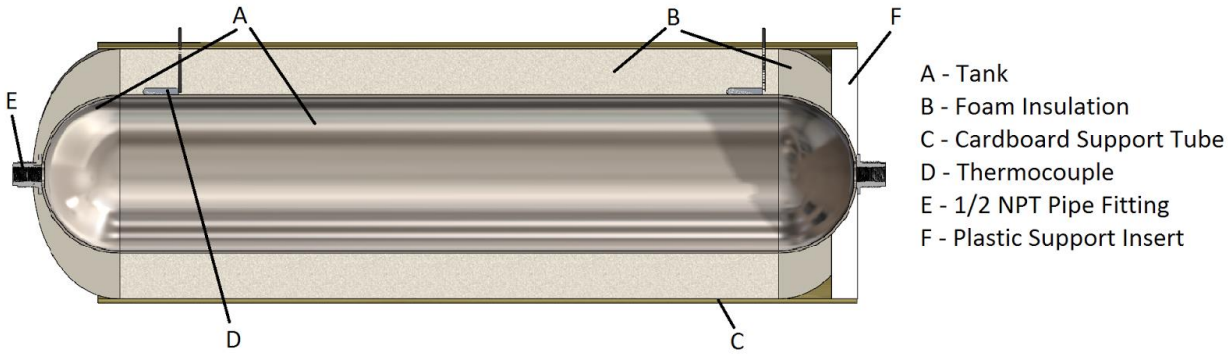

Figure 8.1: Tank Cutaway and Instrumentation Detail

9 Materials

The tank ends (316L steel hemispheres) can be purchased from Arthur Harris & Co. in Chicago, IL.

Pipe stock for the cylinder can be purchased from TW Metals.

Rod stock for the fittings can also be purchased from Online Metals.

10 Testing

The tank should be subjected to hydrostatic pressure testing before use. The tank should be filled with water, pressurized to the test pressure, and checked for leaks. Using an incompressible fluid such as water for the test reduces the stored energy in the pressure vessel. This decreases the hazard to nearby people and test equipment if the vessel fails during the test.

The tests should be performed according to MIL-STD-1522A.

10.1 Qualification test

The qualification test is performed on a few vessels to qualify the design. The minimum qualification requirements of MIL-STD-1522A are for a single vessel to show:

1. No yield after 50 cycles to a pressure of 1.5 * MEOP (8.3 MPa, 1200 psi),
2. then, no burst at a pressure of (burst factor) * MEOP (19 MPa, 2750 psi),
3. finally, test to failure.

10.2 Acceptance test

The acceptance test is performed on every vessel. The MIL-STD-1522A acceptance test pressure is of 1.5 * MEOP (8.3 MPa, 1200 psi).

10.3 Test equipment

A suitable hand-operated pump is available from Enerpac via Grainger. Hydrostatic test hand-pumps are also available from equipment rental companies such as Sunbelt.

11 References

[1] C. R. James and J. A. Letos, "Materials Compatability with Liquid Rocket Propellants," 1970. [Online]. Available: http://www.dtic.mil.libproxy.mit.edu/dtic/tr/fulltext/u2/866010.pdf.

[2] Lincoln Electric, "Common Design Mistakes in Aluminum," [Online]. Available: http://www.lincolnelectric.com/en-us/support/welding-how-to/Pages/aluminum-design-mistakes-detail.aspx.

[3] The Welding Insititute, "Is post weld heat treatment normally required when welding chromium-nickel austenitic stainless steels?," [Online]. Available: http://www.twi-global.com/technical-knowledge/faqs/material-faqs/faq-is-post-weld-heat-treatment-normally-required-when-welding-chromium-nickel-austenitic-stainless-steels/.

[4] "17-7 PH Stainless Steel, RH950, bar and forgings," Aerospace Specification Metals Inc, [Online]. Available: http://asm.matweb.com/search/SpecificMaterial.asp?bassnum=MQM177C.

[5] G. Mathers, "Precipitation hardening stainless steels," [Online]. Available: http://www.twi-global.com/technical-knowledge/job-knowledge/precipitation-hardening-stainless-steels-102/.

[6] American Iron and Steel Institute, "Welding of Stainless Steels and Other Joining Methods," Nickle Development Institute, 1979.

[7] D. Kotecki and F. Armao, "Stainless Steels Welding Guide," Lincoln Electric.

[8] B. Williams, "TIG Welding Austenitic Stainless Steel," IMPO, [Online]. Available: http://www.impomag.com/article/2012/09/tig-welding-austenitic-stainless-steel.

[9] N. Friedrich, G. Posch, J. Tosch, J. Ziegerhofer and W. Berger, "Welding of austenitic stainless steels for cryogenic LNG applications".

[10] AK Steel, "Product Data Sheet: 316/316L Stainless Steel," [Online]. Available: http://www.aksteel.com/pdf/markets_products/stainless/austenitic/316_316l_data_sheet.pdf.

[11] D. Huzel and D. Huang, Modern Engineering for Design of Liquid-Propellant Rocket Engines, Washington, DC: AIAA, 1992.

[12] Federal Aviation Administration, "Metallic Materials Properties Development and Standardization MMPDS-08," 2013.

Test Stand – LHS

Greg Pailet & Juan Salazar | 2017-02-06

This section presents the layout and design of the Liquid Handling System portion of the engine test stand for Viper2. The Pressure and Instrumentation Diagram (PID) on the next page provides reference for this document. The diagram accounts for the instrumentation system, which is meant to collect performance data and send it to a remote location; the cooling system, which pumps H2O to prevent the combustion chamber from overheating; and the LHS itself. There are two primary fluid zones: the GN_2 regulation (indicated by green) zone and cryogenic fluids zone (blue and red). Fluid flow between zones is restricted by a check valve.

Separate sections will cover the instrumentation system, mechanical structure, and control system.

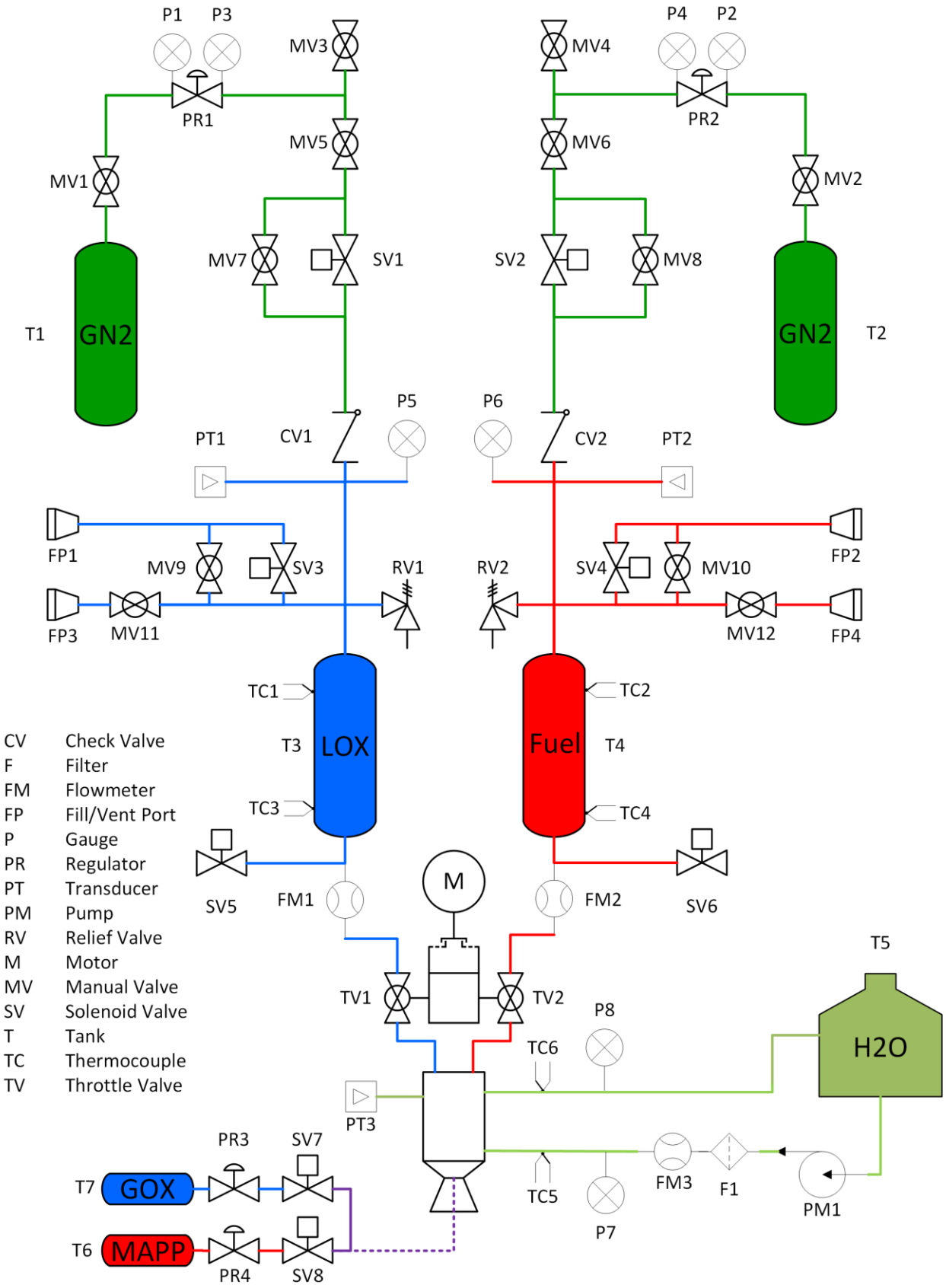
P1
P3
MV3
PR1
MV5
MV1
MV7
SV1
T1
GN2
P4
P2
MV4
PR2
MV6
MV2
SV2
MV8
GN2
T2
P5
P6
PT1
CV1
CV2
PT2
FP1
MV9
SV3
RV1
RV2
SV4
MV10
FP2
FP3
MV11
MV12
FP4
TC1
T3
LOX
Fuel
T4
TC2
TC3
TC4
SV5
FM1
M
FM2
SV6
T5
TV1
TV2
P8
H2O
TC6
PT3
PR3
SV7
T7
GOX
TC5
FM3
F1
PM1
P7
T6
MAPP
PR4
SV8
CV Check Valve
F Filter
FM Flowmeter
FP Fill/Vent Port
P Gauge
PR Regulator
PT Transducer
PM Pump
RV Relief Valve
M Motor
MV Manual Valve
SV Solenoid Valve
T Tank
TC Thermocouple
TV Throttle Valve

1 Requirements

1.1 Usability

1.1.1 Remote Control

The physical design must support remote operation. In the event that control is lost through power failure, the system must fail-safe to prevent damage to components or personnel.

1.1.2 Manual Control

Manual valves are implemented in the system to allow control of fluids during safe scenarios, such as feed pressure adjustment, system purging, and propellant loading.

1.2 Safety

Use of the test stand system comes with potential hazards and thus requires appropriate mitigation. Table 2.1 lists risks and their corresponding mitigations.

Risks	Mitigation
Tank overpressure due to autogenic pressurization	Pressures are monitored at all times and controllable with remotely operated solenoid vent valves. Each tank is also fitted with automatic relief valves in case of control system failure.
Presence of strong oxidizer presenting a chemical and safety hazard	Choice of compatible materials, rigorous cleaning procedures, controlled venting and drainage of gases, and rigorous adherence to detailed operation procedures prevent inadvertent and unsafe contact with LOX.
Exposure to cryogenic fluids	Adherence to Personal Protective Equipment (PPE)

Table 1.1: Risks & Mitigation

1.3 Operation Requirements

1.3.1 Test Operation

Concerning test operation requirements, the system must:

- Sustain consistent mass flow to the engine under continuous burn
- Provide propellant for at minimum 30 seconds of hot fire
- Provide sufficient pressure at the injector inlet, ranging from 600-800 psi.

1.3.2 Instrumentation

The system must support field instrumentation measuring the following at a rate of 100Hz:

- Injection pressure
- Chamber pressure
- Oxygen and fuel mass flows
- Heat flux
- Engine thrust
- Tank temperatures

1.3.3 Adjustability

The system must allow for adjustable flow parameters, including:

- Mass flow of each propellant
- Injection pressure of each propellant
- Ignition Sequence

2 GN_2 Regulation

2.1 Manual and Solenoid Valves

Ball valves from McMaster-Carr were selected for MV3-8, and solenoid valves from Omega were assigned to SV1-2. They regulate flow of GN_2 along the piping illustrated on the P&ID in green. MV1-2 are included on high pressure bottles as shutoff valves.

PID Designation	Purpose
MV1	GN_2 shutoff valve - LOX
MV2	GN_2 shutoff valve - LCH_4
MV3	GN_2 line pressure vent valve - LOX
MV4	GN_2 line pressure vent valve - LCH_4
MV5	Regulated GN_2 shutoff valve - LOX
MV6	Regulated GN_2 shutoff valve - LCH_4
MV7	GN_2 Bypass - LOX
MV8	GN_2 Bypass - LCH_4
SV1	Remote Pressurization - LOX
SV2	Remote Pressurization - LCH_4

Table 2.1: GN2 Regulation Valve Designation

Each valve was selected to meet a maximum desired pressure drop. The pressure drop through each valve is calculated based on the specific gravity of the fluid, the volumetric flow rate, and the flow capacity coefficient C_v. Setting a maximum pressure drop as a requirement allows calculation of the minimum Cv required for known flow rate and fluid properties. This minimum Cv requirement was then used to select appropriate valves in terms of performance and cost.

Valve	Fluid	MEOP (Psi)	Flow Rate (L/s)	C_v Required	C_v Spec	Part No.	Manufacturer
MV1	GN_2	3000	1.024	0.006	-	-	On Tank
MV2	GN_2	3000	1.024	0.006	-	-	On Tank
MV3	GN_2	800	1.132	0.082	1.6	4114T23	McMaster
MV4	GN_2	800	1.024	0.074	1.6	4114T23	McMaster
MV5	GN_2	800	1.132	0.082	1.6	4114T23	McMaster
MV6	GN_2	800	1.024	0.074	1.6	4114T23	McMaster
MV7	GN_2	800	1.132	0.082	1.6	4114T23	McMaster
MV8	GN_2	800	1.024	0.074	1.6	4114T23	McMaster
SV1	GN_2	800	1.132	0.04	0.07	SV12COIL-24DC	Omega
SV2	GN_2	800	1.024	0.036	0.07	SV12COIL-24DC	Omega

Table 2.2: GN2 regulation valve requirements, specifications, and part number.

2.2 Check Valves

Check valves (CV1-2) permit flow in only one direction, important for preventing flow of cryogenic propellants into the GN_2 regulation region. For both cases, the valve must be pressure rated to 800 PSI and have a minimum C_v value of 7.4. In addition, the valves must be compatible with cryogenic fluids and temperatures to function properly and prevent backwards flow.

Valves	Fluid	MEOP (Psi)	Flow Rate (L/s)	C_v Required	C_v Spec	Part Number	Manufacturer
CV1	GN_2	800	1.132	0.07	7.4	CV-500B-T-5	Generant
CV2	GN_2	800	1.024	0.07	7.4	CV-500B-T-5	Generant

Table 2.3: Check valve requirements, specifications, and part number.

2.3 Pressure Regulators

2.3.1 Operating parameters

Regulators (PR1-2) adjust fluid pressure to maintain desired levels. Standard nitrogen gas bottles have an outlet pressure of 3000 psi and are used as the working fluid to pressurize the propellants on the test stand. The regulator outlet pressure requirement is the MEOP of 800 psi for the test stand components. In order to get the most use out of every bottle of GN_2, the C_v requirement was found by requiring the regulator to still function when the supply bottle runs down to 900 psi. CV calculation with a 100 psi pressure drop at the calculated flow rate yields a required CV of 0.007.

2.3.2 Inlet Pressure Effects

All high pressure single stage regulators are subject to a rising output pressure proportional to a decrease in inlet pressure. For the Y11-N115H580 regulator this is specified at 1 psi of rise per 100 psi of inlet pressure drop. Across the 3000 to 900 psi inlet pressure range required, this corresponds to a pressure rise of 21 psi. This can be easily mitigated with periodic adjustment between tests if necessary.

Valves	Fluid	MEOP (psi)	Flow Rate (L/s)	C_v Required	C_v Spec	Part Number	Manufacturer
PR1	GN_2	3000/800	1.132	0.007	0.06	Y11-N115H580	Airgas
PR2	GN_2	3000/800	1.024	0.007	0.06	Y11-N115H580	Airgas

Table 2.4: Pressure regulator requirements, specifications, and part number. Here, 3000 psi is the MEOP for inlet pressure and 800 the MEOP for outlet pressure

2.4 C_v Calculation

Valve sizing is based on its flow capacity coefficient C_v, which is given by the following formula:

$$C_v = Q\sqrt{\frac{SG}{\Delta P}}$$

Where Q = flow rate, SG = specific gravity of the fluid, and ΔP = pressure drop.

2.5 Fitting Requirements

The GN_2 pressurant section consists of National Piping Thread (NPT) 1/4'' fittings for low costs and compact manifolding.

3 Cryogenic System

Liquid oxygen (LOX) is a powerful oxidizer, and accelerates the combustion of all flammable materials to an explosive degree. In order to select valves that are compatible with liquid oxygen, the materials must be have desirable physical properties at cryogenic temperatures, especially the ability to handle fast fluctuations in stress that may result from temperature changes. Such materials that satisfy this property include stainless steel, copper, brass, and bronze [1]. Elastomers and wetted seal materials used in valves must also be compatible with liquid oxygen. Examples of these materials include Teflon (PTFE), Kel-F, and PFA [2].

3.1 Manual and Solenoid Valves

Shut-off valves allow manual On/Off control of fluid flow. On the P&ID, manual valves MV9-12 have shut-off operation. They have a MEOP of 800 psi and are allocated to the vent and fill ports. No fluid flow occurs during operation, only during the filling and venting process. Therefore, they do not have any stringent flow rate or C_v requirements other than permitting filling of the propellant tanks in a reasonable time frame.

Similarly, SV3-6 are used in drain and vent applications and do not have stringent C_v requirements.

PID Designation	Purpose
MV9	Tank manual vent - LOX
MV10	Tank manual vent - LCH_4
MV11	Tank fill - LOX
MV12	Tank fill - LCH_4
SV3	Remote tank vent - LOX
SV4	Remote tank vent - LCH_4
SV5	Remote tank drain - LOX
SV6	Remote tank drain - LCH_4

Table 3.1: GN2 Regulation Valve Designation

Valves	Fluid	MEOP (psi)	Flow Rate (L/s)	C_v Required	C_v Spec	Part Number	Manufacturer
MV9	LOX	800	Vent	-	2.34	SOV-8T	Generant
MV10	LCH_4	800	Vent	-	2.34	SOV-8T	Generant
MV11	LOX	800	Fill	-	2.34	SOV-8T	Generant
MV12	LCH_4	800	Fill	-	2.34	SOV-8T	Generant
SV3	GOX	800	Vent	-	0.06	SV955G56HC0	Valcor
SV4	GCH_4	800	Vent	-	0.06	SV955G56HC0	Valcor
SV5	LOX	800	Drain	-	0.06	SV955G56HC0	Valcor
SV6	LCH_4	800	Drain	-	0.06	SV955G56HC0	Valcor

Table 3.2: Cryogenic fill and vent regulation valve requirements, specifications, and part number.

3.2 Pressure Relief Valves

Pressure relief valves prevent excess pressure build up in both the LOX and LCH4 tanks produced by heating and subsequent boiling of the propellants (autogenic pressurization). The pressure relief valves do not experience fluid flow during operation, but operate as a safety mechanism and therefore do not have stringent flow requirements. The specified valves have a K_d of 0.27 and an orifice diameter of 0.275", are compatible with liquid oxygen at cryogenic temperatures, and are available in the desired relief pressure of 800 psi.

Valves	Fluid	Pressure(Psi)	Flow Rate (L/s)	C_v Required	C_v Spec	Part Number	Manufacturer
RV1	GOX	800	1.132	-	-	HPRV-500SS-T-800	Genarant
RV2	GCH_4	800	1.024	-	-	HPRV-500SS-T-800	Generant

Table 3.3: Cryogenic relief valve requirements, specifications, and part number.

3.3 Fill and Vent Ports

FP1-4 are intended for use when filling and venting the system of cryogenic material. FP3 and FP4 are simply connections for the dewar transfill line so the propellants can be piped into the test stand tanks, while FP1 and FP2 operate as vents to atmosphere. The exact fitting type and configuration of FP3 and FP4 depend on the filling hose specifications and configuration that is used and remain to be determined.

FP1 and FP2 present a topic of conversation. The vents must be in place to safely allow overflow of liquid propellants during filling and a vent pathway during manual purging and remove purging via solenoid valve. RV1 and RV2 also vent to atmosphere, but a scenario can present where both GOX and GCH_4 begin to vent to atmosphere and can very possible form an explosive cloud depending on the ambient air currents and source of ignition. The hot engine, the electrical wiring and circuitry around the stand, and the surrounding area all present potential sources of ignition. More research and discussion into how to safely manage vented gases is required before moving forward with system approval.

3.4 Fitting Requirements

The cryogenic manifold past the check valve has to connect many valves separated by considerable distance due to the size of the propellant tanks. Many cryogenic valves and fittings come with NPT threads that require a sealing compound to make joints leak tight. Because both systems operate at

cryogenic temperatures and LOX is the working fluid in one side, it is essential to use appropriate LOX compatible thread sealant compounds and tapes. When tube fittings are used (such as AN flares or double-ferrule type fittings) it is advisable to use a small amount of Krytox lubricant on the threads to aid in assembly and disassembly after use.

Krytox is a LOX compatible lubricant used in all manner of cryogenic handling situations and is essential to have on hand.

4 Testing

The system will undergo leak testing at room and cryogenic temperatures as well as cold flow testing to measure pressure drop through the network of valves.

5 References

[1] C. R. James and J. A. Letos, "Materials Compatability with Liquid Rocket Propellants," 1970. [Online]. Available: http://www.dtic.mil.libproxy.mit.edu/dtic/tr/fulltext/u2/866010.pdf.

[2] "Chemical Resistance Guide," in The O-Ring Store LLC. [Online]. Available: http://www.theoringstore.com/index.php?main_page=page_3. Accessed: 2017.

Test Stand – Structure

Sam Austin | 2017-02-08

This section describes the proposed test stand structure and layout for the test stand. The test stand is responsible for supporting the engine, propellant tanks, instrumentation, and control system for the duration of the test, and these items will be the focus of this section.

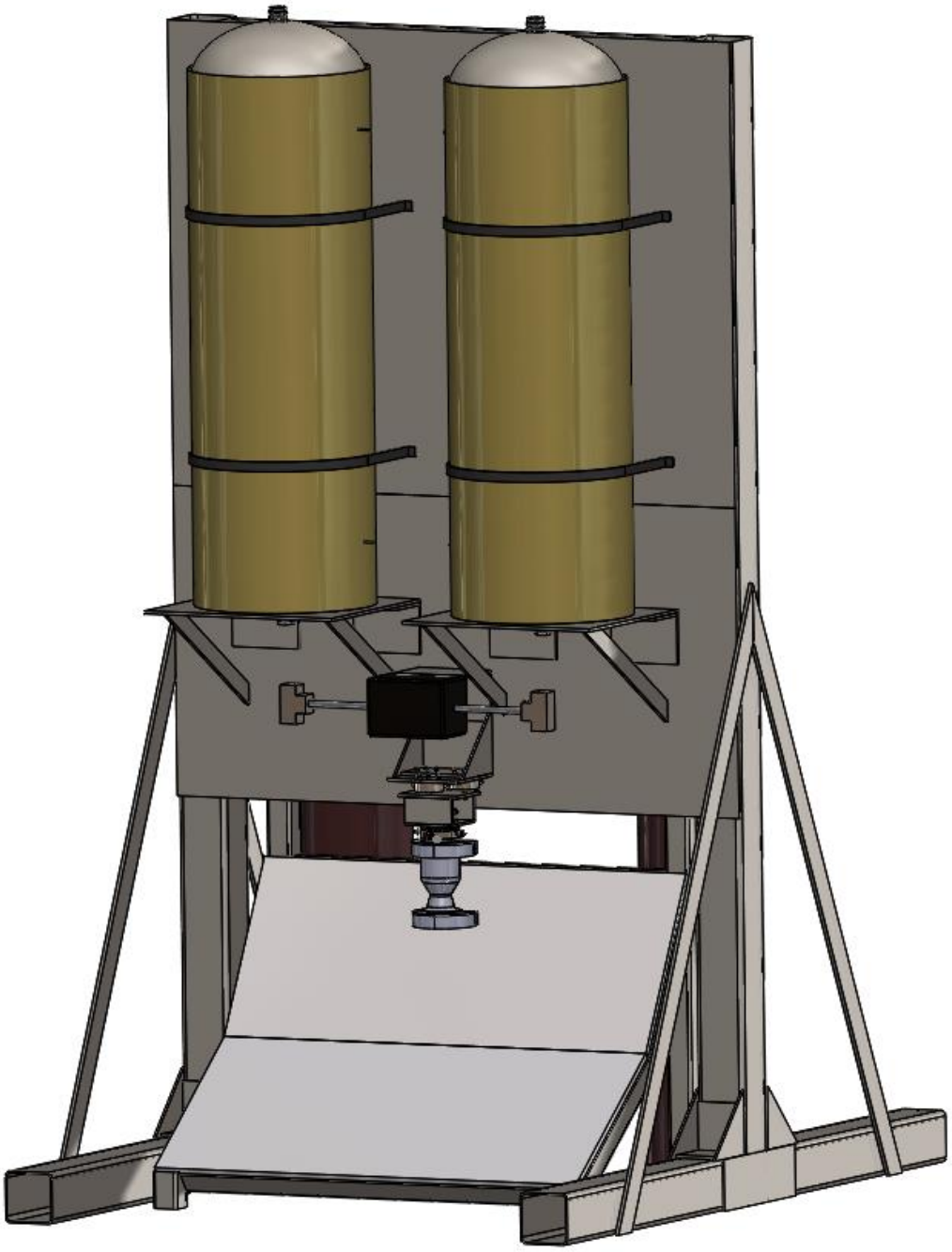

Figure 1.1: Test Stand configured with blast deflector, propellant tanks, and engine assembly

1 Frame

1.1 Structure

The frame supports the engine, tanks, and liquid handling system, as well as the controls and instrumentation. It is constructed from 4-inch hot rolled A500 steel square tubing selected for strength, availability, and weldability. The test stand consists of 7.5 ft. vertical stringers braced by four 2.5 ft. legs at the bottom. Assembly will be accomplished with welds and bolts. Sections of 4 in. by 24 in. by 3/16 in. thick steel plates are attached to the stringers, providing the surface on which to mount the test components. The assembly is further braced by bars running from the horizontal to the vertical stringers.

1.2 Transport and assembly

The test stand must be easily taken apart and transported to the test facility. As the stand will be transported in a small trailer, it must fit within a 6 ft. by 8 ft. by 10 ft. form factor. In addition, the stand must be able to be erected by a small group of people.

The assembled stand already meets the form factor requirements, but in order to ease transport and integration, consideration was given as to which joints would be welded and which would be bolted. The horizontal supports at the base will be welded to the gussets at the base of the vertical stringers, while the gussets themselves will be bolted to the vertical stringers. This allows for the horizontal sections to be removed and for the stand to lay flat during transport. In addition, the mounting plates at the front of the stand will be bolted to the frame for easy removal.

These modularized components decrease the mass that is being carried by the setup crew at any given time, making assembly easier. The tanks will also be removed from the assembly prior to transport.

The team is also looking into a semi-permanent installation at the test site to facilitate assembly, disassembly, and transport, as well as to support larger test stands and engines.

2 Tank Mounting

The tanks must be securely fastened to the test stand and supported by the sides and the bottom. To meet these requirements, the tanks will be mounted vertically and supported from the bottom by a shelf. They will be strapped to the test stand with pipe clamps.

Additional information is contained in the “Tanks” section of this document.

3 Engine and Load Cell Interface

The engine must have a secure connection to the load cell assembly and to the rest of the test stand in order to ensure accurate measurement and safe operation.

To accomplish this, the engine will be mounted to a thrust take-up structure. The thrust take-up structure introduced in the Injector section consists of a 4 inch by 4 inch steel plate bolted to the injector above a spacer ring that gives the plate clearance above the injector bolts. Two vertical plates 2 inches tall are welded to the edges of the base plate. The open sides allow room for the oxygen line and pressure transducer wires to run. The vertical plates are welded to an upper horizontal plate with holes

matching the spacing of the load cells. The assembly is then bolted to the load cells through this plate with spacers.

Alternatives to this design included a dual-hinged bracket assembly that would allow the engine to move up and down while rotating around two fixed points on the test stand wall. However, since the load cells used in this test stand are rated for both tension and compression, it was reasonable to design the thrust take-up structure so that the engine hangs from the load cells in tension before firing and in compression during firing.

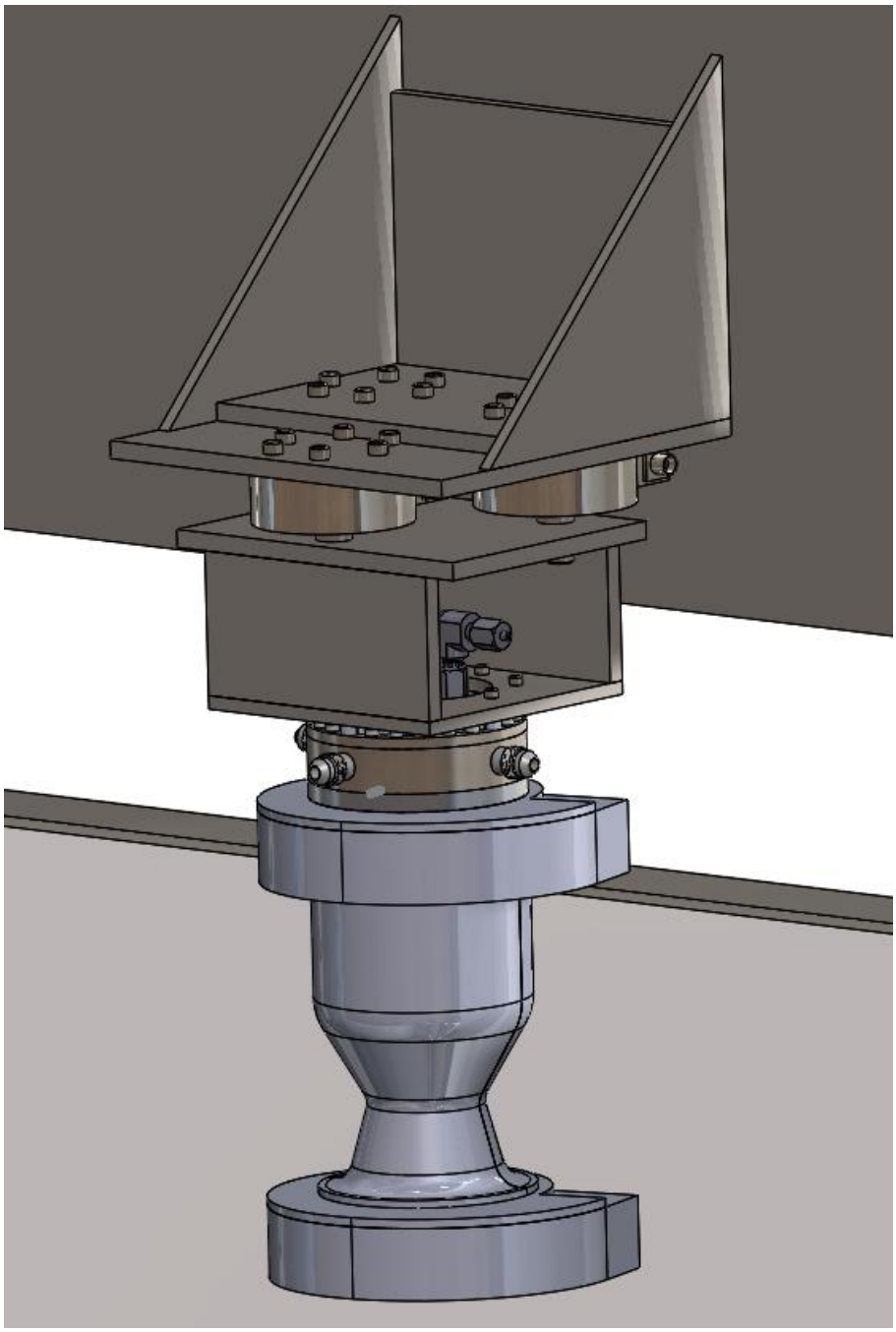

Figure 3.1: Engine and load cell interface mounting configuration

4 Instrumentation and Control Mounting

The instrumentation and control equipment, consisting of the relay box and microcontroller data logger, must be located out of the way of potential ignition sources and secure from vibration and contamination.

To address this, the electronics will be mounted in heavy duty enclosures to protect them from the surrounding test environment. These boxes have fittings for RF antennas and power connectors that will simplify interfacing and integration with their modular form. In order to further protect the electronics from engine exhaust and heat, the boxes will be placed above the engine on the back of the test stand, behind the propellant tanks on a dedicated shelf.

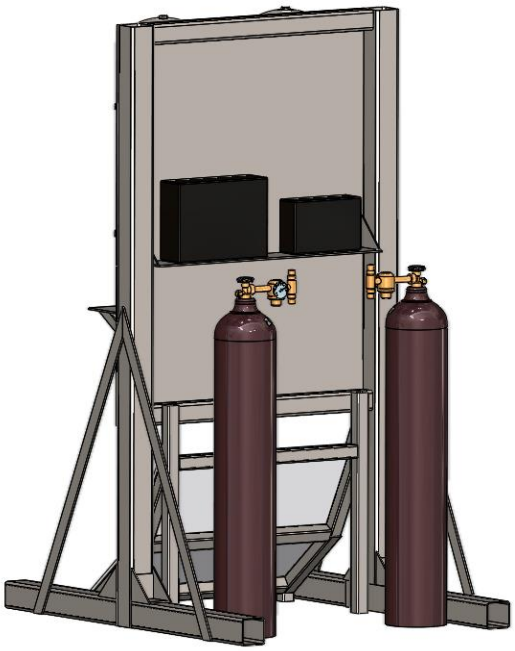

Figure 4.1: Rear view with instrumentation and control boxes visible. Note also the GN_2 bottles in foreground. Welding flowmeters are attached in this photo but rest assured will not be used in operation.

5 Safety

Safe operation is of critical importance in regards to protecting the test stand equipment, surrounding area, and personnel resulting from a failure during testing. Several safety features will be implemented, namely a concrete wall protecting the nitrogen tanks and a flame deflector to prevent the engine's exhaust from reaching the ground.

5.1 Concrete Back Wall

Pending material availability and feasibility of transport, a concrete cinder block wall will be erected behind the test stand to contain debris in the event of a failure during testing. This wall will have three sections, one running parallel to the test stand and two sides angling toward the stand, forming a partial enclosure.

If this wall is constructed, the nitrogen tanks will be placed behind it to protect them from the test environment and possible debris.

As mentioned earlier, the team is considering a semi-permanent installation at the test site. Constructing a permanent wall greatly reduces setup time and allows for sturdier, more secure construction.

Figure 5.1: Proposed concrete wall surrounding rear of test stand.
Note that GN_2 bottles have been moved behind wall.

5.2 Flame Deflector

As the engine's exhaust has the potential to start a serious fire if it hits the ground, the test stand must have a construction to deflect the exhaust away from the ground and the stand. This will be accomplished by two sections of cement fiberboard, mounted on a steel support structure under the test stand. Cement fiberboard is widely available, easy to install, and has superior thermal resistance qualities.

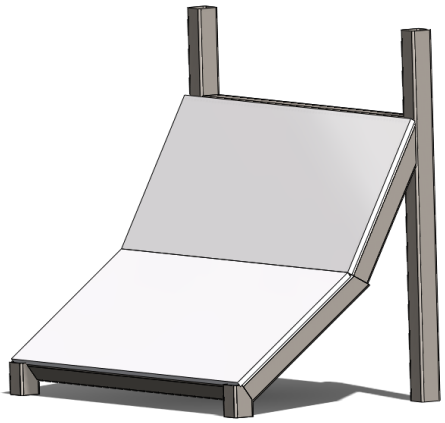

Figure 5.2: Blast Deflector Assembly

6 Stock Material

The cement board flame deflector can be purchased from Home Depot.

The steel elements can be purchased from Online Metals:

- 4 inch square steel tubing
- 3 inch square steel tubing
- 2 inch square steel tubing
- 48 x 36 x 3/16 inch steel plate
- 4 x 4 inch steel angle

Instrumentation & Control

Sam Austin & Josef Biberstein | 2017-02-08

1 Overview

This section presents the proposed controls and instrumentation design and layout for the engine test stand instrumentation and control equipment. The test stand consists of the structure supporting the engine, the LHS, and instrumentation, while the control center consists of the computers, monitors, and control equipment required to conduct the test and operate the test stand equipment remotely. The combined test stand and control center will henceforth be referred to as the "control complex." Detailed in this document is the overall layout of the control and instrumentation electronics and a discussion of each component and its purpose to the test.

The attached PID diagram in the Test Stand – LHS section detailing the LHS and Instrumentation of the test stand accompanies this section, where sensors are referred to by their designations corresponding to the PID.

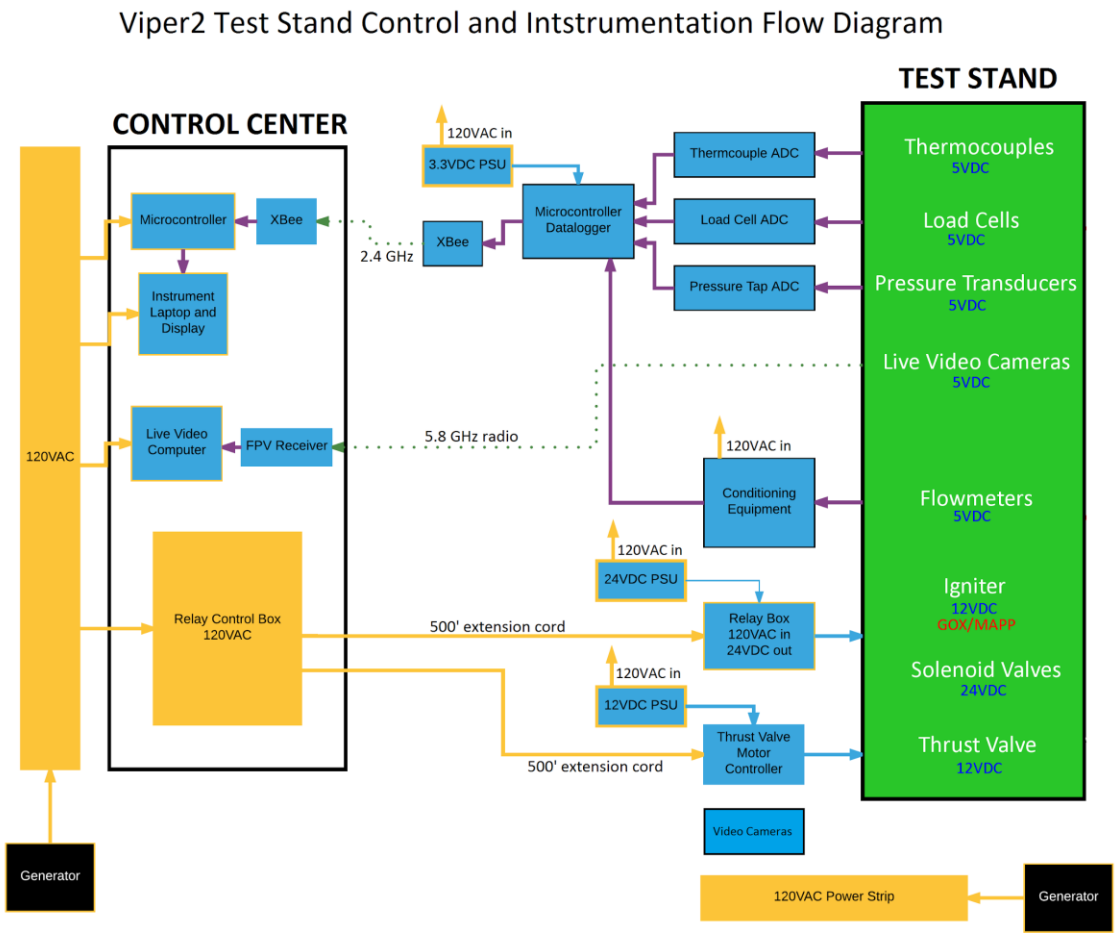

Figure 1.1: Overall test complex layout, including the control center, test stand, power sources, and interfaces

2 Organization

The test complex consists of the test stand and control center, which must be separated from each other by a minimum of 500 feet for safety purposes. The test stand holds instrumentation to monitor various engine and LHS metrics such as engine thrust, line pressures, fluid temperatures, fluid flow, valve positions, and cameras for documentation. Data will be stored locally and transmitted to the control center for live viewing.

In addition, the test stand supports the various valves and actuators responsible for liquid handling and engine control. The test personnel working in the control center are responsible for monitoring received data and controlling valve actuations through a relay box and wired connection.

3 Instrumentation

To collect data mentioned in section 2, test stand instrumentation consists of load cells, pressure transducers, thermocouples, mass flowmeters, valve potentiometers, and cameras. As each sensor will be functioning in a unique environment (i.e. cryogenic, contact with oxygen, etc), special consideration was taken in developing requirements for each instrument.

3.1 Load Cells

Load cells are used to directly measure the thrust produced by the engine. The engine will hang suspended from the three load cells, which are pancake style and rated for tension and compression.

3.1.1 Requirements

The test stand must be capable of accurately measuring the thrust of the engine throughout its burn. Since the engine is expected to produce a maximum thrust of 2355 N, the load cells must have a range of at least 1.5 times that maximum, or 3533 N. In order to better characterize the burn profile, the load cells must be mounted in a way that allows for the determination of any thrust vectors. In addition, the engine assembly must be easily attached and removed from the test stand. The cells should interface easily with test equipment and be sampled at a rate of 100Hz.

3.1.2 Designed Solution

3.1.2.1 Load Cell Type

In order to facilitate mounting and data collection, the load cells selected were pancake style cells rated for both tension and compression, a common choice in the aerospace industry. The use of tension/compression cells alleviates the need to support the engine from the bottom when not firing or when building up to thrust less than its own weight. In addition, this means that the compressive range of the load cell need not be as great as compression only cells, as part of its load will be tension due to the hanging mass of the engine.

As mentioned previously, the engine will hang supported from the cells. The engine is mounted vertically to facilitate propellant loading and flow, as common in liquid engine test stands. Mounting the engine and attachment assembly directly to the load cells alleviates the need for extra mounting equipment such as isolated travel brackets, although this will be explored if the current option does not work.

3.1.2.2 Thrust Vector Measurement

In order to accurately characterize the engine's performance, a system was designed that could detect any thrust vectors, should they arise during the burn. Instead of a single load cell supporting the engine, it will hang from a cluster of three load cells. Having three load cells enables detection of differential loads, and thus the calculation of potential thrust vectors. This approach also spreads the loads among several smaller cells instead of one large one, which allows for the use of smaller cells.

3.1.2.3 Electrical Interface

The output of the load cells will be a standard mV/V analog signal. In order to collect this signal accurately, we will use a 16-bit AD7705 analog to digital converter. This will be able to give us measurements in sub 1 pound resolution with a millivolt input signal. This chip can be purchased on a breakout board or included in a simple circuit on a custom PCB.

3.2 Pressure Transducers

Pressure transducers are used to electronically measure pressure in various locations in the LHS. In particular, three pressure transducers will be used, one on each propellant tank and one connected to the combustion chamber.

3.2.1 Requirements

The pressure transducers installed on the propellant tank manifolds (PT1, PT2) must be rated to handle cryogenic temperatures (or suitably insulated) and vapor compatible with GOX and CH4. The transducer in the engine (PT3) must be rated to handle the high temperatures of combustion. As the propellant tank MEOP is 800 psi, the propellant tank transducers must be rated for 1.5 times that value, or 1,200 psi. Likewise, the engine transducer must be capable of handling pressures up to 750 psi, 1.5 times greater than the combustion pressure of 500psi. All sensors must easily integrate and interface with test equipment.

3.2.2 Designed Solution

Suitable pressure sensors are widely available from Omega, Futek, and Honeywell. Cryogenic models are likely cost prohibitive so transducers PT1 and PT2 will be placed upstream of the tanks to aid in insulation from cryogenic temperatures with extended tube runs. Similarly, the combustion chamber pressure sensor PT3 will be insulated from temperature through a long, thin tube extending from the engine. Packing the tube with grease or a thick oil is also possible to prevent corrosive gases from contacting the transducer element.

The common signal output types of analog voltage, mV/V, and current output are equally easy to work with and standardized.

3.3 Thermocouples

Thermocouples electronically provide temperature data from various parts of the LHS, allowing evaluation of propellant tank performance and thermal properties of the engine.

3.3.1 Requirements

The thermocouples installed on the propellant tanks must be capable of operating accurately at cryogenic temperatures. All thermocouples must easily integrate and interface with test equipment. They must also be cost effective.

3.3.2 Designed Solution

3.3.2.1 Thermocouple locations

Two thermocouples will be mounted on each propellant tank, one at each end to measure tank temperature during the filling process and while in use (TC1-4). In addition, there will be two thermocouples in the water cooling flow, one in the water inlet and one in the outlet (TC5-6). By measuring the temperature differential between the inlet and outlet, the heat flux through the combustion chamber can be calculated, aiding in the thermal analysis of the engine.

3.3.2.2 Electrical Interface

Type K thermocouples were chosen for their abundance and low price. These thermocouples operate over a large temperature range, and are suited for operation in cryogenic environments. Thermocouple amplifiers using the MAX31855K will be utilized in order to perform cold-junction compensation and communicates via the SPI protocol. The thermocouples have a one meter wire that will be extended if they are too short.

3.3.2.3 Mechanical Interface

Wire-bead type thermocouples can be spot welded directly to the tanks for TC1-4 or taped on the exterior with aluminum tape. Thermocouples TC5 and TC6 in the water flow will be housed in waterproof thermowells inserted through thermocouple pass through fittings, offered by Swagelok and Hylok.

3.4 Mass Flowmeters

In order to precisely measure mass flow of propellants and water coolant, mass flowmeters FM1 and FM2 will be added to the propellant lines leading to the thrust valves. In addition, FM3 placed on the water coolant line will monitor coolant mass flow.

3.4.1 Requirements

Primarily, the flowmeters must be capable of measuring flows up to 0.6 L/s at a MEOP of 800 psi, the maximum calculated propellant flow rate for Viper2. In addition, they must be able to withstand cryogenic operation and use compatible materials for the propellants. The water flowmeter does not have such stringent requirements, but must measure up to 5 L/s at a MEOP of 150 psi.

3.4.2 Designed Solution

Hoffer Flow Controls offers a very broad range of cryogenic flowmeters and signal conditioning systems for rocket test applications. The test stand will be outfitted with HO series turbine flowmeters with a maximum operating pressure of 1000 psi, cleaned for service with LOX and cryogenic methane down to 77°K, and a calibrated flow range up to 4.7 L/s. Each flowmeter has a 1” AN fitting easily integrated with the rest of the system.

Water flow meters are readily available from industrial suppliers Grainger and MSC. FM3 has yet to be selected but the flow and pressure requirements are well within the range of available products.

3.4.2.1 Electrical Interface

Each flow meter is provided with a CAT3 signal conditioner and transmitter providing a linear 5v frequency pulse output to the data collector.

3.5 Valve Potentiometers

One potentiometer on each thrust valve, TV1 and TV2, will directly measure the position of the valve with respect to time. Measurement of these positions and comparison with the flow rate curves produced by the flow meters allows capture of the startup sequence of the engine.

3.5.1 Requirements

The instrumentation system must capture the position of each valve at a minimum of 100 Hz at a measurement resolution of 0.5 degrees to allow accurate analysis of the startup sequence.

3.5.2 Designed Solution

The potentiometers mounted on each valve shaft produce a ratiometric output when supplied with a fixed voltage and configured as a voltage divider. Capture of this analog voltage is accomplished with an analog to digital converter (ADC). The ADS1115 is capable of measuring up to four analog signals at 860 Hz with 16-bit resolution with a selectable input range up to 6.144V. Given a standard 1-turn potentiometer configured as a voltage divider, a 5V drive voltage translates to 13.88mV per degree of rotation. Because the valves only actuate 90 degrees, the change in output voltage is only 1.25V. Using the ADS1115 at a full scale range of 2.048V therefore provides a measurement resolution of 0.03mV, equal to 0.002 degrees. The ADS1115 communicates via the I2C protocol.

Other solutions include encoder modules or digital potentiometers that require no voltage measurement on the instrumentation board. This solution may be superior if the potentiometers are not precise or repeatable during testing.

3.6 Live Webcams

Mechanical pressure gauges will be mounted on the propellant tanks as a redundancy for the pressure transducers and to aid in testing. These pressure gauges will be monitored by cameras sending a live video feed back to the control center.

3.6.1 Requirements

The test stand will include several cameras which broadcast live video from the test stand to the control station with low latency. The signal must be broadcast to the control center and be available for live viewing.

3.6.2 Designed Solution

Live video will be transmitted from the test stand via FPV camera units on the 5.8GHz band. The data will be received at the ground station and transferred to a computer via an analog video to USB capture card. Cameras positioned at the ground station will broadcast on different channels, allowing the operator at the control station to switch between views with the receiver.

3.7 Test Stand Cameras

In addition to the live video of the pressure gauges broadcast to the control center, there will also be several cameras shooting video recorded locally to capture details of the test sequence.

3.7.1 Requirements

The cameras must be capable of recording in high resolution to allow for post-test analysis. In addition, the cameras must have battery and storage capacity to record continuously for a minimum of 20

minutes during the fueling and checkout process. Several shooting modes, including slow motion, time lapse, and normal speed are desired.

3.7.2 Designed Solution

Four GoPro cameras will be used on and around the test stand to record the engine firing and other events. They will be mounted on tripods and adjusted so as to best capture the intended target. If necessary, external battery power supplies will be connected to the cameras to ensure the required runtime of at least 20 minutes. GoPro cameras are capable of frame rates up to 240fps at low resolution and a maximum resolution of 4k at 30 fps. Four cameras and a wide range of quality vs. frame rate settings meets the desired requirements.

4 Control

In addition to the instrumentation implemented to monitor various aspects of test performance, the test conductors must have a way to control the test through the actuation of valves and ignition of the engine. This will be accomplished through various solenoid valves to remotely pressurize, vent, and drain the propellant tanks, a motor driven thrust valve to initiate a test, and activating the engine igniter. These electrical components, mounted on the test stand, will interface with the control center through a wired connection to a relay box.

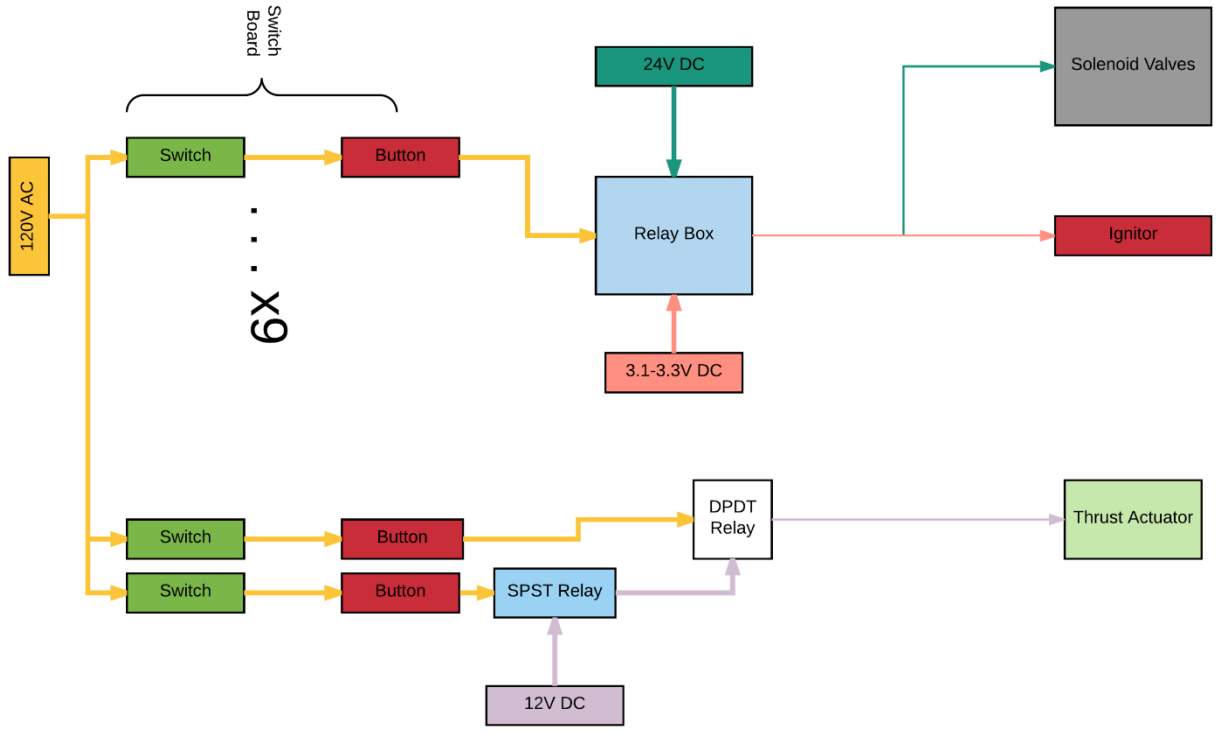

Figure 4.1: Block diagram of the control system for the test stand

4.1 Solenoid Valves

Solenoid valves are electromechanical actuators use DC current to actuate a valve controls fluid flow. They can be operated remotely and take the place of a valve otherwise actuated manually. This allows

for increased safety during test progress because critical and potentially hazardous activities (i.e. tank pressurization, tank relief, draining, and ignition) can be accomplished at a distance.

4.1.1 Requirements

The selected valves for SV1-6 require 24V with a peak power of 15W each. SV7 and SV8 require 12V and also have a peak power draw of 15W each.

4.1.2 Designed solution

4.1.2.1 Power Requirements

Two power supplies are needed to power all 8 solenoid valves: one supply rated 24V at 90W and the other rated to supply 12V at 30W. Although there should never be a case where all valves are activated at one time, the supply should be capable of supporting any combination of valve activations. 12V and 24V power supplies in this power range are readily available from electronics distributors such as Digikey and there are many available on campus for use at no cost.

4.1.2.2 Control

Controlling the solenoid valves directly from 500 feet is infeasible due to resistance in a long control cable leading to each valve. Instead switches in the control box will send 120V AC signals to relays at the test stand, where the DC supplies are located.

4.2 Thrust Valves

The flow of propellants into the combustion chamber will be controlled by the thrust valves TV1 and TV2. The valves are mechanically linked to the same drive motor, and will be actuated simultaneously.

4.2.1 Requirements

Exact specifications of the drive motor are not yet known due to the need to do empirical torque testing on TV1 and TV2 when cooled to cryogenic temperatures. A maximum power of 750W has been set at an upper limit, with a maximum drive voltage of 24V. An adjustable power supply will be used to allow changing the drive voltage to adjust motor speed and subsequently valve actuation speed.

4.2.2 Designed solution

Control of the DC gear motor will be through a DPDT relay switch connected to the control box through the 500 foot control line. In series with the power supply for the motor will be a SPST relay allowing the motor to turn in both directions and be stopped and started at any time.

4.3 Ignition

The engine will be ignited by the combustion of a mixture of GOX and MAPP gas in the main combustion chamber. Ignition of the gas will be achieved by heating a resistive nichrome wire passed across the opening of the GOX/MAPP inlet. The mixture is ignited as it flows across the nichrome, releasing enough energy to ignite the propellants.

4.3.1 Requirements

The ignition system requires powering the nichrome wire to light the main ignition torch as well as controlling gas flow through the appropriate solenoid valves for GOX and MAPP gas. Solenoid control was covered in section 4.1. The nichrome wire requires 14.1A at a supply voltage of 3.2V.

4.3.2 Designed Solution

Power for the nichrome will be provided by a Mean Well LRS-100-3.3 AC-DC power supply unit, with a peak capacity of 20A. This supply has a nominal output of 3.3V with an adjustable range of 2.97V to 3.6V. This voltage will be controlled by a 20A relay with an AC coil operated by switches in the control center.

5 Data Collection and Transmission from Test Stand

5.1 Requirements

- The data sampled from the test stand should be both stored locally and available live to the test operators. Data stored locally will be sampled at a minimum rate of 100Hz, and data which is available live will be transmitted at a minimum of 10Hz.
- The data collected will be stored in plain text in a Comma Separated Values (.csv) file for ease of post processing.
- Time stamps will be recorded with each set of data.
- The microcontroller used to collect the data will be housed in a robust enclosure to prevent damage from water ingress and environmental conditions.
- Data transmission to the control station will be viewed through a program running on a laptop computer. This program will also store collected data in the event that data collected by the microcontroller is lost.

5.2 Designed Solution

Data from all sensors will be aggregated by a Teensy 3.6 microcontroller. The Teensy 3.6, running at 120MHz, has the necessary speed to collect and stream data at the required rate (100 Hz from the test stand and 10 Hz to the control center). It also has sufficient input/output capabilities to interface with all instrumentation. The Teensy 3.6 is equipped with a built-in SD card adapter which will allow the logging incoming data without using an SD breakout board. To send the data back from the test stand to the control station, we will use an Xbee Pro S1 operating in serial pass-through mode. This Xbee module has sufficient range and bandwidth to transfer the required data. The software to view the Xbee's output at the control station and aggregate and store the data at the test stand will be developed by the team.

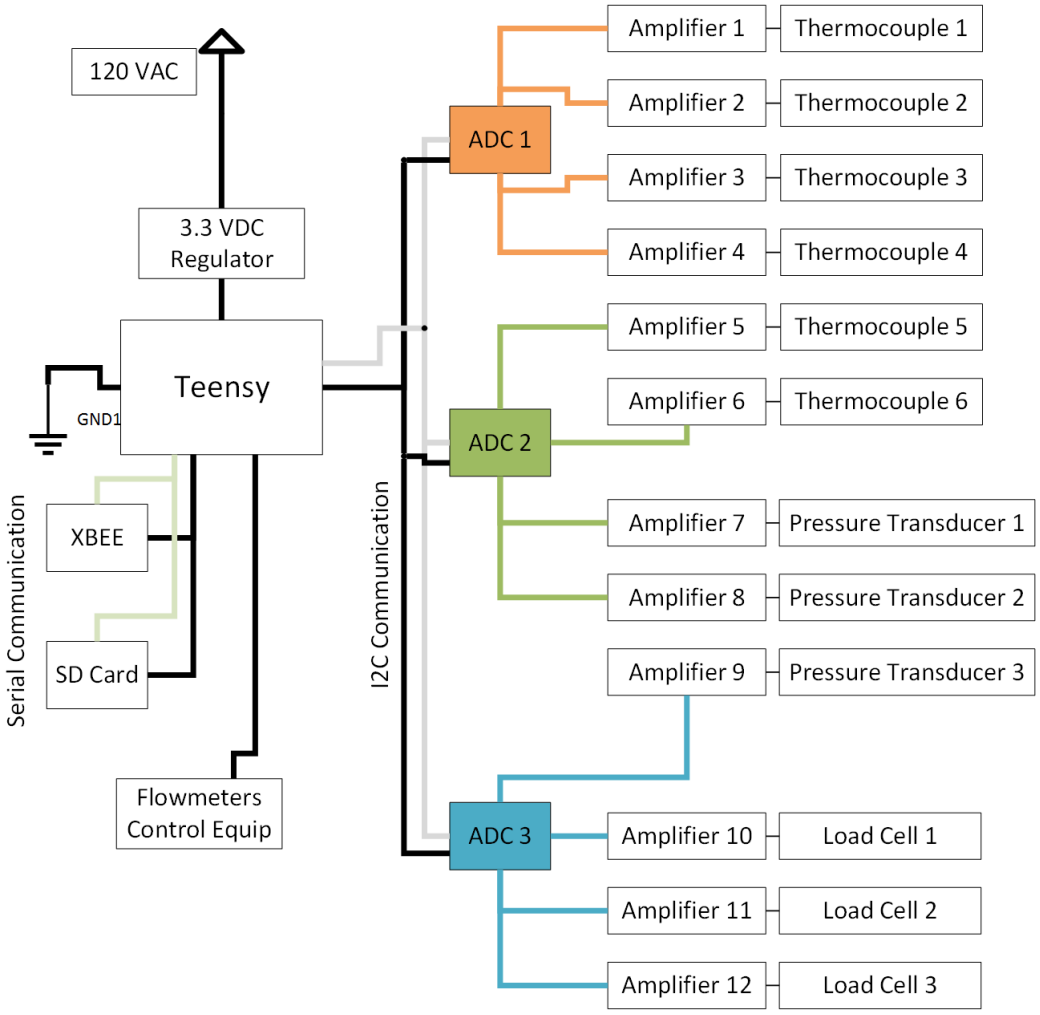

Figure 5.1: Data collection and transmission package at test stand

6 Control Center

The control center coordinates test operations such as propellant loading, tank pressurization, engine firing, and data collection and live monitoring.

6.1 Instrumentation and Live Monitoring

Data will be collected and stored locally at the test stand at a sample frequency of 100 Hz. In addition, data will be streamed wirelessly through an XBee communication module operating at 2.4 GHz, with packets being sent at 10 Hz. At the control center, a second XBee module will be connected to a laptop receiving the data and sending it over a serial connection. This data will be processed and displayed in a graphical format on the monitor using Processing or a similar graphics language.

6.2 Live Video Monitoring

The cameras at the test stand will monitor the propellant pressure gauges and transmit over the 5.8 GHz band to a receiver at the control station. The A/V receiver is connected through a digital capture card to the USB port on a laptop running the live feed. Since two cameras will be present, the transmitters will

run on different channels and video switching will be accomplished by changing channels at the receiver. The signal will be displayed on the live video laptop.

6.3 Relay Control System

6.3.1 Test Stand Control Box

Valve control will be accomplished through a relay system, comprised of boxes at the control center and at the test stand. All remotely controlled valves and systems including the igniter, the solenoid valves, and the thrust valve motor will be operated this way. Each valve is controlled by a separate AC relay, which operates on 120VAC that is routed into the box at the control center. A series of AC switches controls the activation of the relays. Each relay circuit features an “arm” switch in series with the main valve actuation switch for safety.

6.3.2 Control Center/Test Stand Communication

The outputs from the control box connect via extension cords to the relay box at the test stand. Other alternatives considered were wireless communication with the relay box at the test stand and DC wired communication. As the proper operation of the valves is critical to test success and safety, preference was given to a simple and reliable system. The wireless communication system might be subject to packet loss or other signal problems and could cause errors such as erratic valve actuation or not actuating on command.

A DC wired signal could suffer high voltage drops due to the long cable it is passed through. While these problems could be solved by a series of optocouplers and comparators, it is not the simplest solution, and preference was given to the AC wired extension cord system.

6.3.3 Test Stand Relay Box

The relay box at the test stand consists of a set of AC inputs from the control center extension cords and a set of DC outputs to the solenoid valves and motors. In this situation, relays with a 120 VAC coil and DC rated contactor will be used. The AC control circuit is completely isolated from the solenoid valve and motor actuation circuit, and DC power will be supplied to the control circuit through the relay box power supplies and a generator near the test stand.

The relays for the solenoid valves will have contact ratings for a minimum of 24V at 2A in order to be compatible with the selected valves. The relays contacts for the thrust valve motor control will be be rated for 24V at 40A in order to be compatible with the thrust valve motor.

7 Safety and Equipment Checkout

7.1 Safety

Safety is a critical aspect of the design, and is addressed in several ways. Primarily, the 500 foot distance between the control center and the test stand is enough to contain any failures that may occur during testing, and all test personnel and spectators will remain in or behind the control center while testing is in progress. The valve control circuit is designed with a arming switches to minimize risk of unwanted actuation. The wired AC connection to test stand control elements ensures maximum reliability, and was deemed the best choice in executing desired valve operation while avoiding noise in the circuit and potential software problems present in digital control. Class B fire extinguishers will be available both at the test stand and at the control center.

7.2 Equipment Checkout

All equipment will be tested prior to engine testing. This will consist of a visual circuit inspection, as well as incremental integration of the circuitry to ensure that each piece of the circuit is working before connecting another branch. For example, before testing the entire valve actuation circuit with both control boxes, the control center relay box will be tested for proper functionality, followed by the addition of the extension cords and then finally the test stand control box. Similar procedures will be followed for the instrumentation, data logging, and transmission circuits.